Electrostatically Enhanced Thioureas: Synthesis, Reactivity and Selectivity

A THESIS SUBMITTED TO THE FACULTY OF
UNIVERSITY OF MINNESOTA
BY

Yang Fan

IN PARTIAL FULFILLMENT OF THE REQUIREMENTS
FOR THE DEGREE OF
DOCTOR OF PHILOSOPHY

Dr. Steven R. Kass, Advisor

July, 2018

Acknowledgements

First I'd like to express my special thanks to my advisor Dr. Steven Kass, who has guided and supported my five-year graduate study with his profound knowledge, patience and generosity. His scientific way of thinking and kind personality will always affect me in my future career.

I also want to deeply appreciate my family for their continuous substantial and emotional support, without which I couldn't succeed in my study abroad.

Finally, I'd like to acknowledge all previous and current group colleagues for their selfless contributions in creating a good academic and laboratory environment and I have really benefit and learned a lot from them.

Abstract

Hydrogen bonding exhibits its importance in enzyme-catalyzed chemical transformations, naturally occurring three-dimensional architectures and molecular recognition. In recent years, synthetic chemists have successfully exploited hydrogen bonds and developed many enantioselective organocatalysts. As a result, small molecule hydrogen bond donors along with organometallic species and enzymes are now recognized as playing a major role in asymmetric synthesis.

Thiourea derivatives are among the most common and widely-developed hydrogen bond catalysts. Impressive results in terms of both yields and enantioselectivities in asymmetric syntheses have been obtained. A key feature in their success is the ability of these compounds to simultaneously donate two hydrogen bonds to a substrate, despite their relatively weak acidity. This provides highly stereoconfined environments when chiral moieties are incorporated into the thiourea and has made them the subject of extensive research efforts.

The work described in this thesis focuses on the development of a class of positively charged acidity-enhanced thiourea catalysts which make use of an alkylated pyridinium substituent and an appropriate non-coordinating counteranion to enhance their N–H acidities and improve their catalytic activities by orders of magnitude in a variety of transformations. A series of these catalysts have been synthesized and their reactivities in both asymmetric and non-asymmetric transformations were explored. Simple and highly efficient synthetic schemes and excellent catalytic results have been discovered for these novel species.

Table of Contents

List of Tables

Chapter 1

Chapter 2

Chapter 3

Chapter 4

Chapter 5

Appendix for Chapter 2

Appendix for Chapter 3

Appendix for Chapter 4

Appendix for Chapter 5

List of Figures

Chapter 1

Chapter 2

Chapter 3

Chapter 4

Chapter 5

Appendix for Chapter 3

List of Schemes

Chapter 1

List of Abbreviations

Ac: acetyl

aq: aqueous

Ar: aromatic

ATR: attenuated total reflectance

BAr^F_4: tetrakis(3,5-bis(trifluoromethyl)phenyl)borate

BINOL: 1,1'-bi-2-naphthol

Bn: benzyl

Boc: *tert*-butyloxycarbonyl

calcd: calculated

cat.: catalyst

conv.: conversion

DCM: dichloromethane

DMF: *N*,*N'*-dimethylformamide

DMAP: dimethylaminopyridine

DMSO: dimethylsulfoxide

DNA: deoxyribonucleic acid

dr: diastereomeric ratio

ee: enantiomeric excess

eq.: equivalent or equation

e.r.: enantiomeric ratio

ESI: electrospray ionization

EtOAc: ethyl acetate

Gly: glycine

h: hours

His: histidine

HPLC: high-performance liquid chromatography

HRMS: high-resolution mass spectroscopy

IR: infrared

LUMO: lowest unoccupied molecular orbital

mg: milligram

MHz: megahertz

min: minutes

mL: milliliter

mM: millimolar

mol%: mole percent

mp: melting point

MPa: megapascal

MPLC: Medium-pressure liquid chromatography

MS: molecular sieve

Ms: methanesulfonyl

nm: nanometer

NMR: nuclear magnetic resonance

Nu: nucleophile

OTf: triflate

OTs: *p*-toluenesulfonate

Ph: phenyl

ppm: parts per million

PPN: bis(triphenylphosphine)iminium

Py: pyridinium

rt: room temperature

Ser: serine

SFC: solvent free conditions

SI: supporting information

TADDOL: α,α,α',α'-tetraaryl-1,3-dioxolan-4,5-dimethanol

TBA: tetra-*n*-butylammonium

TBS: *tert*-butyldimethylsilyl

temp: temperature

TFA: trifluoroacetic acid

TFAA: trifluoroacetic anhydride

THF: tetrahydrofuran

TLC: thin-layer chromatography

TMS: tetramethylsilane

tosyl: *p*-toluenesulfonyl

μL: microliter

UV: ultraviolet

Vis: visible

Chapter 1. Background and Introduction*

1.1. Hydrogen Bonds

Hydrogen bonding is very common in nature and accounts for a large number of inter- and intramolecular interactions in our surrounding environment, from the complex properties of bulk water and protein folding to the specificity of DNA base pairing (Figure 1).[1]

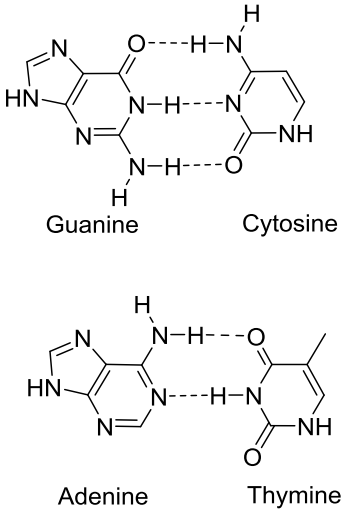

Figure 1. Hydrogen bonding in DNA base pairing.

By definition, a hydrogen bond is the electrostatic attraction that results from the association of hydrogen atom bound to a relatively electronegative atom A, and a second electronegative atom B which possesses an unshared electron pair.[2] These electronegative atoms typically are fluorine, oxygen and nitrogen but sometimes A or B can be carbon. In

*This chapter is reproduced from my 2013 written preliminary examination at the University of Minnesota and this dossier is used as the template for the subsequent sections.

this A–H···B interaction, the A–H part is referred to as a hydrogen bond donor and the electronegative atom B is called a hydrogen bond acceptor.

In addition to its importance in forming natural three-dimensional structures, the hydrogen bond also plays key roles in various other areas. For instance, hydrogen bonds are also an extremely powerful tool in molecular recognition,[3] crystal engineering[4] and the construction of supramolecular architectures.[5] Moreover, hydrogen bonding has tremendous potential in catalysis.

1.2. Hydrogen Bonding Catalysis

1.2.1. Nature

In nature, many biochemical compounds are synthesized by enzymes in living cells. Enzymes are nature's catalysts and accelerate a wide variety of biochemical transformations.[6] A typical example is illustrated by serine protease-catalyzed hydrolysis of amides (Figure 2).[6a] Serine proteases form an oxyanion hole and simultaneously donate two hydrogen bonds to the carbonyl group of an amide, thereby activating it electrophilically and stabilizing the high-energy tetrahedral oxyanion intermediate formed in the amide hydrolysis reaction. Other enzymes using hydrogen bonding interactions to catalyze reactions include chorismate mutase,[7] type II adolases,[8] *etc*.

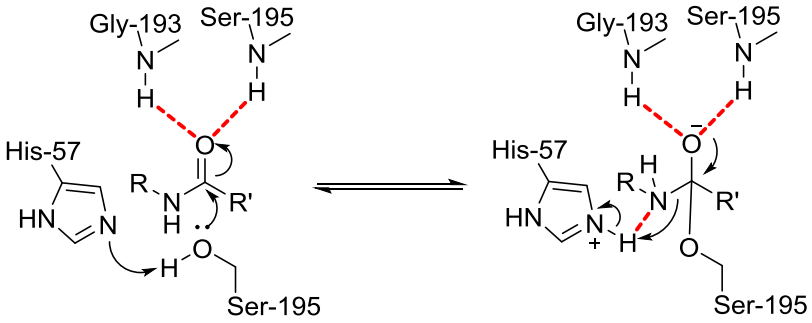

Figure 2. Serine protease-catalyzed amide hydrolysis.[6a]

1.2.2. Hydrogen Bonding Organocatalysis

Since the mid-1980s, there has been an increasing focus on hydrogen bond donors as enzyme mimics and catalysts for organic transformations.[9,10] In the intervening three decades, synthetic chemists have successfully exploited hydrogen bonds in the development of small-molecule organocatalyst systems.[10]

The major principle behind hydrogen bonding catalysis is to mimic an oxyanion hole and facilitate nucleophilic reactions. From a detailed mechanistic point of view, this is accompanied by donation of one or more hydrogen bonds to an electrophile, thereby decreasing the energy of its lowest unoccupied molecular orbital (LUMO) and activating nucleophilic attack. The resulting transition state is stabilized, and consequently this leads to rate acceleration. This process can end with generating either a protonated (proton transfer to substrate after transition state) or unprotonated (no proton transfer) intermediate.[11]

With respect to the numbers of hydrogen bonds donated by hydrogen bond donors, the hydrogen bonding catalysts can be divided into three categories: (1) single hydrogen

bond donor catalysts; (2) double hydrogen bond donor catalysts and (3) multi-hydrogen bond donor catalysts[12] (Figure 3).

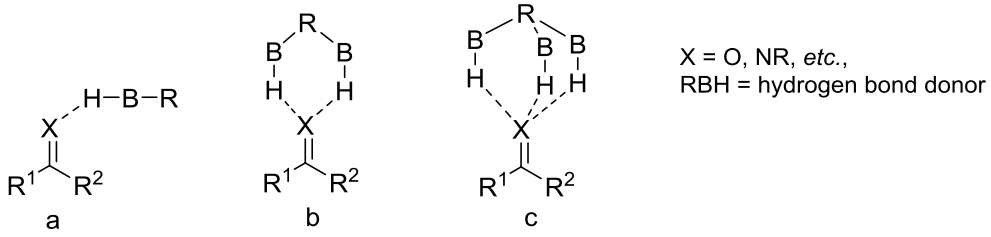

Figure 3. An activation mode of electrophiles by (a) single, (b) double and (c) multiple hydrogen bond donors.

Single hydrogen bond donor catalysts are less developed than double hydrogen bond donors due to the moderate strength and the difficulty in controlling directionality of a single hydrogen bond.[1] Typical species such as α,α,α',α'-tetraaryl-1,3-dioxolan-4,5-dimethanol (TADDOL, **1**), 1,1'-bi-2-naphthol (BINOL, **2**) and other kinds of diols constitute the majority of single hydrogen bond donor catalysts (see Section 1.3 for more details). These single hydrogen bond donors are proposed to form an intramolecular hydrogen bond between the two hydroxyl groups. This interaction increases the acidity and defines the orientation of the O–H bond that is not engaged in the intramolecular hydrogen bond (Figure 4). Diarylphosphoric acids are also typically regarded as single hydrogen bond donors, in spite of their relatively strong acidity.

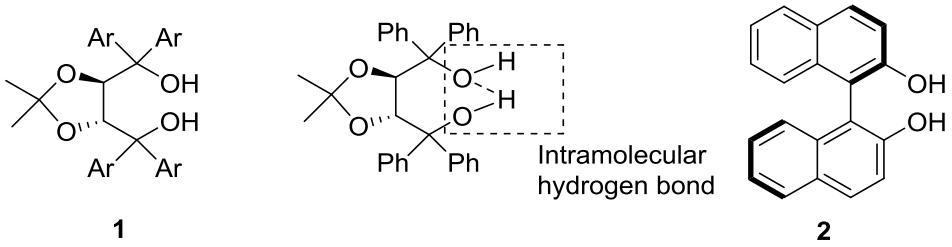

1 **2**

Figure 4. TADDOL (**1**) and BINOL (**2**) as single hydrogen bonding catalysts.

Double hydrogen bonding donor catalysts have become a widespread and powerful implement for substrate activation in hydrogen bonding catalysis. In this hydrogen bonding catalytic strategy, the activation of substrates occurs via either binding of the hydrogen bonding donor to an electrophile substrate to increase its electrophilicity or formation of a substrate/catalyst ion pair in the transition state. Double hydrogen bonding is advantageous over single hydrogen bonding in both bond strength and directionality. Some substrates that can be activated by double hydrogen bond donors include aldehydes, ketones, esters, a variety of imine derivatives, *N*-acyliminium ions, nitro compounds and epoxides.[1] This class of hydrogen bonding donor catalysts consists of ureas, thioureas, chiral guanidinium and amidinium ions among others (Figure 5). Of these, the most successful and widely developed species are thiourea derivatives.

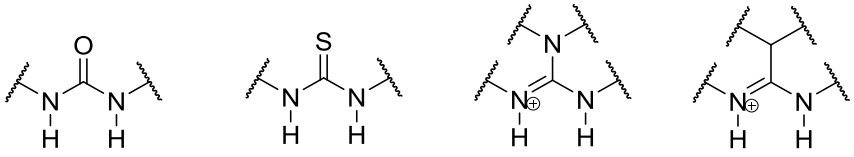

Figure 5. Urea, thiourea, guanidium and amidinium ions as double hydrogen bonding catalysts.

Nowadays, asymmetric organocatalysis is widely recognized as a major area of enantioselective synthesis, complementary to metal complexes and enzyme-mediated catalysis.[10h,13] In particular, small-molecule chiral hydrogen bond donors have emerged as a powerful tool for asymmetric organocatalysis.[10] These organocatalysts have many advantages over traditional metal-based catalysts. The core aspect is that they do not contain any metals and are thus less toxic. Also, being more economical, environment-friendly and air- and moisture-stable species with good tunability, these readily available species are promising candidates for the development of practical and useful organic reagents. Meanwhile, the loading requirement for most organocatalysts can remain at a relatively low level (usually $\leq$ 10 mol%).[10h]

1.3. Various Hydrogen Bonding Catalysts

Recent progress in this field has provided numerous structurally distinct hydgrogen bonding catalysts that cover a wide acidity range of about 20 pK_a units.[1,10c,10d] In this section, several typical structural motifs will be briefly discussed. As the focus of my research projects, thioureas will be exclusively discussed in detail in Section 1.4.

1.3.1. TADDOL and BINOL Derivatives

As has been discussed in the previous section, TADDOL derivatives belong to single hydrogen bond donors which feature an intramolecular hydrogen bond between two O–H groups. The surrounding aryl substituents provide further stereochemical control by introducing additional steric and electronic contributions. TADDOL derivative **1** (Ar = 1-

naphthyl) was initially reported to effectively catalyze an asymmetric hetero-Diels–Alder reaction of aminodienes with aldehydes (Scheme 1) in moderate yield and good ee.[14]

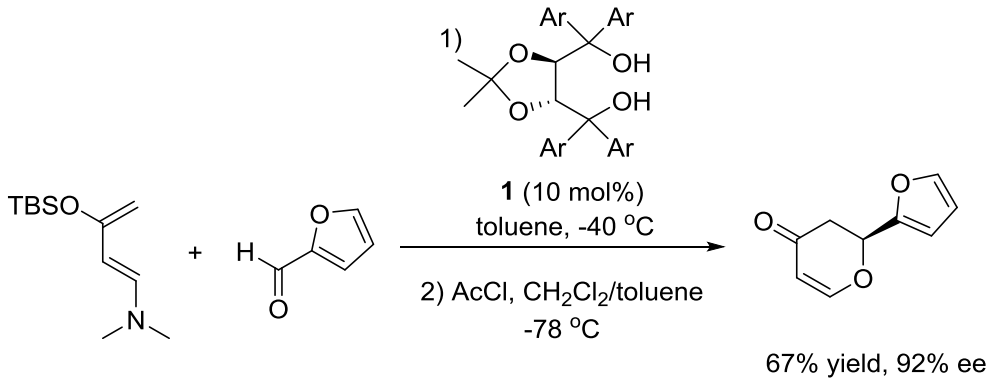

Scheme 1. TADDOL-catalyzed asymmetric hetero-Diels–Alder reactions of an aminodiene with an aldehyde.

Schaus *et al.*[15] reported the enantioselective Morita–Baylis–Hillman reaction of aliphatic aldehydes catalyzed by BINOL derivative **3** in the presence of an organic base, affording the corresponding adducts with high ee.

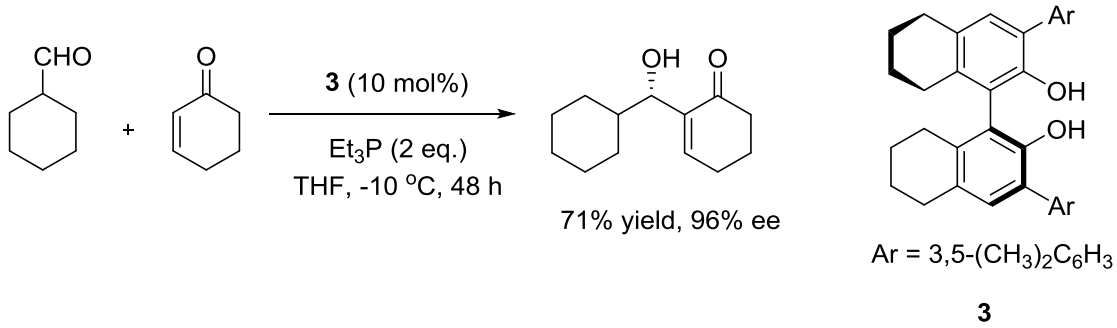

Scheme 2. Enantioselective Morita–Baylis–Hillman reaction of an aliphatic aldehyde catalyzed by BINOL derivative **3**.

1.3.2. Phosphoric Acids

Chiral phosphoric acids are among the most extensively developed single hydrogen bond donors with relatively strong acidity (DMSO pK_a around 2-4[16]).[17] In this regard, the bifunctional BINOL-derived chiral phosphoric acids bearing both acidic and basic sites and 3,3'-substituents for asymmetric induction are the most commonly employed structural motif (Figure 6).

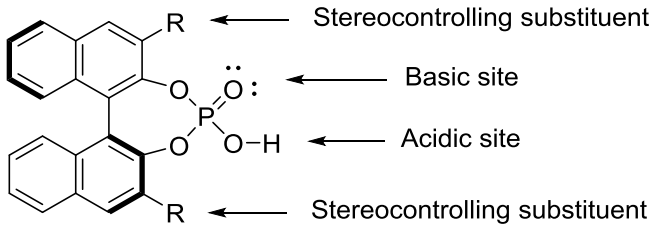

Figure 6. BINOL-derived chiral phosphoric acids.[10c]

For example, phosphoric acid **4** was found to be an effective catalyst in the enantioselective Mannich-type reaction of aldimines and silyl ketene acetals, and the *syn* product was formed in good yield and enantioselectivity (Scheme 3).[18]

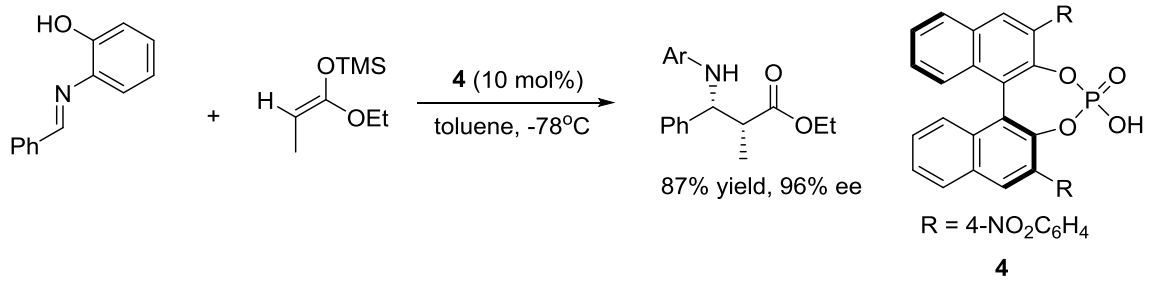

Scheme 3. Enantioselective Mannich-type reaction of an aldimine and a silyl ketene acetal catalyzed by **4**.

Phosphoric acid **5** bearing different aryl substituents at the 3,3'-positions was reported by Terada *et al*. to have good catalytic performance in the Mannich reaction of 2,4-pentandione with aldimines (Scheme 4).[19]

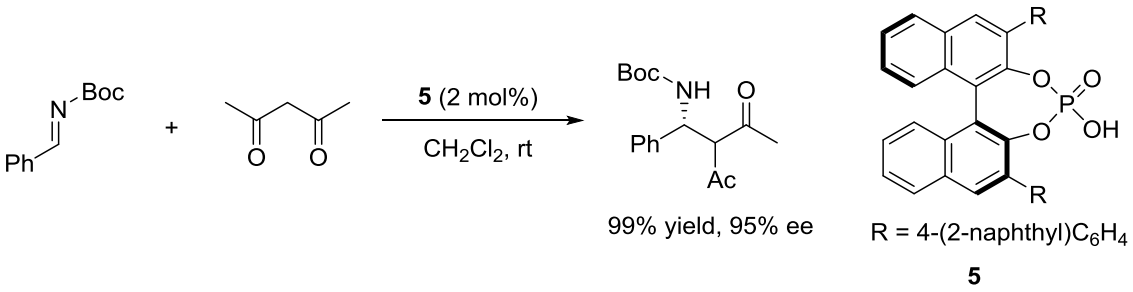

Scheme 4. Mannich reaction of an aldimine with 2,4-pentandione catalyzed by **5**.

1.3.3. Squaramides

Within the scope of double hydrogen bond donors, thioureas and squarmides serve as two common classes (see Section 1.4 for a detailed discussion on thioureas). With regard to asymmetric catalysis, the two hydrogen bonds provide not only stronger coordination to the substrate but also a well-defined organization of the complex required for asymmetric induction.

Rawal *et al*. took advantage of chiral squaramides since they have a wider spacing between the two N–H bonds than thioureas and this was demonstrated by both crystallographic and computational data (Figure 7).

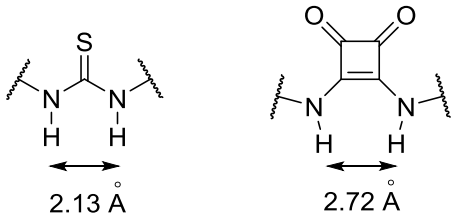

Figure 7. Crystallographic and computational data of N–H distances in thiourea and squaramide.[20]

Cinchona-squaramide **6** was identified as an effective catalyst for the conjugate addition of 2,4-pentanedione to *trans*-β-nitrostyrene, giving the enantiomerically pure product (Scheme 5).[20]

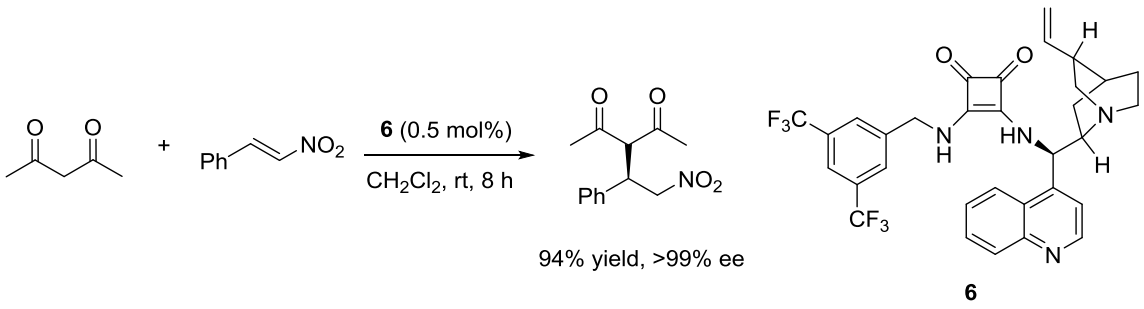

Scheme 5. Conjugate addition of 2,4-pentanedione to *trans*-β-nitrostyrene catalyzed by **6**.

The same research group later reported an asymmetric Friedel–Crafts reaction between *N*-tosyl imines and indole using 2.5 mol% of cyclohexanediamine-squaramide catalyst **7** (Scheme 6).[21] In this reaction, the 3-indolyl methanamine products have been obtained in up to 96% yield and ee.

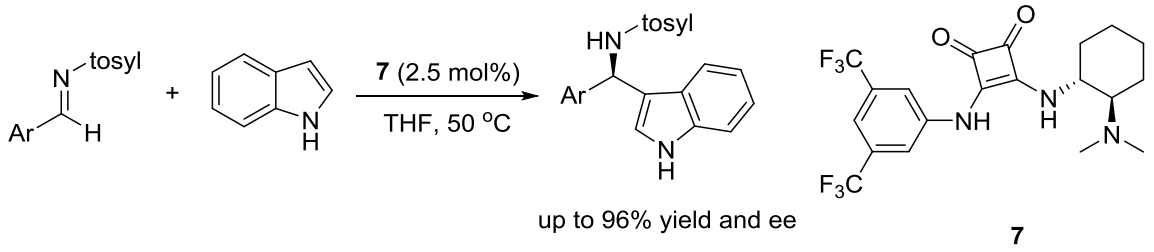

Scheme 6. Asymmetric Friedel–Crafts reaction between *N*-tosyl imines and indoles catalyzed by **7**.

1.3.4. Silanediols

Mattson *et al*. initially reported the successful use of silanediol catalysis based upon its good anion recognition ability of acetate.[22] As a double hydrogen bond donor, the silanediol was proposed to bind strongly to electrophiles with bifurcated binding sites such as nitroalkenes (Figure 8). Its catalytic potential was then confirmed in the Friedel–Crafts addition of *trans*-β-nitrostyrene with indole promoted by **8**, affording an 81% yield after 24 h (Scheme 7).[23]

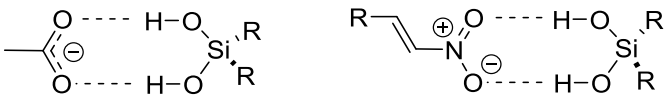

Figure 8. Binding pattern of silanediol with acetate and nitroalkenes.

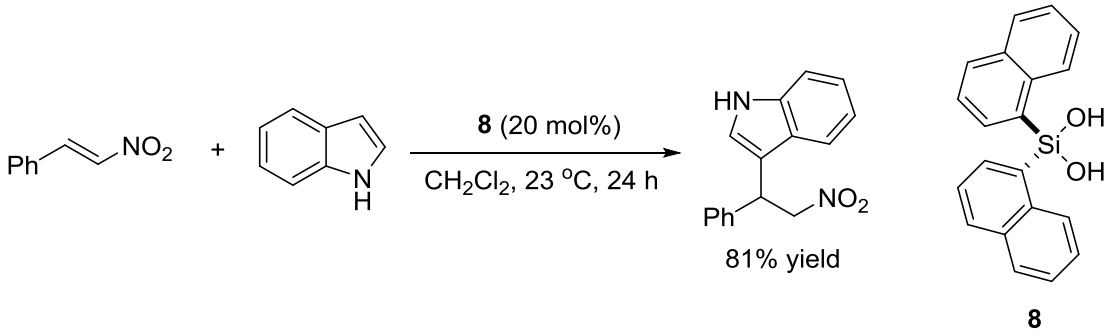

Scheme 7. Silanediol-promoted Friedel–Crafts addition of *trans*-β-nitrostyrene with indole.

An independent study suggested a cooperative hydrogen bonding effect in silanediol catalysis, where an O–H group is acidified by self-association (Figure 9).[24] This was supported by NMR binding, X-ray and computational data.

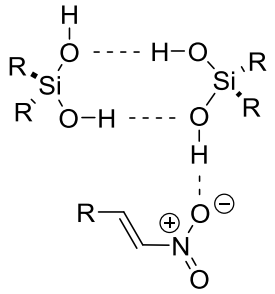

Figure 9. Cooperative hydrogen bonding effect via self-association of silanediol.

As a result, the novel fluorinated silanediol **9** was developed and not only improved the yield in Friedel–Crafts addition to 92% under the same reaction conditions, but also demonstrated excellent catalytic reactivity in the more challenging Michael addition of *trans*-β-nitrostyrene with *N*,*N*-dimethyl-*m*-anisidine (Scheme 8).

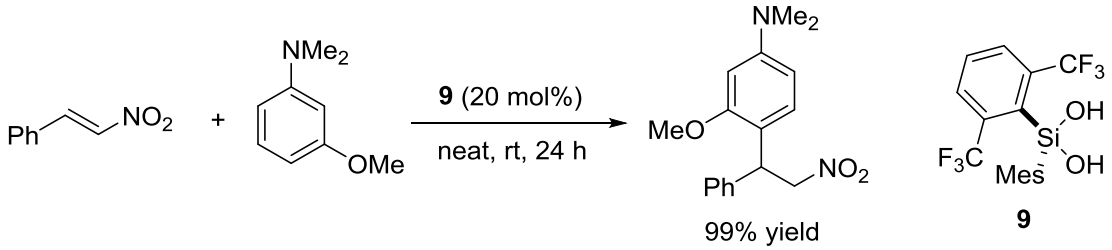

Scheme 8. Michael addition of *trans*-β-nitrostyrene with *N*,*N*-dimethyl-*m*-anisidine promoted by **9**.

1.3.5. Polyols

Many enzymes are known to employ elaborate hydrogen bond networks with two or three hydrogen bonds being used to stablize one oxygen atom center in the transition state of a variety of chemical transformations.[25] This interaction lowers the energy gap between the ground state and transition state resulting in an increased reaction rate.[26] These findings provided our group the impetus to develop a new class of Brønsted acid catalysts. Recent progress in our group includes a new series of aliphatic polyhydroxy alcohols **10-12**, the so-called "polyols", which exploit hydrogen bond networks containing up to six hydrogen bonds to enhance their acidities by stabilizing an oxygen atom negative-charged center in their mono-deprotonated conjugate base structures (Figure 10).[27] We call this type of catalysts single-centered hydrogen-bonded enhanced acidity acids (SHEA acids).

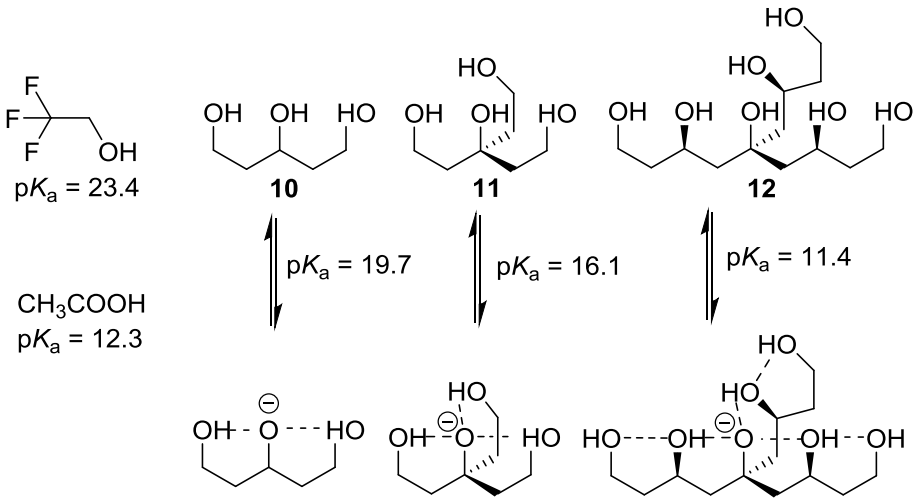

Figure 10. Various polyols **10-12** with their conjugate bases (pK_a values are measured in DMSO; for pK_a value of acetic acid, see ref. 28).

Our group also successfully incorporated electron-withdrawing trifluoromethyl (–CF_3) substituents into this series of polyols to afford even stronger Brønsted acids.[29] The catalytic abilities of three CF_3-containing polyols **13-15** were explored in the Friedel–Crafts alkylation reaction between β-nitrostyrene and *N*-methylindole and in the aminolysis of styrene oxide (Scheme 9). The results demonstrated that all three polyols promote these two transformations in accord with their increasing acidities (**13** < **15** < **14**) in terms of both the reactivity and regioselectivity (Table 1). Hydrogon bonding catalysis is proposed as the mechanism of these reactions.

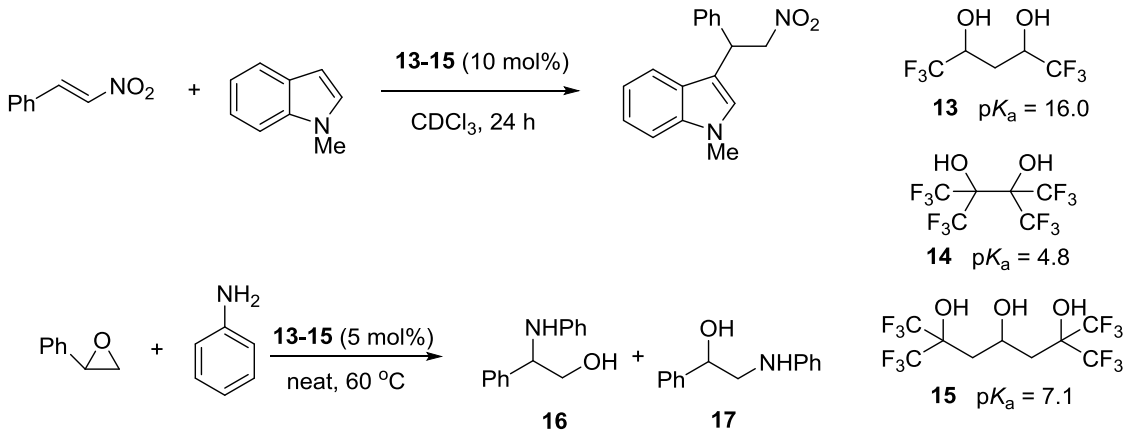

Scheme 9. Friedel–Crafts alkylation and aminolysis reactions catalyzed by three fluorinated polyols **13-15**.

Table 1. Catalytic results of Friedel–Crafts alkylation and aminolysis reactions catalyzed by fluorinated polyols **13-15**.[a]

Catalyst	pK_a (in DMSO)	Conversion (%)[b]		**16** : **17**
		Friedel–Crafts Alkylation	Aminolysis[c]	
13	16.0	19	89	73:27
14	4.8	95	100	88:12
15	7.1	53	100	81:19
No catalyst	-	4	5	53:47

[a]This table is regenerated from ref. 27. [b]Determined by ^{1}H NMR. [c]Reaction time = 2.75 h except for when **14** was used, then it was 20 min.

This type of catalyst is advantageous in its simple atomic constitution (C, H, O and sometimes F), relatively low catalyst loadings and sensitivity to heat, and the presumed benign properties of polyols with respect to the environment. Other such species

developed by our group include a series of *scyllo*-inositol-derived and 1,3,5-triarylbenzene-derived polyols (**18** and **19**, respectively, Figure 11).[12b,30]

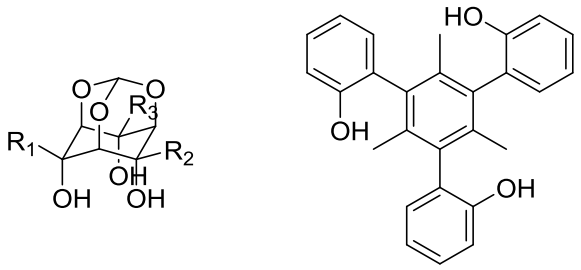

18 **19**

Figure 11. Two types of polyols developed by our group.

1.4. Thioureas

Urea and thiourea derivatives belong to a widely-used hydrogen bonding catalyst family that effectively utilizes two hydrogen bonds to interact with organic substrates to provide sufficient activation to accelerate a wide variety of chemical processes despite their relatively weak acidities (pK_a = 8-20 in DMSO).[31] Moreover, chiral urea and thiourea catalysts can provide highly stereoconfined environments in addition to their relatively strong and directional hydrogen bonds.[1,32]

From a mechanistic point of view, thiourea derivatives catalyze reactions by (a) directly activating an electrophile substrate toward nucleophilic attack by forming two hydrogen bonds and (b) promoting the formation of a stable substrate/catalyst ion pairs (Figure 12). It is also worth mentioning Pathway (c), which can be viewed as a special case of pathway (b), since an ion pair intermediate is present but no resonance stabilization is involved. It proceeds via formation of a reactive carbenium intermediate

in an S_N1 fashion by direct abstraction of an anionic leaving group by hydrogen bonding with the thiourea.

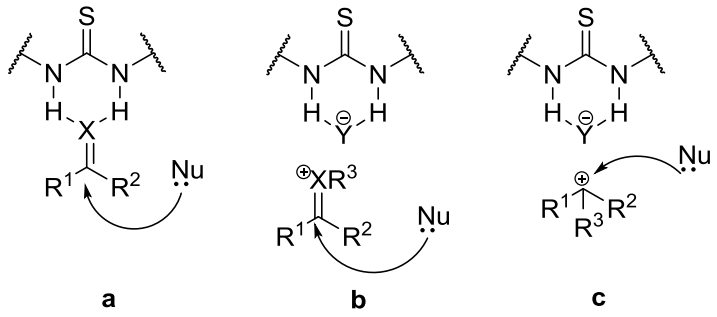

Figure 12. Three proposed pathways of thiourea catalysis through double hydrogen bonding.

1.4.1. Early Studies of Ureas

Etter *et al*. first reported that *N,N'*-diarylureas possessing electron-withdrawing substituents can form co-crystals with a wide variety of Lewis bases such as carbonyl compounds (Figure 13).[33] This discovery inspired the vibrant development of ureas and thioureas as general acid catalysts.

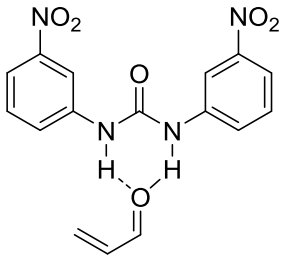

Figure 13. A carbonyl compound activated by Etter's urea.

An early example of urea catalysis came from Curran *et al*. who found that substoichiometic amounts of diarylurea with an electron-withdrawing CF_3 group on the aryl backbone (i.e., **20)** enhanced the yield of a Claisen rearrangement[34] (Scheme 10) and the diastereoselectivity of an allylation reaction[35] (not shown).

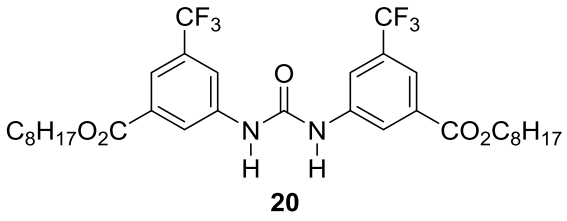

20

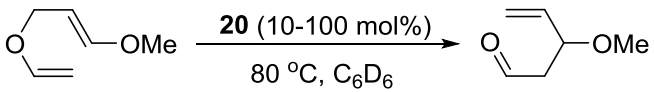

20 (mol%)	k_{rel}
0	1.0
10	2.7
40	5.0
100	22.4

Scheme 10. Claisen rearrangement catalyzed by Curran's diarylurea **20**.

Since Curran's pioneering work, various types of novel urea and thiourea derivatives acting as general acid catalysts have been developed to catalyze nucleophilic addition reactions with impressive diastereo- and enantioselectivities. Their catalytic versatility has been successfully demonstrated by several groups on various reactions (see below).

1.4.2. Schreiner's Catalysts

Based on Curran's discovery, Schreiner and co-workers developed an array of achiral diaryl thiourea catalysts **21-23** for carbonyl activation processes (Figure 14).[36] These thiourea catalysts are advantageous in terms of their straightforward preparation and

increased solubility compared to their urea analogs due to the absence of intermolecular hydrogen bonding.[32b,36b]

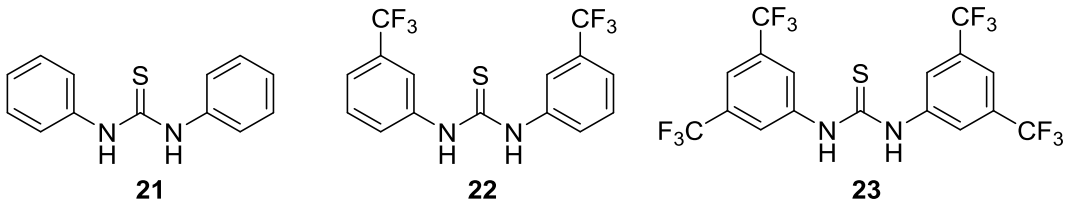

Figure 14. Schreiner's diaryl thiourea catalysts **21-23**.

Thiourea catalysts **22** and **23**, bearing highly electron-withdrawing CF_3 groups at the 3- and/or 5-position(s) of the aromatic rings, have a remarkable catalytic rate enhancement effect. Several reasons are responsible for this acceleration.[32b,36b] First, from an enthalpic point of view, the catalysts with CF_3 substituents have significantly more acidic N–H hydrogens relative to the unsubstituted ones. Second, from an entropic perspective, the attractive interaction between the hydrogen atoms at the 2-positions on the aromatic rings, which are polarized by the adjacent electron–withdrawing CF_3 groups, and the basic sulfur atom of the thiourea moiety (Figure 15) leads to a high rotational barrier and a relatively rigid conformation. This rigidity minimizes the entropic loss in complexation of electrophilic substrates and thus facilitates catalysis. In addition, the thiocarbonyl group is a relatively weak hydrogen bonding acceptor and decreases self-association.

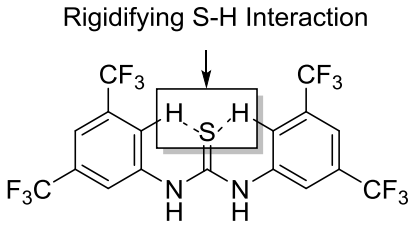

Figure 15. Rigidifying S–H interaction in catalyst **23**.

The results of Diels–Alder reactions between enone **24** and acyloxazolidinone **25** with cyclopentadiene catalyzed by **21–23** are displayed below (Schemes 11 and 12).[32b,36b] Appreciable rate accelerations and remarkable yields were obtained. As expected from these experiments, they identified thiourea **23**, which has two CF_3 groups at the 3,5-positions of the aromatic rings, as the most efficient catalyst among the group.

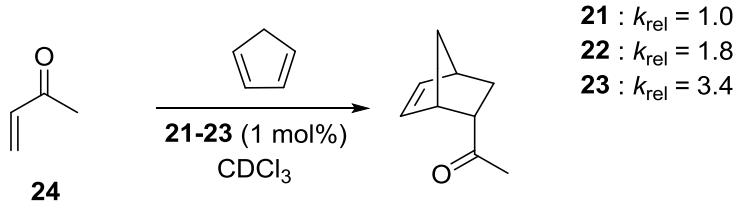

Scheme 11. Diels–Alder reaction of enone **24** and cyclopentadiene catalyzed by thioureas **21-23**.

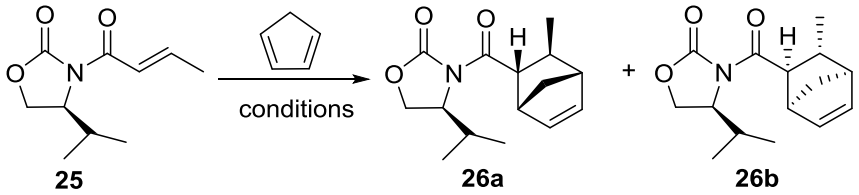

Reaction Conditions	% Yield	**26a** : **26b**
22 (25 mol%), $CHCl_3$, rt	74	77 : 23
23 (25 mol%), $CHCl_3$, rt	78	81 : 19

Scheme 12. Diels–Alder reaction of acyloxazolidinone **25** and cyclopentadiene catalyzed by thioureas **22** and **23**.

1.4.3. Jacobsen's Catalysts

Over the past two decades Jacobsen's group has focused on the activation of alkyl- and acyl-substituted imines by a series of urea and thiourea catalysts bearing various optimized Schiff-base moieties for asymmetric transformations such as the Strecker, nitro-Mannich (Henry), hydrophosphonylation and acyl Pictet–Spengler reactions.[1,10d] In the late 1990's, Jacobsen *et al.* first reported the asymmetric hydrocyanation of imines (i.e., the Strecker reaction of *N*-allyl aldimines with a Schiff-base thiourea catalyst **27**, Scheme 13).[37] In their studies, a combination of parallel synthetic libraries and conventional linear optimizations were utilized and they identified that L-*tert*-leucine, (*R*,*R*)-1,2-diaminocyclohexane along with 3-*tert*-butyl-5-methoxysalicylaldehyde in **27** are critical for good enantiomeric ratios (70-91% ee) in the hydrocyanation product.

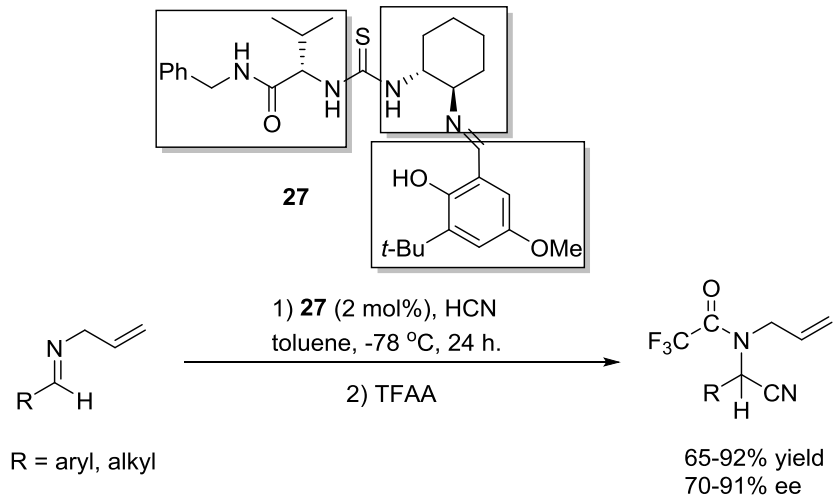

Scheme 13. Asymmetric Strecker reaction of *N*-allyl aldimines with a Schiff-base thiourea catalyst **27**.

To design improved catalysts, they carried out both spectral studies and high-level computations to elucidate the mechanism of the reaction and the binding pattern of the catalyst. Initially, they found Michaelis–Menten kinetic behaviour in these reactions.[38] This indicated that the substrate binds to the catalyst reversibly. It was also found that the thiourea preferentially binds to the *Z*-isomer of imines via a double hydrogen bond as shown in Figure 16 as this binding motif minimizes the steric interaction between the catalyst and large imine substituents R^L. This mechanistic proposal led to the design of an improved 5-pivaloyl-substituted Schiff base thiourea catalyst **28**, which displays both superior reactivity and selectivity profiles. For example, the Strecker reaction of *N*-benzyl imines **33** gave up to a nearly perfect 99.3% ee.[38]

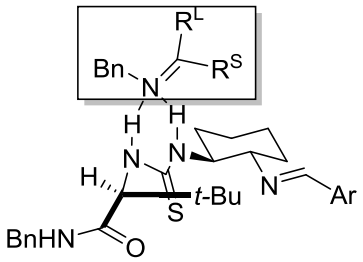

Figure 16. Intially proposed interaction of thiourea catalyst **28** with *Z*-imine isomer through a bifurcated hydrogen bond structure.[32a]

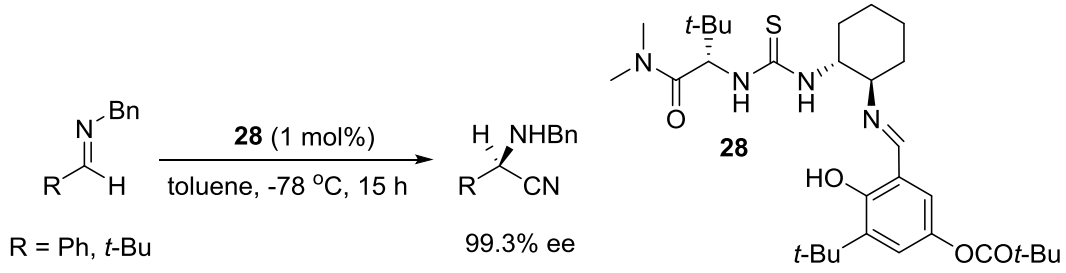

Scheme 14. Asymmetric Strecker reaction catalyzed by **28**.

A later report in 2009 from the same research group, however, proposed a different mechanism for this transformation.[39] Experimental and computational data indicated that rather than directly activating the imine, the catalyst promotes the protonation of the imine by HCN. This leads to a diastereomeric iminium/cyanide ion pair that is stabilized by multiple hydrogen bond interactions with the catalyst (Figure 17). Nucleophilic attack of cyanide anion in this ion pair affords the observed enantiomeric products, which depends on different extents of iminium ion stabilization among different catalysts and diastereomeric transition structures.

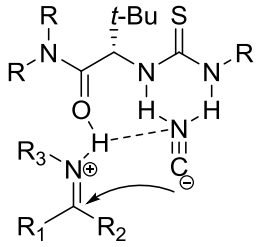

Figure 17. Iminium/cyanide ion pair stabilized by hydrogen bonding in enantioselective Schiff-base thiourea-catalyzed Strecker reactions.[39]

Despite the huge success of Schiff-base thiourea catalysts in asymmetric Strecker reactions, their application is not limited to just this type of reaction. It has been shown that fine-tuning and simplifying the catalyst structure can be used in other processes without an accompanying decline in enantioselectivity. For example, catalysts **28** and **29** were used to catalyze the hydrophosphonylation reactions of *N*-benzyl imine with phosphite[40] (Scheme 15) and Mannich reactions of *N*-Boc imines and silyl ketene acetals[41] (Scheme 16), respectively. A Schiff-base moiety was also found to be unnecessary to promote the acyl-Pictet–Spengler reaction of tryptamine with an aldehyde in the presence of acetyl chloride to afford the cyclized product with high enantioselectivity (95% ee) (Scheme 17).[42] Likewise, a further simplified thiourea **31** with an acetamide group promoted the Henry (nitro-Mannich) reaction of *N*-Boc imines with nitroalkanes to provide *syn* adducts with both high enantio- and diastereoselectivity (97% ee and 16/1 dr, Scheme 18).[43]

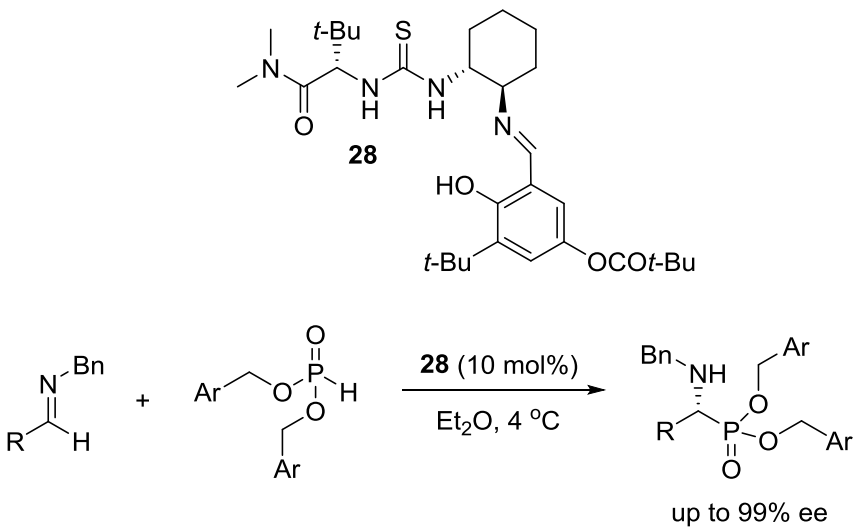

Scheme 15. Hydrophosphonylation reactions of *N*-benzyl imines with phosphites catalyzed by **28**.

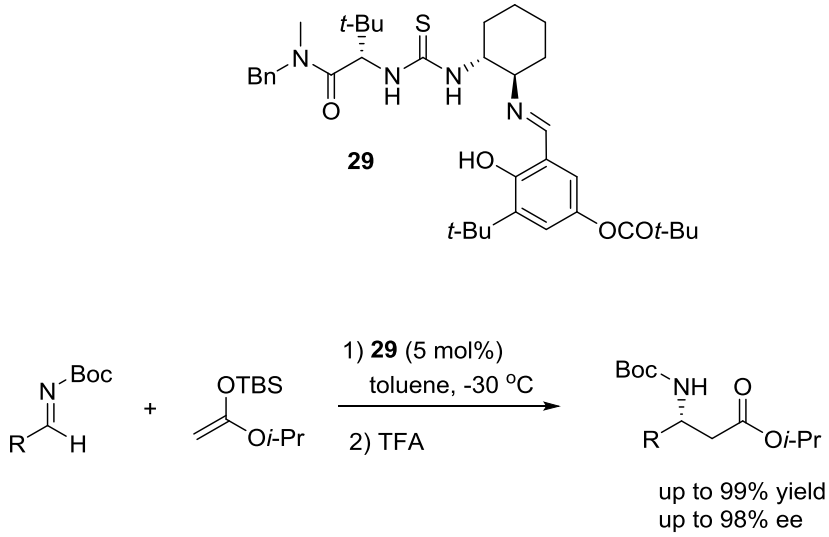

Scheme 16. Mannich reactions of *N*-Boc imines and a silyl ketene acetal catalyzed by **29**.

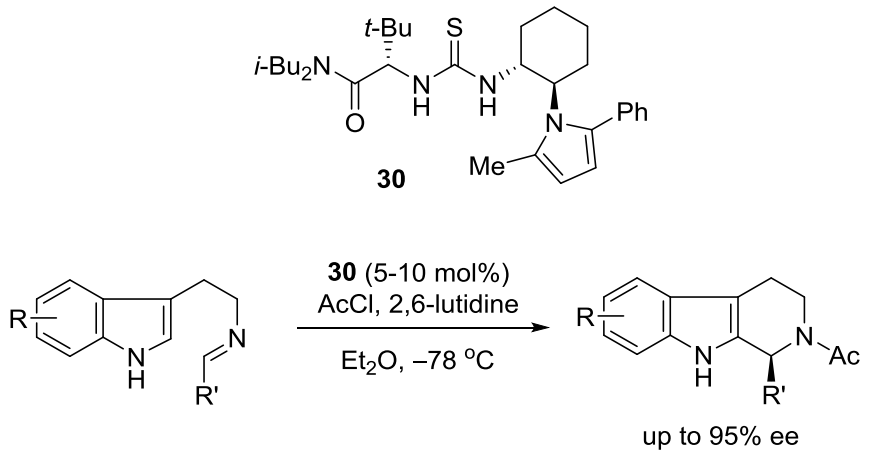

Scheme 17. Enantioselective acyl-Pictet-Spengler reaction promoted by **30**.

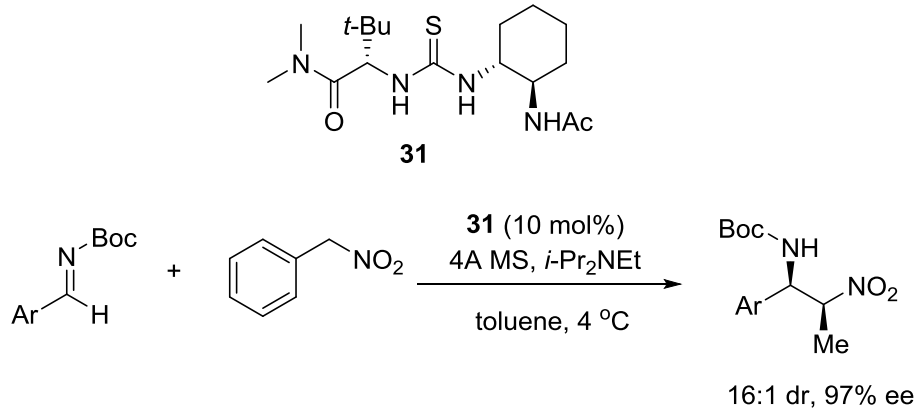

Scheme 18. Henry reaction of *N*-Boc imines with a nitroalkane catalyzed by **31**.

1.4.4. Takemoto's Catalysts

Despite the success of Jacobsen's thiourea derivatives, they are only useful for reactions involving aldimines and ketoimines. To overcome this limitation and further expand the scope of thiourea asymmetric catalysis, Takemoto *et al*. designed and

prepared the so-called "bifunctional thiourea catalyst" based on the remarkable performance of Schreiner's achiral diarylthiourea catalyst.[44] The resulting series of compounds (**32–34**) have a tertiary amino group bearing a cyclic or acyclic 2-(*N*,*N'*-dimethylamino)ethane derivative instead of one of the 3,5-bis(trifluoromethyl)phenyl groups in Schreiner's diaryl thiourea **23** (Figure 18).

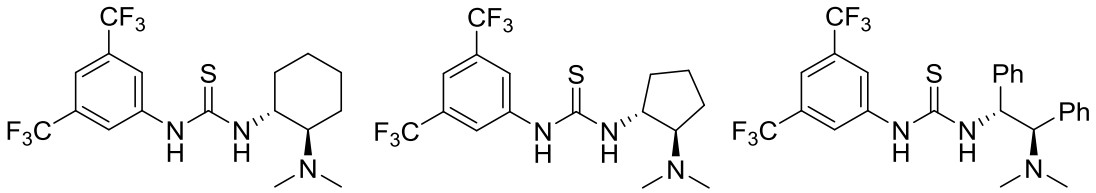

Figure 18. Takemoto's bifunctional thiourea catalysts **32-34**.

These catalysts are special in that the diaminoethane moiety serves as both a chiral scaffold and a basic functional group in addition to the enhanced acidity of the 3,5-bis(trifluoromethyl)phenyl thiourea. It is important, however, that the basic amine is tertiary so that the interaction with the acidic thiourea moiety is very weak and the two functional groups don't deactivate each other.[45]

This is apparent in the X-ray crystallographic structure of thiourea **32** in Figure 19 (left), which shows that the acidic N–H bond and the basic amine only interact weakly (i.e., the NH···N bond distance is 2.70 Å). In addition, the dimethylamino and thiourea groups are positioned equatorially in the chair conformation of the cyclohexane ring, which is an ideal spatial arrangement for the dual activation of both nucleophiles and electrophiles. In contrast, **33** has a cyclopentyl moiety instead of the cyclohexyl ring, and

in this case the two N–H bonds of the thiourea are *anti* to each other so as to facilitate the intramolecular hydrogen bonding between the tertiary amine and the N–H hydrogen (Figure 19, right).

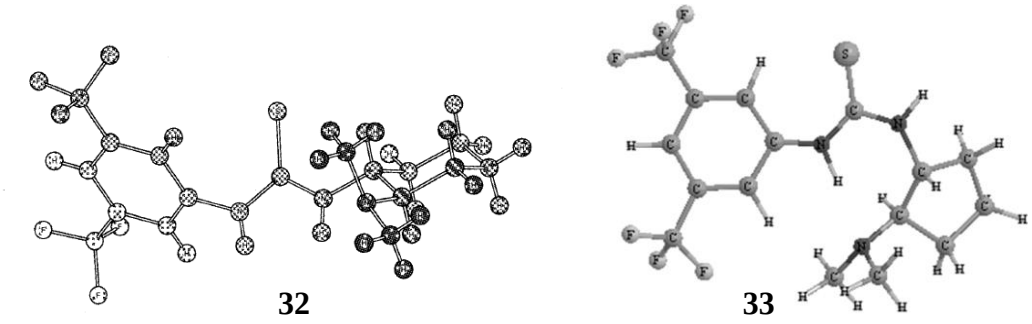

32 **33**

Figure 19. X-ray crystallographic structures of thiourea **32** and **33**.[46]

Takemoto *et al*. demonstrated that these catalysts are highly effective for a variety of catalytic asymmetric nucleophilic additions by dual-activation of both the electrophile and the nucleophile (Figure 20). The electrophilic substrates in these reactions include electron-deficient alkenes and imines. For example, 10 mol% of **32-34** catalyze the Michael reaction of *β*-nitrostyrene with diethyl malonate (Scheme 19). Thiourea **32** bearing the 2-(*N,N'*-dimethylamino)cyclohexane substituent turned out to be the best of the three catalysts in terms of the reaction rate, yield and enantioselectivity.[44] These results also suggest that the rigidity of the chiral diamine scaffold plays a key role in this transformation. This catalyst was also used in the aza-Henry reaction of various nitroalkanes with phenyl *N*-Boc-imine, and gave good yields, diastereoselectivities (*syn* vs. *anti*) and enantioselectivities (Scheme 20).[47]

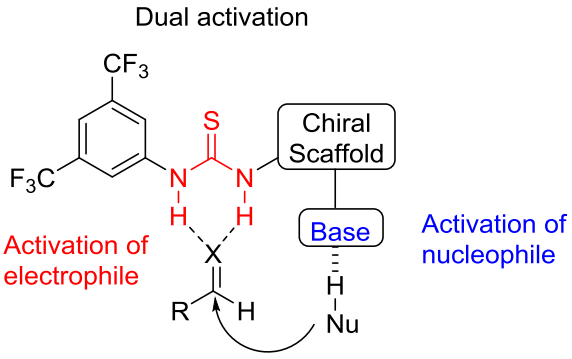

Figure 20. Dual-activation mode of Takemoto's catalysts (reproduced from ref. 48).

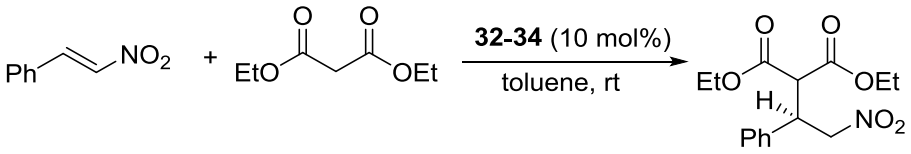

catalyst	time(h)	% yield	% ee
32	24	86	93
33	48	56	84
34	48	52	64

Scheme 19. Michael reaction of β-nitrostyrene with diethyl malonate catalyzed by **32-34**.

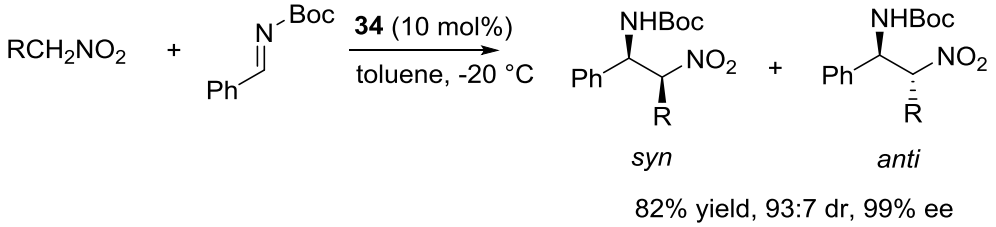

Scheme 20. Aza-Henry reaction of nitroalkanes with a *N*-Boc-imine catalyzed by **34**.

The proposed mechanism for the latter transformation involves coordination and activation of the nitroalkane by forming two hydrogen bonds to the thiourea followed by an intramolecular proton transfer to the neighboring tertiary amine.[47] A subsequent

complex involving the addition of the imine was invoked as the product-forming transition state (Figure 21).

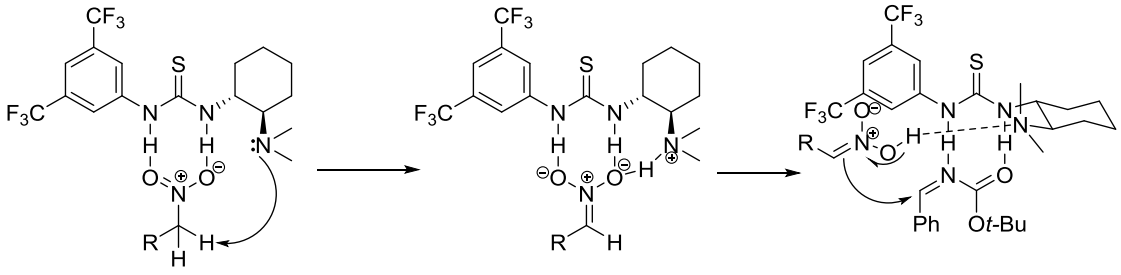

Figure 21. Proposed mechanism for the aza-Henry reaction.

1.4.5. Thiourea Catalysis via Anionic Leaving Group Abstraction

A special type of thiourea catalysis worth mentioning involves a mechanism in which an anionic leaving group is abstracted. This type of process takes advantage of the powerful anion-binding ability of ureas and thioureas.[32e] Jacobsen *et al*. reported that a Takemoto analog (**35**) catalyzed the enantioselective alkylation of *α*-arylpropionaldehydes by a novel ion-pairing mechanism (Scheme 21).[49] Mechanistic studies strongly suggested that the reaction proceeds via the formation of an enamine intermediate and that the subsequent activation of the electrophile by the thiourea occurs by halide abstraction. The resulting stabilized ion pair of a halide and a carbocation leads to the electrophilic attack of the enamine and the formation of the new C–C bond. Hydrolysis of the resulting iminium ion regenerates the catalyst and leads to the ketone product.

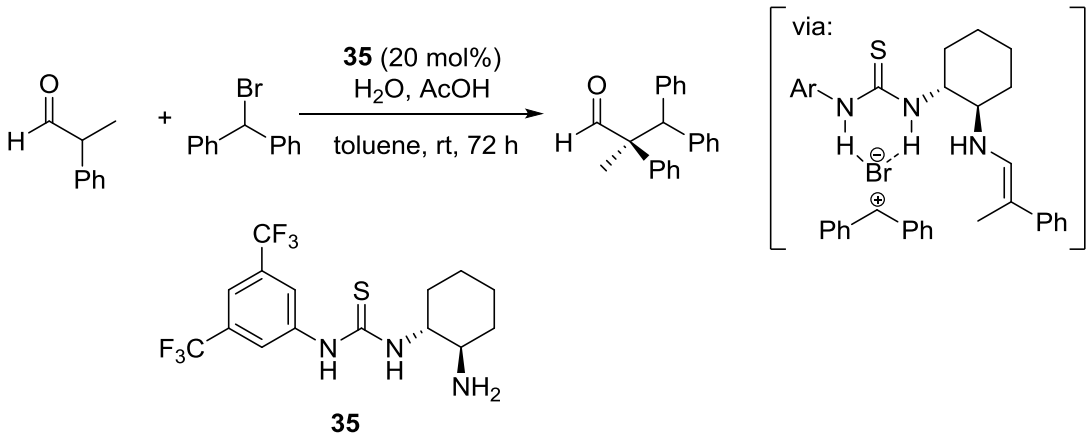

Scheme 21. Enantioselective alkylation via an ion-pairing mechanism.

1.5. Acidity-enhancing Strategy by Charged Substituents

In a very recent report by our research group, an IR spectroscopic study showed that phenols with charged substituents and weakly coordinating anions (**36** and **37**) have enhanced relative acidities in nonpolar media compared non-charged analogs.[50] In this study, it was found that a red shift in the O–H stretching frequency ($\Delta\nu$) was observed for a series of *meta*- and *para*-substituted phenols when placed in a 1% CD_3CN:CCl_4 (v/v) solution (Figure 22). Interestingly, these shifts are in better accord with the gas-phase acidities than the DMSO pK_a values for the phenols. As a result, the observed shifts can be used as an indicator of acidity in nonpolar media (Table 2). This is evidenced in the catalytic Friedel−Crafts reaction between β-nitrostyrene and *N*-methylindole, where depending upon the reaction conditions, phenol **36** and **37** are 26 and 750 times more active than *p*-nitrophenol, respectively (Scheme 22).

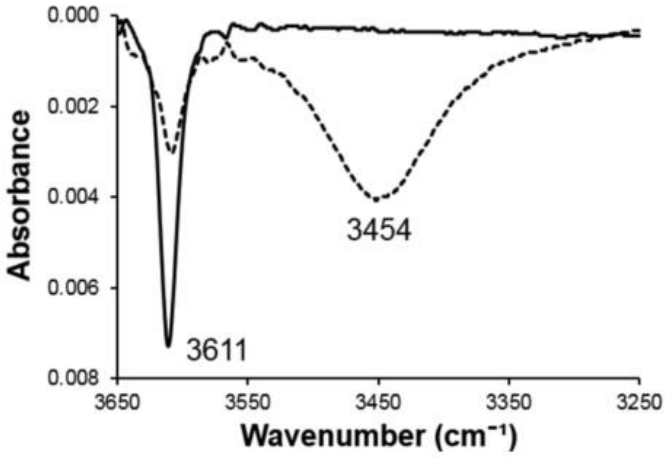

Figure 22. Representative IR spectrum of phenol in CCl_4 (solid line) and in 1% CD_3CN/CCl_4 (dotted line; reprinted with permission from ref. 50. Copyright ACS).

Table 2. Hydroxyl O–H stretching frequency shifts, DMSO pK_a and gas-phase acidity values for *p*-nitrophenol and charged analogs **36** and **37**.[a]

Catalyst	$\Delta\nu$ (cm^{-1})	pK_a (DMSO)	$\Delta G°_{acid}$ (kcal mol^{-1})
p-nitrophenol	221	10.8	320.9 ± 2.0
36	329	12.5 ± 1.0	261.4[b]
37	370	12.4 ± 1.1	231.1[b]

[a]All values come from ref. 50 unless otherwise indicated. [b]Computed values.

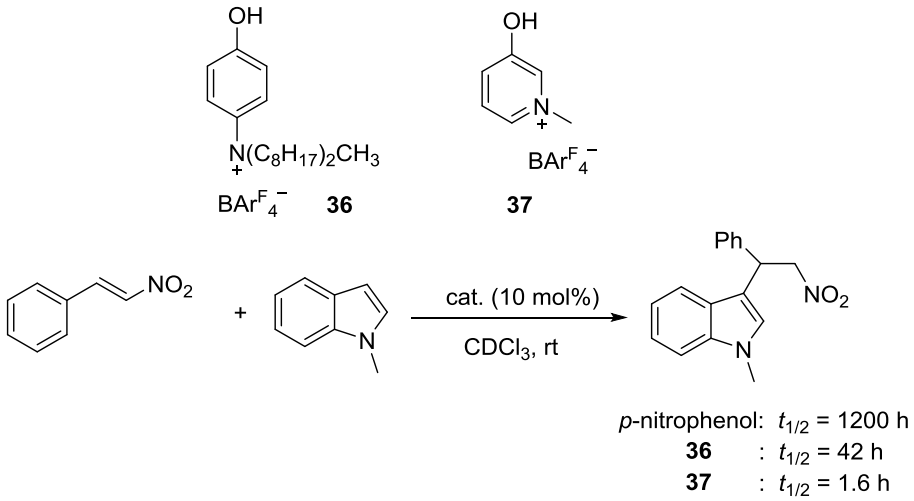

Scheme 22. Kinetic analysis of a Friedel−Crafts reaction catalyzed by *p*-nitrophenol, **36** and **37**.

These findings suggest a novel strategy for enhancing Brønsted acidity and catalytic activity of hydrogen bonding catalysts without introducing additional hydrogen bonding sites.[50] Subsequent studies along this line include the development of charged phosphoric acids[51] and charged thioureas. This latter area is the focus of this thesis.

1.6. Thesis Focus

This dissertation will focus on the study of a series of thiourea catalysts bearing charged substituents and weakly coordinating anions. Their synthesis, characterization and utility will be discussed in detail in the following chapters. The initial report of electrostatically enhanced thioureas and their catalytic activities compared to neutral analogs in three organic transformations are shown in Chapter 2. The family of electrostatically enhanced thioureas is expanded in Chapter 3, and a UV spectroscopic

approach is introduced to gauge their reactivity. Chapter 4 deals with the application of charged thioureas in the catalytic cycloaddition of CO_2 with styrene oxide. In Chapter 5, a series of charged thioureas bearing chiral indanol substituents are utilized to catalyze the enantioselective Friedel−Crafts reaction of β-nitrostyrene with indole.

Chapter 2. Electrostatically Enhanced Thioureas*

Small molecule metal-free hydrogen bond catalysis has become an active and vibrant research area over the past two decades.[1] Numerous classes of compounds have been explored including BINOLs,[2] silane diols,[3] squaramides[1e,4] and a,a,a,a-tetraaryl-1,3-dioxolane-4,5-dimethanols (TADDOLs)[5] among others, but no species have received more attention than thioureas.[6] Of these, *N*,*N*'-bis(3,5-bis(trifluoromethyl)phenyl)thio-urea [$(3,5\text{-}(CF_3)_2C_6H_3NH)_2CS$], also known as Schreiner's thiourea,[7] occupies a privileged position because it is an especially effective catalyst leading to relatively rapid transformations. This has been attributed to its enhanced acidity due to the four electron withdrawing trifluoromethyl groups[8] and weak C–H···S hydrogen bonds that are thought to play a factor in stabilizing the reactive *Z*,*Z*-conformer.[7b,c]

Cationic hydrogen bond donors such as amidinium,[9] ammonium,[10] guanidinium,[11] pyridinium,[12] and quinolinium[13] ions also have been extensively explored.[14] These species correspond to protonated neutral bases and consequently are more acidic than their corresponding conjugate bases. This may account for their enhanced reactivities, but conformational rigidity, changes in the binding site, and the potential use of an additional hydrogen bond are also important contributing effects. A different strategy for increasing the reactivity of neutral hydrogen bond catalysts, especially in nonpolar solvents where organic transformations of this sort are typically carried out, is to incorporate a charged

*Fan, Y.; Kass, S. R. Electrostatically Enhanced Thioureas. *Org. Lett.* **2016**, *18*, 188-191. Copyright ACS. Reproduced with permission.

center without introducing a new hydrogen bond site. A recent report by Berkessel et al. exploiting this novel approach to develop Coulombic anion-binding catalysts,[15] and our observation that the catalytic ability of a phenol can be enhanced by orders of magnitude by the presence of a charged site[16] suggests that electrostatic enhancement of hydrogen bond catalysts is a new general design strategy.[17]

To explore this hypothesis, thioureas with one and two *N*-methyl pyridinium ion centers were prepared and their reactivities in several different types of transformations were examined. These new catalysts were compared to *N*,*N*'-diphenylthiourea (**1**) and Schreiner's thiourea (**2**) (Figure 1) and are found to be orders of magnitude more reactive in nonpolar solvents.[18]

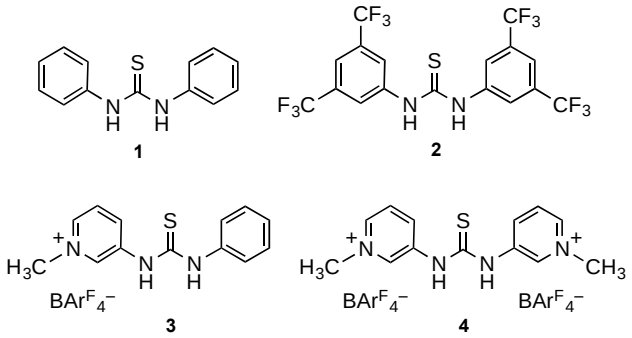

Figure 1. Thiourea catalysts employed in this work.

Mono and di *N*-methylpyridinium ions **3** and **4** were readily synthesized starting with commercially available 3-amino-pyridine (**5**) as illustrated in Figure 2. Thiophosgene was used to convert this amine into its isothiocyanate,[19] and this product was subsequently alkylated with methyl iodide to afford the corresponding pyridinium ion **7**. This key intermediate was reacted with aniline to afford the iodide salt of **3** (**3I**). Alternatively,

methylation of 3-aminopyridine occurs at the more nucleophilic ring nitrogen atom,[20] and the resulting pyridinium iodide **8** was reacted with **7** to yield the doubly charged thiourea derivative of **4** (**4I**). Both iodide salts have limited solubilities in weakly polar solvents

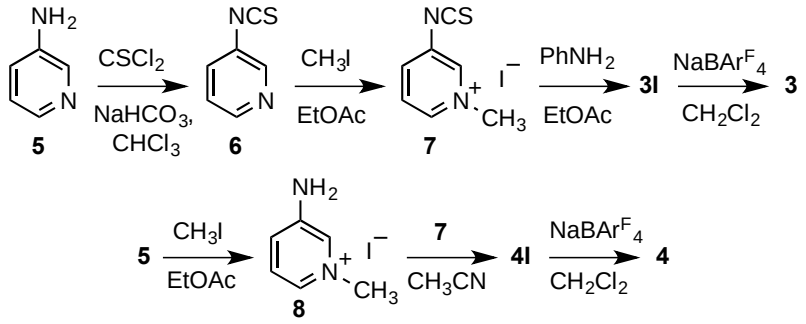

Figure 2. Synthetic routes for thioureas **3** and **4**.

and presumably form deactivating NH···I⁻ hydrogen bonds so they were converted to their tetrakis(3,5-bis(trifluoromethyl)phenyl)borate (BAr^F_4) salts **3** and **4**. These metathesis reactions were readily accomplished by stirring **3I** or **4I** with $NaBAr^F_4$ in CH_2Cl_2.

To evaluate the catalytic activity of electrostatically enhanced thioureas **3** and **4**, the Friedel–Crafts alkylation of *trans*-β-nitrostyrene with *N*-methylindole was examined in $CDCl_3$ at room temperature (eq 1). This transformation was chosen because the reaction

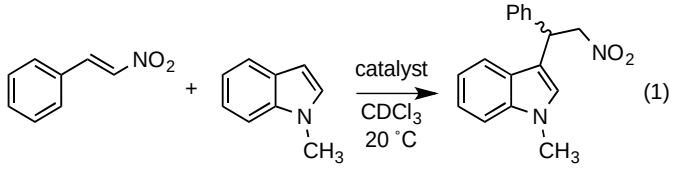

rate has been observed to correlate with the acidity of hydrogen bond catalysts whereas acetic acid does not promote this process.[21,22] Second-order rate constants were determined by monitoring the reaction via ^{1}H NMR spectroscopy and the data are

summarized in Table 1. Diphenylthiourea **1** is a poor catalyst in that it only speeds up the uncatalyzed process by a factor of 1.4 and more than a month is needed for half of the starting material to be converted to product. Schreiner's thiourea is 28 times more effective than **1**, but this transformation is still slow and has a half-life of 29 hours. *N*-Methylpyridinium ion containing thioureas **3** and **4** are much more active than **2** and have half-lives of 5 hours and 4 minutes, respectively. An acidic impurity in **3** or **4** acting as the active catalyst was discounted since 1 mol % of *p*-toluenesulfonic acid (*p*-TsOH) did not afford any observable product by ^{1}H NMR over 20 h. These results indicate that the one charged center in **3** is more effective than the four CF_3 groups in **2** by a factor of 7, and that the presence of two cationic sites affords an even more active catalyst that is 400 times more reactive.

Table 1. Kinetic data for the room temperature Friedel–Crafts reaction of *trans*-β-nitrostyrene with *N*-methylindole.

entry	cat.	mol%	solvent	k (M^{-1} h^{-1})	$t_{1/2}$ (h)	k_{rel}
1			$CDCl_3$	2.8 x 10^{-3}	1,100	
2	**1**	10	$CDCl_3$	3.9 x 10^{-3}	820	0.035
3	**2**	10	$CDCl_3$	1.1 x 10^{-1}	29	1.0
4	**3**	10	$CDCl_3$	7.1 x 10^{-1}	4.5	6.5
5	**4**	10	$CDCl_3$	45	0.071 (4.3 m)	410
6	**4**	5	$CDCl_3$	11	0.29 (17 m)	
7	**4**	2.5	$CDCl_3$	9.1 x 10^{-1}	3.5	
8	**4**	1	$CDCl_3$	1.6 x 10^{-2}	200	
9	**4**	5	$C_6D_5CD_3$	14	0.23 (14 m)	
10	**4**	5	CD_2Cl_2	55	0.058 (3.5 m)	

Catalyst loading was explored for **4** (Table 1, entries 5-8) and as expected the Friedel-Crafts reaction rate increases with the amount of added catalyst. A linear dependence was not observed but a straight line was obtained from a plot of the second-order rate constants versus the square of the catalyst concentrations (Figure 3). This suggests that the dimer of **4** is the active catalyst in this transformation which is consistent with a previous report on thiourea catalysts.[23]

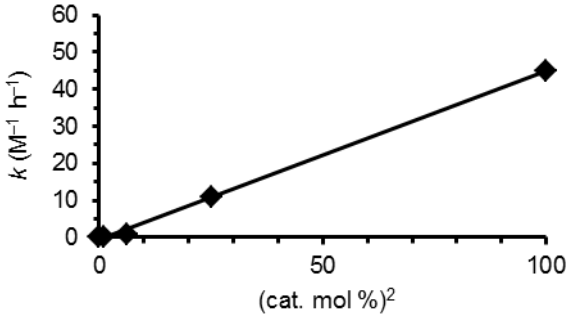

Figure 3. A linear least squares fit of the second-order Friedel–Crafts rate constants vs. (cat. %)^2; k = 0.46(cat. %)^2 - 0.70, r^2 = 0.999; Table 1 entries 5-8.

Carrying out the Friedel–Crafts alkylation in a few different solvents was also examined. Little impact was noted by switching from $CDCl_3$ to toluene-d_8, but a 5-fold increase was observed when the reaction was carried out in CD_2Cl_2. All three of these solvents have dielectric constants of less than 10, but the most polar one of these leads to the fastest transformation. This may be a reflection of the aggregation state of **4** in these solvents. In any case, the doubly charged thiourea salt is soluble in nonpolar media and displays excellent performance characteristics.

We next turned our attention to the Diels–Alder reaction between cyclopentadiene and methyl vinyl ketone (eq 2), in part because Schreiner's thiourea previously has been

reported to catalyze this transformation.[7b] At room temperature in $CDCl_3$ with 1 mol % of the catalyst, **2** accelerates this cycloaddition by less than a factor of 1.5 relative to the uncatalyzed process (Table 2). In contrast, the charge containing thioureas **3** and **4** enhance the background-corrected rates by one and two orders of magnitude,respectively. The half-life for the latter transformation is also under 4 minutes. As for the selectivity, the major product is the *endo* isomer in each instance as expected. Its relative contribution, however, increases from 71% for the uncatalyzed process to 81% with Schreiner's thiourea and 88% when either **3** or **4** is used.

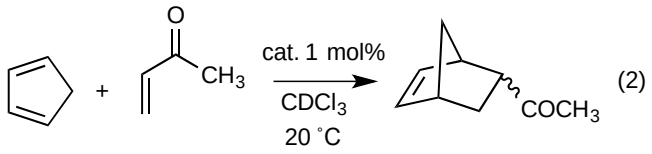

Table 2. Diels–Alder kinetic data.

entry	cat.	k (M^{-1} h^{-1})	$t_{1/2}$	k_{rel}[a]	*endo*:exo
1		0.72	2.2 h		71:29
2	**2**	1.0	1.6 h	1.0	81:19
3	**3**	7.3	13 m	24	88:12
4	**4**	28	3.5 m	97	88:12

[a]Corrected for the rate of the uncatalyzed reaction.

Lastly, the ring-opening aminolysis of styrene oxide with aniline was explored under solvent free conditions (SFC, eq 3). Product formation was monitored for each transformation and zero and first-order processes were found to fit the data depending upon which catalyst, if any, was used. Consequently, qualitative results are reported (Table 3), but it is apparent that **3** and **4** are much more effective catalysts than **2**. That is,

significantly higher selectivities and greater conversions are observed (e.g., **4** gives a 93% conversion in 0.5 h whereas only 39% of the starting material has reacted in 2.33 h with **2**). The dicharged thiourea was also found to outperform **2** even when 10 times less was used (i.e., 0.1 mol % of **4** led to a 53% conversion in 0.5 h whereas 39% of the reactant went on to product in 2.33 h with 1 mol % of **2**).[24]

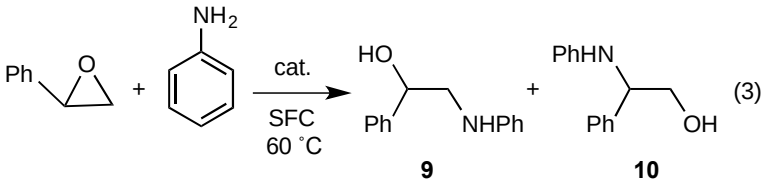

Table 3. Catalytic results for the solvent free aminolysis of styrene oxide with aniline.

entry	cat.	mol%	*t* (h)	% conv	**9** : **10**
1			2.33	5.8	38:62
2	**2**	1	2.33	39	35:65
3	**3**	1	2.33	55	13:87
4	**4**	1	0.5	93	10:90
5	**4**	0.1	0.5	53	10:90

Charged substituents are not especially effective in enhancing acidities and lowering pK_a values in polar solvents.[16,25] Based upon the 2.4 and 1.3 pK_a unit acidifying effect of a *m*-CF_3 group on phenol and *N*,*N*'-diphenylthiourea,[8,26] respectively and the recently measured 5.5 pK_a difference between phenol and 3-hydroxy-*N*-octylpyrinium ion[16] all in dimethyl sulfoxide (DMSO), one can estimate that pK_a(**3**) = 10.4.[27] This value is essentially the same as incorporating two meta trifluoromethyl groups into **1** and consequently **3** is ~2 pK_a units less acidic than Schreiner's thiourea.[8] In nonpolar solvents, a reversal in their relative acidities undoubtedly takes place. As a result, incorporation of

a single positively charged center into a thiourea without adding a new hydrogen bond site was found to be catalytically more effective than the four electron withdrawing trifluoromethyl groups in Schreiner's thiourea.[28] Addition of a second ionic center presumably enhances the DMSO acidity of **4** so that it is similar to **2** but leads to rate accelerations of ~10^2 - 10^3. These results represent a new strategy for activating hydrogen bond catalysts, and a potential means for improving stereoselectivities since lower temperatures typically can be employed when transformations occur more rapidly at room temperature.[29]

2.1. Experimental

General. All solvents and reagents were purchased from Sigma Aldrich and Alfa Aesar except for tetrakis-(3,5-bis(trifluoromethylphenyl)borate ($NaBAr^F_4$) and the deuterated solvents which came from Matrix Scientific and Cambridge Isotope Laboratories, respectively. These materials were used as received without further purification. Glassware including flasks, vials, syringes and NMR tubes was oven dried. TLC analyses were carried out with Merck precoated 250 mm silica gel 60 F-254 plates and were visualized with a hand held UV lamp. Medium pressure liquid chromatography was carried out with a Biotage Isolera 1 using silica gel columns (Sorbent technology's premium R_f silica gel, 60 Å, 40-75 um). Uncorrected melting points were determined with a Thomas Hoover Uni-Melt apparatus in unsealed tubes. Proton and ^{13}C NMR spectra were obtained with Varian VI 300 and 500 MHz instruments, and chemical shifts are given in ppm and were referenced as follows: ^1H spectra, 7.26 ($CHCl_3$), 5.32

($CHDCl_2$), 2.50 (CHD_2SOCD_3), 2.08 ($C_6D_5CHD_2$) and 1.94 d (CHD_2CN); ^{13}C spectra, 77.2 ($CDCl_3$), 53.8 (CD_2Cl_2), 39.5 ($(CD_3)_2SO$) and 1.3 d (CD_3CN). IR spectra were recorded with an ATR iD5 source on a Nicolet iS5 FT-IR and high resolution mass data were obtained with a Bruker ESI-BioTOF instrument using methanol and acetonitrile solutions and polyethylene glycol as an internal standard.

3-Isothiocyanatopyridine (**6**).[19] 3-Aminopyridine (2.0 g, 21 mmol) was dissolved in 50 mL of chloroform and an equal volume of saturated aqueous $NaHCO_3$ was added at room temperature. The resulting solution was stirred and 2.0 mL (26 mmol) of thiophosgene in 20 mL of $CHCl_3$ was added dropwise. After 1.5 h, the reaction mixture was filtered and the aqueous layer was extracted twice with 25 mL portions of $CHCl_3$. The combined organic material was dried over anhydrous $MgSO_4$ and concentrated under reduced pressure with a rotary evaporator. Medium pressure liquid chromatography of the residue (10 : 90 to 50 : 50 ethyl acetate/hexanes) afforded 2.0 g (69%) of **6** as a brown oil (R_f = 0.18 in 10 : 90 ethyl acetate/hexanes). ^1H NMR (500 MHz, $CDCl_3$) δ 8.54 (d, J = 2.1 Hz, 1H), 8.51 (dd, J = 1.5 and 4.9 Hz, 1H), 7.53 (ddd, J = 1.5, 2.1 and 8.4 Hz, 1H), 7.32 (dd, J = 4.9 and 8.4 Hz, 1H). ^{13}C NMR (126 MHz, $CDCl_3$) δ 147.6 147.1, 139.1, 132.3, 129.5, 123.9. IR (ATR source), 2980, 2020, 1575, 1417, 1372, 1240, 800 cm^{-1}. HRMS-ESI: calcd for $C_6H_5N_2S$ $(M + H)^+$ 137.0168, found 137.0176.

3-Isothiocyanato-1-methylpyridinium iodide (**7**). In a 6 dram vial, 0.20 g (1.47 mmol) of 3-isothiocyanatopyridine was dissolved in 2 mL of ethyl acetate and 0.18 mL (2.89

mmol) of methyl iodide was added dropwise at room temperature under argon. The reaction mixture was allowed to stir overnight and the resulting precipitate was filtered, washed with 5 mL of ethyl acetate and dried under vacuum to afford 0.25 g (61%) of **7** as a pale yellow solid (mp 132 – 135 ˚C). ^{1}H NMR (300 MHz, DMSO-d_6) δ 9.32 (s, 1H), 8.93 (d, J = 6.0 Hz, 1H), 8.62 (d, J = 9.0 Hz, 1H), 8.17 (dd, J = 6.0 and 9.0 Hz, 1H), 4.32 (s, 3H). ^{13}C NMR (75 MHz, DMSO-d_6) δ 143.6 141.5, 141.3, 131.7, 128.1, 107.4, 48.2. IR (ATR source), 2082, 1496, 1291, 1160, 809 cm^{-1}. HRMS-ESI: calcd for $C_7H_7N_2S$ (M – I)$^+$ 151.0324, found 151.0333.

3-Amino-1-methylpyridinium iodide (**8**).[20] 3-Aminopyridine (2.0 g, 21 mmol) was dissolved in 10 mL of ethyl acetate in a 6 dram vial at room temperature under an inert atmosphere. Methyl iodide (2.7 mL, 43 mmol) was added dropwise with stirring and the reaction was allowed to proceed overnight. The resulting precipitate was filtered, washed with 5 mL of ethyl acetate and dried under vacuum to give 4.6 g (92%) of **8** as a white solid (mp 118 – 121 ˚C). ^{1}H NMR (300 MHz, DMSO-d_6) δ 8.06 (d, J = 5.9 Hz, 1H), 7.98 (t, J = 2.2 Hz, 1H), 7.68 (dd, J = 5.8 and 8.5 Hz, 1H), 7.55 (dd, J = 2.2 and 8.9 Hz, 1H), 6.62 (s, 2H), 4.18 (s, 3H). ^{13}C NMR (75 MHz, DMSO-d_6) δ 148.1, 131.7, 128.8, 127.6, 126.7, 47.9. IR (ATR source) 3352, 3283, 3185, 1508, 1484, 1321, 1167, 794, 669. HRMS-ESI: calc for $C_6H_9N_2^+$ (M – I)$^+$ 109.0760, found 109.0771.

1-Methyl-3-(3-phenylthioureido)pyridinium iodide (**3I**). In a 6-dram vial, 0.15 g (0.54 mmol) of 3-isothiocyanato-1-methylpyridinium iodide was dissolved in 3 mL of CH_3CN

under argon. Aniline (55 μL, 0.60 mmol) was added dropwise and the reaction mixture was allowed to stir overnight at room temperature. A minimal amount of a 1 : 1 mixture of ethyl acetate and pentane was subsequently added (~ 3mL) and the resulting precipitate was filtered, washed with 5 mL of ethyl acetate and dried under vacuum to afford 0.14 g (70%) of **3I** as a yellow solid (mp 163 – 167 ˚C). ^{1}H NMR (300 MHz, DMSO-d_6) δ 10.57 (s, 1H), 10.43 (s, 1H), 9.25 (s, 1H), 8.69 (d, J = 5.9 Hz, 1H), 8.55 (d, J = 9.5 Hz, 1H), 8.06 (dd, J = 6.2 and 8.8 Hz, 1H), 7.43 (m, 4H), 7.23 (m, 1H), 4.34 (s, 3H). ^{13}C NMR (126 MHz, DMSO-d_6) δ 180.0, 140.2, 140.1, 139.8, 138.4, 138.3, 128.8, 126.9, 125.6, 124.2, 48.2. IR (ATR source) 3061, 1552, 1494, 1322, 1194, 756. HRMS-ESI: calc for $C_{13}H_{14}N_3S^+$ $(M - I)^+$ 244.0903, found 244.0907.

1,3-bis-3-(1-Methylpyridylium)thiourea iodide (**4I**). 3-Isothiocyanato-1-methylpyridinium iodide (0.10 g, 0.36 mmol) was dissolved in 3 mL of CH_3CN under an inert atmosphere at room temperature in a 6-dram vial. 3-Amino-1-methylpyridinium iodide (85 mg, 0.36 mmol) was added and the resulting solution was stirred at room temperature overnight. The resulting precipitate was filtered and washed with 5 mL of CH_3CN to afford 0.10 g (52%) of **4I** as a pale yellow solid (mp 192 – 194 ˚C). ^{1}H NMR (300 MHz, DMSO-d_6) δ 11.09 (br s, 2H), 9.23 (s, 2H), 8.79 (d, J = 6.0 Hz, 2H), 8.60 (d, J = 8.7 Hz, 2H), 8.13 (dd J = 6.0 and 8.7 Hz, 2H), 4.38 (s, 6H). ^{13}C NMR (126 MHz, DMSO-d_6) δ 181.1, 141.4, 140.6, 139.2, 138.9, 127.3, 48.4. IR (ATR source) 2977, 1565, 1498, 1317, 1220, 747. HRMS-ESI: calc for $C_{13}H_{15}N_4S^+$ $(M - H - 2I)^+$ 259.1007, found 259.1014 and calc for $C_{13}H_{16}N_4S^{2+}$ $(M - 2I)^{2+}$ 130.0542, found 130.0564.

1-Methyl-3-(3-phenylthioureido)pyridinium tetrakis(3,5-bis(trifluoromethyl)phenyl)-borate (**3**). To a 6 dram vial, 24 mg (27 μmol) of sodium tetrakis(3,5-bis(trifluoromethyl)phenyl)borate, 10 mg (27 μmol) of 1-methyl-3-(3-phenylthio-ureido)pyridinium iodide and 1 mL of CH_2Cl_2 were added. This mixture was stirred at room temperature under an argon atmosphere until the solid material was totally dissolved and a cloudy suspension formed. Stirring was then stopped and the solution was left undisturbed until a white solid precipitated and a clear solution formed. The reaction mixture was then filtered and concentrated under reduced pressure to afford 25 mg (84%) of **3** as a yellow solid (mp 140 – 144). ^{1}H NMR (500 MHz, CD_2Cl_2) δ 9.91 (s, 1H), 8.40 (br s, 1H), 8.11 (m, 2H), 8.03 (br s, 1H), 7.83 (t, J = 6.5 Hz, 1H), 7.73 (s, 8H), 7.56 (s, 4H), 7.54 (t, J = 7.5 Hz, 2H), 7.46 (t, J = 7.5 Hz, 1H), 7.37 (d, J = 8.0 Hz, 2H), 4.35 (s, 3H). ^{13}C NMR (126 MHz, CD_2Cl_2) δ 179.4, 162.1 (q, $^{1}J_{B\text{-}C}$ = 49.2 Hz), 141.1, 139.2, 138.7, 138.6, 138.1, 135.2 (d, $^{2}J_{B\text{-}C}$ = 31.3 Hz), 131.0, 130.7, 129.3 (qq, $^{3}J_{B\text{-}C}$ = 2.8 Hz and $^{2}J_{F\text{-}C}$ = 36.1 Hz), 128.5, 126.3, 125.0 (q, $^{1}J_{F\text{-}C}$ = 273 Hz), 117.9 (d, $^{3}J_{F\text{-}C}$ = 37.2 Hz), 49.7. IR (ATR source) 3356, 1354, 1273, 1109, 888, 682. HRMS-ESI: calc for $C_{13}H_{14}N_3S^+$ $(M - C_{32}H_{12}BF_{24}^-)^+$ 244.0903, found 244.0912 and calc for $C_{32}H_{12}BF_{24}^-$ $(M - C_{13}H_{14}N_3S^+)^-$ 863.0654, found 863.0669.

1,3-bis-3-(1-Methylpyridylium)thiourea tetrakis(3,5-bis(trifluoromethyl)phenyl)borate (**4**). To a 6 dram vial, 34 mg (39 μmol) of sodium tetrakis(3,5-bis(tri-fluoromethyl)phenyl)borate, 10 mg (19 μmol) of 1,3-bis-3-(1-methylpyridylium)thiourea iodide and 1 mL of CH_2Cl_2 were added. This heterogeneous solution was stirred at room temperature

under an inert atmosphere until the solids totally dissolved and a cloudy suspension formed. Stirring was then stopped and the resulting mixture was left alone until a white solid precipitated and a clear solution resulted. It was then filtered and concentrated under reduced pressure to afford 32 mg (85%) of **4** as a pale yellow solid (mp 68 – 72 ˚C). ^{1}H NMR (500 MHz, CD_2Cl_2) δ 10.39 (br s, 2H), 9.76 (s, 2H), 8.45 (d, J = 8.7 Hz, 2H), 8.17 (d, J = 6.3 Hz, 2H), 7.86 (dd, J = 5.9 and 8.5 Hz, 2H), 7.72 (s, 16H), 7.55 (s, 8H), 4.34 (s, 6H). ^{13}C NMR (126 MHz, CD_2Cl_2) δ 179.2, 162.2 (q, $^{1}J_{B\text{-}C}$ = 49.3 Hz), 140.3, 140.1, 138.4, 135.2 (d, $^{2}J_{B\text{-}C}$ = 25.6 Hz), 129.3 (qq, $^{3}J_{B\text{-}C}$ = 2.1 Hz and $^{2}J_{F\text{-}C}$ = 31.2 Hz), 129.0, 128.8, 125.0 (q, $^{1}J_{F\text{-}C}$ = 273 Hz), 118.0 (d, $^{3}J_{F\text{-}C}$ = 28.6 Hz), 50.1. IR (ATR source) 1507, 1353, 1272, 1110, 886, 688 cm^{-1}. HRMS-ESI: calc for $C_{13}H_{15}N_4S^+$ (M – H – $2(C_{32}H_{12}BF_{24})^-)^+$ 259.1007, found 259.0989 and calc for $C_{32}H_{12}BF_{24}^-$ (M – $C_{13}H_{16}N_4S^{2+}$ – $C_{32}H_{12}BF_{24}^-)^-$ 863.0654, found 863.0638.

Friedel–Crafts reactions. Oven-dried NMR tubes were charged with 0.0075 g (0.050 mmol) of *trans*-β-nitrostyrene, 19 ml (0.15 mmol) of *N*-methylindole and the desired amount of catalyst in 0.6 mL of a deuterated solvent at room temperature under an inert atmosphere. Reaction progress was monitored by ^{1}H NMR using signals for *trans*-β-nitrostyrene (8.04 δ ($CDCl_3$ and CD_2Cl_2) and 7.43 δ (toluene-d_8)) and the alkylation product (5.23 δ ($CDCl_3$), 5.18 δ (CD_2Cl_2) and 5.00 (toluene-d_8)). Second-order rates constants and the first half-lifes of the limiting reagent were obtained using the integrated rate law (i.e., ln([*N*-methylindole][β-nitrostyrene]$_o$/[β-nitro-styrene][*N*-methylindole]$_o$) = k([*N*-methylindole]$_o$ – [β-nitrostyrene]$_o$)t) where [β-nitrostyrene]$_o$ and [*N*-methylindole]$_o$

are the initial concentrations and [β-nitrostyrene] and [*N*-methylindole] are the concentrations at different times.

Diels–Alder transformations. Freshly prepared solutions of cyclopentadiene (25 μL, 0.30 mmol), methyl vinyl ketone (8.1 μL, 0.10 mmol) and 1 mol% of the catalyst were dissolved in 0.60 mL of $CDCl_3$ at room temperature under argon in NMR tubes. Reaction progress was monitored by ^1H NMR using the signals at 6.33 (methyl vinyl ketone) and 5.86 ppm (cycloaddition products). *Endo* and *exo* product ratios were measured using their resonances at 2.14 and 2.22 ppm, respectively while the second-order rate constants and half lifes were determined as described for the Friedel–Crafts reaction.

Aminolyses of styrene oxide. In a 3 dram vial, 0.093 g (1.0 mmol) of aniline, 0.12 g (1.0 mmol) of styrene oxide and 0.1 or 1.0 mol% of the desired catalyst were added under argon at 60 ˚C. Aliquots were removed at select times and diluted with 1 mL of $CDCl_3$ to monitor the reaction progress. Proton NMR chemical shifts at 4.97, 4.52 and 2.83 ppm corresponding to **9**, **10**, and styrene oxide, respectively were used for this purpose.

Chapter 3. Quantification of Catalytic Activity for Electrostatically Enhanced Thioureas via Reaction Kinetics and a UV-Vis Spectroscopic Measurement*

3.1. Introduction

Nature exploits noncovalent interactions such as hydrogen bonds to reduce the activation energy barriers of enzyme-catalyzed chemical transformations.[1] A wealth of small-molecule organocatalysts that mimic this behavior have been developed over the past two decades and this field has emerged as a fast-growing research area.[2] Metal-free catalysts that use hydrogen bonds most commonly activate electrophiles towards nucleophilic attack by lowering their LUMO energies to enhance the overall reaction rates, but other pathways have been proposed and are operational.[3]

Thioureas are a widely used class of hydrogen bond donors that can simultaneously provide two N−H activating sites.[4] Of these compounds, incorporation of four electron withdrawing trifluoromethyl groups into *N*,*N*'-diphenylthiourea (**1**) to afford *N*,*N*'-bis(3,5-bis(trifluoro-methyl)phenyl)thiourea (**2**, Schreiner's thiourea)[5] is regarded as a seminal contribution. This is due to the enhanced acidity of the latter compound, the generally assumed stabilization of its active *Z*,*Z*-conformer via internal C−H···S hydrogen bonds, an increase in solubility in nonpolar media and the significantly greater reactivity observed when **2** is used.[6] As a result, the 3,5-bis(trifluoromethyl)phenyl ring has been

*Fan, Y.; Kass, S. R. Quantification of Catalytic Activity for Electrostatically Enhanced Thioureas via Reaction Kinetics and a UV-Vis Spectroscopic Measurement. *J. Org. Chem.* Submitted.

incorporated into most thiourea catalysts and occupies a privileged position in the field of organocatalysis.[7]

Inspired by the use of Schreiner's thiourea and the wealth of chiral variants, we recently reported on the synthesis and reactivity of several electrostatically enhanced thioureas that possess one or two activating *N*-methylpyridinium ion centers along with an appropriate noncoordinating counteranion (3 and 4, Figure 1).[8] These compounds were found to outperform Schreiner's thiourea in several organic transformations by leading to rate enhancements of 1–3 orders of magnitude without changing the hydrogen

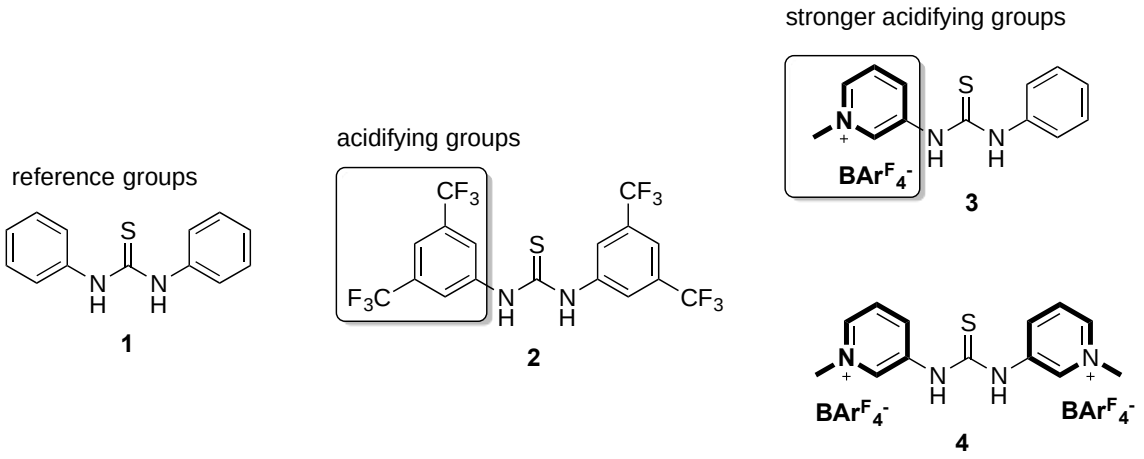

Figure 1. *N*,*N*'-Diphenylthiourea (**1**), Schreiner's thiourea (**2**), and charged thiourea salts **3** and **4**, where $BAr^{F}_{4}{}^{-} = (3,5\text{-}(CF_3)_2C_6H_3)_4B^{-}$.

bonding arrangement of the catalyst. As they also can be readily prepared, and a chiral variant was found to give good enantioselectivities while still maintaining the enhanced activity,[9] a quick and direct manner for quantitatively assessing their catalytic abilities in nonpolar media was sought.

A variety of different types of hydrogen bond donating catalysts have been developed and their measured pK_a values in DMSO commonly are used as a guide to their activity.[10] That is, for related compounds, more acidic derivatives typically are found to be more reactive catalysts. Substituent effects in a polar aprotic medium, however, need not be the same as in nonpolar solvents, and it is the latter conditions that are usually employed with hydrogen bond catalysts. Other physical measures for structure-reactivity relationships therefore might be more valuable. Building upon the work of Reed et al.,[11] we reported an IR method for determining the acidities of phenols in carbon tetrachloride by comparing the free O–H stretch with the lower frequency band resulting from the formation of a O–H···$NCCD_3$ hydrogen bond upon addition of a small amount of acetonitrile-d_3.[12] The resulting frequency shifts of twenty *meta*- and *para*-substituted phenols were found to better correlate with their gas-phase acidities (ΔG°_{acid}) than their DMSO pK_a values. This approach is more challenging when the Brønsted acid is a double hydrogen bond donor, however, especially if there is conformationally flexibility as is the case for thioureas.

To our delight, Kozlowski et al. recently reported a colorimetric sensor molecule, 7-methyl-2-phenylimidazo[1,2a]pyrazine-3(7H)-one (**S**, Figure 2) for quantitatively determining the electrophilic activating ability of a large number (i.e., 33 compounds) of single and double hydrogen bond donors with different structural motifs.[13] In this approach, **S** is titrated with a hydrogen bond donor HY in dichloromethane and UV-Vis spectra are recorded over the course of this process. The absorption maxima (λ_{max}) of the resulting hydrogen bonded complexes **S**···HY empirically were found to be blue shifted

to lower wavelengths, and the inverse of the change relative to the unbound sensor ($\Delta\lambda_{max}^{-1}$) correlate with the logarithm of the equilibrium association constant (K) and catalyzed reaction rate constants (*k*).

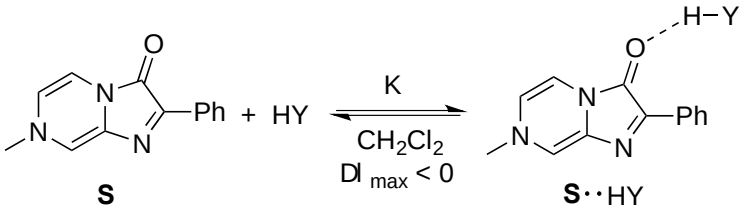

Figure 2. UV-Vis sensor **S** which is responsive to hydrogen bond interactions with Brønsted acids HY.

In this contribution we report kinetic data for Friedel−Crafts alkylations of *N*-methylindole with *trans*-β-nitrostyrene catalyzed by a variety of charged thiourea salts. Solvent effects, catalyst loading and substrate scope were also investigated with our most active thiourea derivative. In addition, the UV-Vis method reported by Kozlowski et al. was successfully applied to a series of 10 thioureas and a good correlation between their catalytic activity and hydrogen bond donating ability was observed.

3.2. Results and Discussion

Based upon recent communications dealing with electrostatically enhanced thioureas and phosphoric acids,[8,14] a series of thourea derivatives with one and two *N*-alkylpyridinium ion centers (**3-10**, Figure 3) were synthesized from commercially available arylamines. These compounds differ in their structural symmetry, alkyl chain

length and the identity of the counteranion, and were prepared by reacting *N*-alkylated isothiocyanates (which were readily obtained from their corresponding amines) with an *N*-alkylated aminopyridine or aniline (Scheme 1).[8] The final step in this process was the exchange of an iodide or triflate anion to a tetrakis(3,5-bis(trifluoromethyl)phenyl)borate

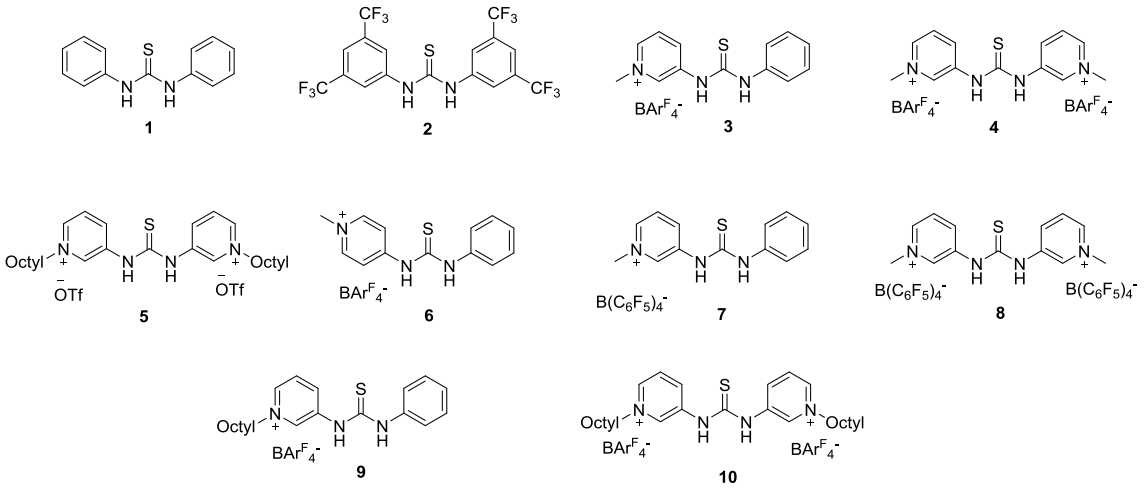

Figure 3. Thiourea catalysts screened in this work.

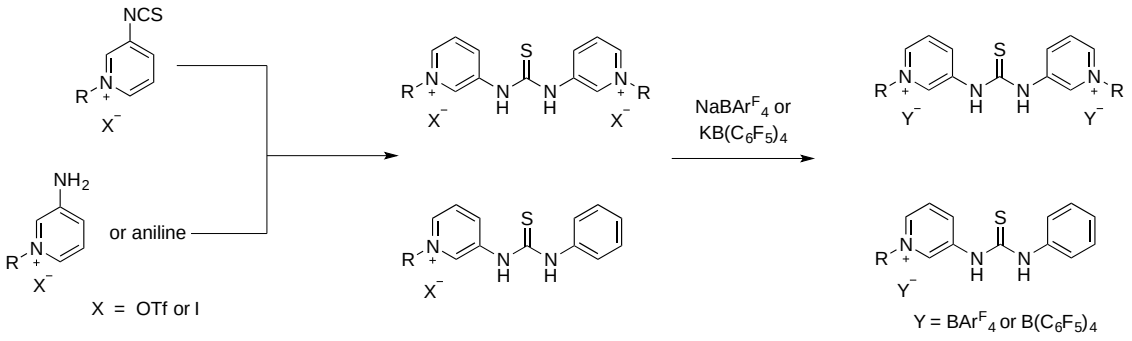

Scheme 1. General synthetic route for the preparation of thioureas **3-10**.

($BAr^F_4^-$) or tetrakis(pentafluorophenyl)borate ($B(C_6F_5)_4^-$) counterion. This transformation was readily accomplished by stirring the thiourea precatalyst in dichloromethane with the

sodium or posttasium salt of the tetraarylborate anion and subsequently filtering away the insoluble NaX (X = I or OTf) salt. This anion interchange is critical as the iodide salts typically are poorly soluble in nonpolar solvents such as CH_2Cl_2 and both the iodides and triflates are much less active catalysts, presumably due to the formation of NH···I^- and NH···$OSO_2CF_3^-$ hydrogen bonds.

To evaluate the catalytic activity of *N*-alkylpyridinium ion containing thiourea salts **3-10** along with noncharged reference compounds **1** and **2**, the Friedel−Crafts alkylation of *N*-methylindole with *trans*-β-nitrostyrene (eq. 1) was examined. This transformation was selected because it has been well-studied and reaction rates with Brønsted acid and hydrogen bond catalysts have been found to correlate with their acidities.[15] Second-order rate constants and the first reaction half-lifes were determined in $CDCl_3$ at room temperature with a 10 mol% catalyst loading via ^{1}H NMR spectroscopy (Table 1).

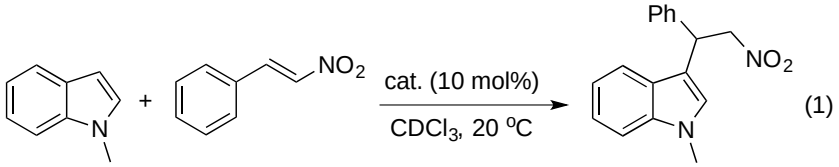

(1)

The uncatalyzed reaction is extremely slow and takes more than a month for half of the *trans*-β-nitrostyrene to be consumed (entry 1). Diphenylthiourea (**1**) is an ineffective catalyst in that the reaction rate is only 40% larger than the background process and a month is still needed to convert 50% of the limiting reagent (i.e., *trans*-β-nitrostyrene) to the product (entry 2). Schreiner's thiourea (**2**), which was reported as a good catalyst for this transformation,[16] is much better than **1** (entry 3), but still requires more than a day to

Table 1. Reactivity data for the Friedel–Crafts alkylation of *N*-methylindole with *trans*-β-nitrostyrene catalyzed by thiourea catalysts **1-10**.[a]

entry	catalyst	k (M^{-1} h^{1})	$t_{1/2}$ (h)	k_{rel}
1		0.0028	1,100	
2	**1**	0.0039	820	0.010[b]
3	**2**	0.11	29	1.0
4	**3**	0.71	4.5	6.5
5	**4**	45	0.071 (4.3 min)	400
6	**5**	0.0048	640	0.018[b]
7	**6**	1.0	3.1	9.1
8	**7**	0.33	9.3	3.0
9	**8**	8.1	0.38 (23 min)	74
10	**9**	2.4	1.3	22
11	**10**	18	0.17 (10 min)	160

[a]These reactions were carried out in NMR tubes with *N*-methylindole and *trans*-β-nitrostyrene concentrations of 250 and 83 mM, respectively. [b]This value is corrected for the uncatalyzed reaction rate.

convert half of the *trans*-β-nitrostyrene to product under the employed reaction conditions. The *N*-alkylpyridinium containing thioureas were found to be much more active than **2**. One charged site makes **3** a more active catalyst than Schreiner's thiourea by a factor of 7 (entry 4). Incorporation of a second charged site in **4** leads to the most effective catalyst of the examined series corresponding to a 400-fold rate acceleration relative to **2**, and a reaction half-life of just 4 min (entry 5). Catalyst **6** with the positively charged center at the *para* position outpaces its *meta* analogue **3** (entry 7) presumably because conjugation makes this derivative more acidic. When the $BAr^{F}_{4}{}^{-}$ counteranion is switched to $B(C_6F_5)_4{}^{-}$, this leads to a decrease in catalytic activity as reflected by the

performances of **7** and **8** (entries 8 and 9) compared to those of **3** and **4**, respectively. A much greater decrease is observed when $CF_3SO_3^-$ is used as the counterion (entry 6) as **5** is found to be less active than Schreiner's thiourea and only marginally better than diphenyl thiourea. This deactivation of the catalyst can be attributed to one or two $NH\cdots OSO_2CF_3^-$ hydrogen bonds and emphasizes the importance of a weakly coordinating anion as the counterion. Finally, when *N*-octyl substituents are used instead of methyl groups, this leads to a rate enhancement of a factor of 3 for the mono charged species (i.e., **9** vs **3** (entries 10 and 4)) but a 2.5-fold reduction for the doubly charged thioureas (**10** vs. **4** (entries 11 and 5)). This reversal is indicative of more than one effect being involved and suggests that sterics are an issue when both aromatic rings are alkylated.

Solvent effects and catalyst loadings were also explored with **4**, the most active thiourea catalyst examined (Table 2). When the Friedel–Crafts reaction between *N*-methylindole and *trans*-β-nitrostyrene is carried out in toluene-d_8 instead of $CDCl_3$ there is little difference in the observed rates (entry 1 vs 6). A 5-fold increase is observed when CD_2Cl_2 is used as the solvent (entry 2 vs 6) presumably because it has a larger dielectric constant than toluene and chloroform but does not have a good hydrogen bond accepting

Table 2. Solvent and catalyst loading effects.

entry	**4** mol%	solvent	k ($M^{-1}h^{-1}$)	$t_{1/2}$ (h)
1	5	$C_6D_5CD_3$	14	0.23 (14 min)
2	5	CD_2Cl_2	55	0.058 (3.5 min)
3[a]	10	C_6D_6	0.95	3.2
4[b]	10	THF-d_8	no rxn	

5	10	$CDCl_3$	45	0.071 (4.3 min)
6	5	$CDCl_3$	11	0.29 (17 min)
7	2.5	$CDCl_3$	0.91	3.5
8	1	$CDCl_3$	0.016	200

[a]Catalyst **4** is only partially soluble in C_6D_6. [b]No reaction was observed after 24 h.

site. For the two other nonpolar solvents examined, benzene-d_6 is a much less effective medium and no reaction was observed after 24 h in tetrahydrofuran-d_8. These latter two results can be attributed to the limited solubility of **4** in C_6D_6 and the hydrogen bond accepting oxygen atom in THF-d_8. Catalyst loading was also explored (entries 5-8), and a linear correlation between the rate constant and the square of the catalyst concentration was found. This is indicative of a second-order dependence on the thiourea and suggests that its dimer is the catalytically active species in accord with previous findings.[8,17]

To examine the scope of the Friedel−Crafts alkylation, a series of substituted aromatic *trans*-β-nitroalkenes were explored (eq 2, Table 3). All of these reactions afforded the corresponding addition products efficiently and with excellent conversions in a 20 min time period regardless of the electron donating or withdrawing ability of the substituent. Incorporation of a methyl group at C2 in *N*-methylindole (i.e., R = CH_3 in eq. 2) also only had a small effect. These perfectly atom economical transformations are clean processes and the products are robust compounds that can be readily purified by column chromatography. All of this suggests that this reaction can be successfully scaled up, and this was accomplished by increasing the reaction scale by a factor of 10. That is, after allowing *N*-methylindole and *trans*-β-nitrostyrene to react in the presence of 10

mol% of **10** for 0.5 hr, 146 mg of the product was isolated after chromatography in an essentially quantitative yield.

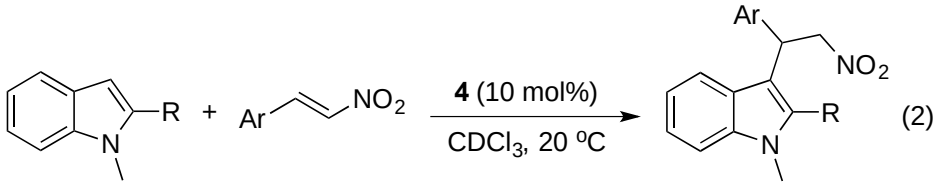

(2)

Table 3. Substrate scope for the catalytic Friedel−Crafts alkylation of *N*-methylindoles with aromatic nitroalkenes.[a]

entry	Ar	R	conversion (%)[b]
1	Ph	H	91
2	4-ClC_6H_4	H	96
3	4-BrC_6H_4	H	98
4	4-FC_6H_4	H	88
5	4-MeC_6H_4	H	92
6	4-$OMeC_6H_4$	H	83
7	4-$CF_3C_6H_4$	H	91
8	2-furyl	H	88
9	Ph	Me	86

[a]Standard reaction conditions at room temperature of 0.25 M *N*-methylindole, 0.083 M *trans*-β-nitrostyrene and 10 mol% of **4** were used. [b]Reaction conversions were obtained directly by ^{1}H NMR without isolation of the product.

All of the *N*-alkylpyridinium ion containing thiourea salts examined in this work are substantially more active catalysts for the Friedel−Crafts alkylation of *N*-methylindole with *trans*-β-nitrostyrene than *N*,*N*′-diphenyl- and Schreiner's thioureas with the

exception of **5**. This latter charged salt has two deactivating hydrogen bond accepting trifluoromethylsulfonate counteranions, and is the only *N*-alkylpyridinium substituted thiourea that was used without a non-coordinating tetraarylborate anion. To rationalize the entire reactivity order, we turned to Kozlowski's UV-Vis spectroscopy approach.[13] This method is carried out in CH_2Cl_2, a nonpolar solvent in which our catalysts operate, and a common medium for hydrogen bond catalysis studies. In contrast, pK_a's of organic compounds are usually measured in DMSO, which is an unsuitable solvent for most catalytic investigations due to its strong hydrogen bond accepting ability.

A series of titrations of a colorimetric sensor S (red) with thioureas **1**-**10** were carried out. Two hydrogen bonds to the carbonyl group can be formed in the bound sensor···thiourea complex (eq. 3), and blue shifts in the UV-Vis spectra and visible color changes to the naked eye were observed (Figure S1). That is, upon adding increasing

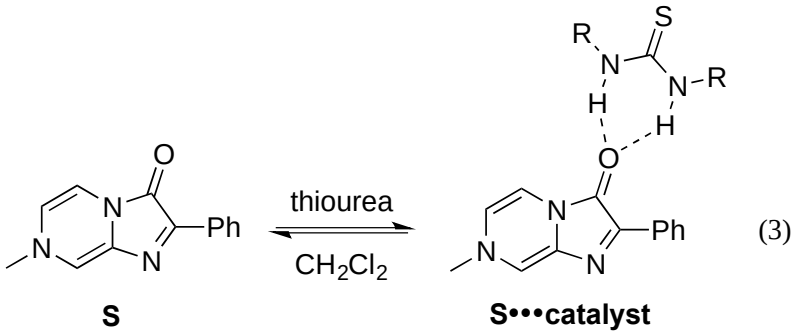

(3)

concentrations of **1**-**10**, the observed values for λ_{max} decreased from the value for **S** (498.6 nm) to lower wavelengths. This hypsochromic shift continued until an endpoint was reached where the sensor fully exists as the bound complex, S···thiourea. This is illustrated for the data with **4** (Figures 4 and S2), and from the resulting titration curve the

equilibrium association constant can be determined.[13] The measured values along with λ_{max} for the bound complexes, and the rate constants for the Friedel–Crafts reaction of *N*-methylindole with *trans*-β-nitrostyrene catalyzed by **1-10**, are given in Table 4.

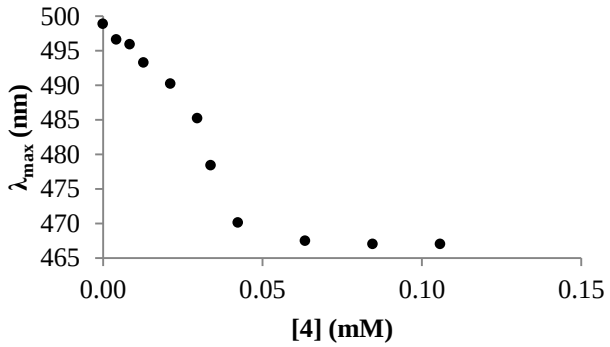

Figure 4. Changes in the observed UV-Vis absorption maxima values upon titrating a 2.22 x 10^{-5} M solution of **S** in CH_2Cl_2 with thiourea **4**.

Table 4. Wavelength shifts, equilibrium association constants and catalyzed reaction rate constants for the Friedel–Crafts alkylation of *N*-methylindole with *trans*-β-nitrostyrene.[a]

catalyst	λ_{max} (nm)	K (M^{-1})	*k* ($M^{-1}\cdot h^{-1}$)
1	495.0	20.0	0.0011[a]
2	479.5	1,210	0.11
3	475.5	4,120	0.71
4	467.0	2.08×10^5	45
5	495.6	972	0.0020[a]
6	473.5	1.01×10^4	1.0
7	480.8	2,650	0.33
8	470.7	6.41×10^4	8.1
9	472.0	4,260	2.4
10	468.8	1.02×10^5	18

[a]Background corrected rate constant.

Bound complexes of the sensor with thioureas **1-10** were found to have λ_{max} absorptions of 495.0 to 467.0 nm, and these values correspond to shifts of 3.6 to 31.6 nm relative to **S**. The equilibrium association constants track these changes and span a 10,000-fold range. A plot of the natural logarithm of K versus the change in the reciprocal values of λ_{max} upon complexation of **S** with a thiourea (i.e., $\lambda_{max}(S\cdots thiourea)^{-1} - \lambda_{max}(\mathbf{S})^{-1}$) is linear (Figure 5). This indicates that the absorption maximum of 7-methyl-2-phenylimidazo[1,2a]pyrazine-3(7H)-one complexed to a thiourea is a good surrogate for the corresponding equilibrium association constant. The only exception is for **5**, which has two triflate counterions that can serve as hydrogen bond acceptors even though this anion is the conjugate base of a strong acid. Interactions of this sort between the thiourea and one or both of the triflate ions would lead one to expect that K should be diminished, and that **5** would display a negative deviation from the line in Figure 6. This is not the case, and suggests that one or both of the triflate ions are able to energetically interact with **S** in a favorable manner. To assess this possibility, both B3LYP and M06-2X geometry optimizations were carried out with the cc-pVDZ basis set on a single bound conformer structure. The resulting geometries are similar, and as illustrated for the latter case in Figure 6, the two triflate anions coordinate with both the thiourea and the sensor via a number of hydrogen bonds.

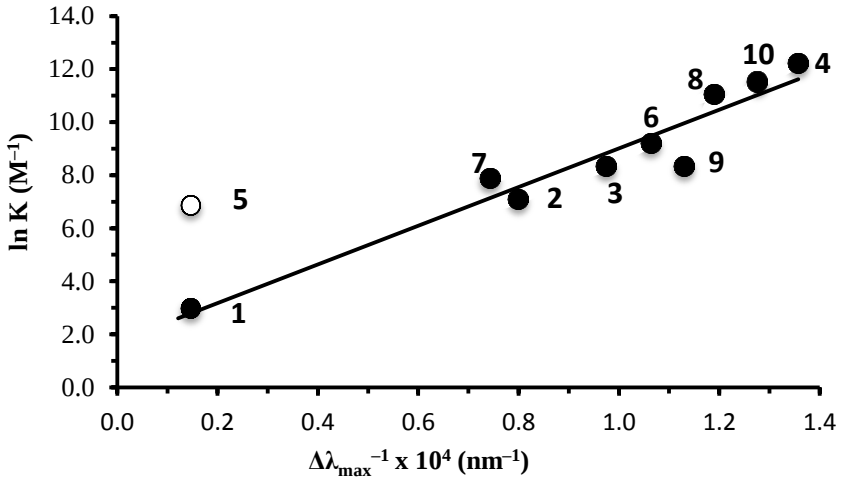

Figure 5. Changes in the reciprocals of the absorption wavelength maxima of **S** and **S···**thiourea compared to the logarithms of the corresponding equilibrium association constants. The equation for the linear least-squares fit of the data is ln K (M^{-1}) = 7.29 x $\Delta\lambda_{max}^{-1}$ (nm^{-1}) + 1.72, r^2 = 0.92, where the value for **5** was omitted from the analysis.

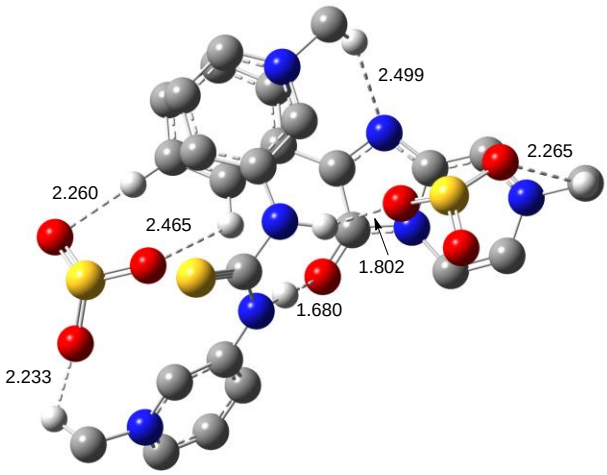

Figure 6. An M06-2X/cc-pVDZ optimized structure of **S···5**. Select interactions are illustrated with dashed lines and the given distances are in Angstroms. Both trifluoromethyl groups and the majority of the hydrogen atoms have been omitted for clarity sake.

A plot of ln *k* versus $\Delta\lambda_{max}^{-1}$, where *k* are the measured rate constants for the thiourea-catalyzed Friedel−Crafts reactions of *N*-methylindole with *trans*-β-nitrostyrene is also linear (Figure 7). In this case the data for all ten catalysts (**1-10**) fit on the correlation including the result for **5**, the doubly charged salt with two triflate counterions. These rate constants span a sizable range of $10^4 - 10^5$, but are well correlated with the UV-Vis spectroscopic changes induced by hydrogen bond formation. Non-charged thioureas, mono- and bis-charged derivatives with two different noncoordinating tetraarylborate counteranions, and a deactivated species with two hydrogen bond accepting triflate anions are all well behaved with respect to Kozlowski's spectroscopic approach. Since this methodology is relatively insensitive to water, the requisite sensor can be readily obtained, and micromolar solutions can be used, it is well suited for rapidly screening charged thiourea catalysts.

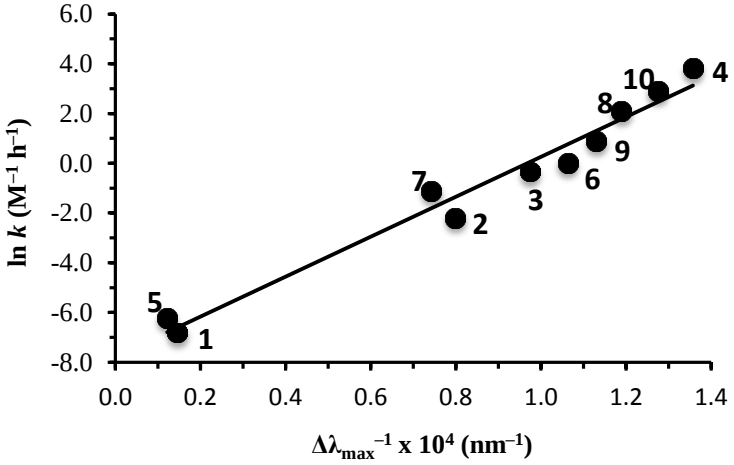

Figure 7. A linear correlation between the logarithm of the reaction rate constant for the transformation given in eq. 1 and $\Delta\lambda_{max}^{-1}$, where the equation of the line obtained by a least-squares fit of the data is ln *k* (M^{-1} h^{-1}) = 8.03 x $\Delta\lambda_{max}^{-1}$ (nm^{-1}) – 7.76, r^2 = 0.97.

3.3. Conclusion

A series of electrostatically enhanced thiourea catalysts were prepared and their performance in the Friedel−Crafts alkylation of *N*-methylindoles with *trans*-β-nitroalkenes was evaluated. Reactivity enhancements of 2–3 orders of magnitude were observed relative to Schreiner's thiourea, which for the past 15 years has been widely regarded as the benchmark in this area of organocatalysis. The concept of introducing a non-coordinating positively charged center and a non-interacting counteranion suggests a new strategy for catalyst development. A UV-Vis spectroscopic method developed by Kozlowski et al. can be used to rationalize the catalytic abilities of **1-10**, and should be of value in rapidly screening subsequent derivatives.

3.4. Experimental

General. All chemicals were obtained and used as received from Sigma Aldrich, Alfa Aesar and Matrix Scientific except for deuterated solvents which came from Cambridge Isotope Laboratories. Glassware (i.e., flasks, vials, syringes and NMR tubes) was oven-dried before use and reactions were carried out under an argon atmosphere. Uncorrected melting points were obtained with a Uni-Melt apparatus in unsealed tubes. Proton and ^{13}C NMR spectra were acquired with a 500 MHz instrument and the respective chemical shifts were referenced in ppm as follows: δ 7.26 and 77.2 ($CDCl_3$), 5.32 and 53.8 (CD_2Cl_2), 2.50 and 39.5 (DMSO-d_6), 2.08 (toluene-d_8), and 2.05 and 29.8 (acetone-d_6). IR spectra were recorded with a FT-IR equipped with an ATR source, and high resolution mass spectrometry data were obtained with an ESI-BioTOF instrument using methanol

solutions and polyethylene glycol as an internal standard. UV-Vis spectra were obtained with a Lambda XLS spectrometer and a 10 mm septum-covered quartz cell. Catalysts **3-4** and their requisite precursors along with related kinetic data were previously reported in a recent communication.[8]

3-Amino-1-(1-octyl)pyridinium triflate. In a 6 dram vial, 50 mg (0.53 mmol) of 3-aminopyridine was dissolved in 1 mL of CH_2Cl_2 and 0.28 g (1.07 mmol) of 1-octyl triflate[18] was added at room temperature. The reaction mixture was allowed to stir overnight before being concentrated under reduced pressure. The resulting residue was washed with 2 mL of pentane and dried under vacuum to afford the product as a yellow oil (0.19 g, 100%). ^{1}H NMR (500 MHz, $CDCl_3$) δ 8.23 (s, 1H), 7.75 (d, J = 5.4 Hz, 1H), 7.59 (d, J = 8.8 Hz, 2H), 7.48 (dd, J = 5.9, 8.8 Hz, 1H), 5.81 (s, 2H), 4.28 (t, J = 7.8 Hz, 2H), 1.88 (m, 2H), 1.37 – 1.02 (m, 10H), 0.81 (t, J = 6.9 Hz, 3H). ^{13}C NMR (126 MHz, $CDCl_3$) δ 149.0, 130.5, 128.9, 128.1, 127.9, 120.6 (q, $J_{C\text{-}F}$ = 320 Hz), 62.2, 31.7, 31.3, 29.0, 28.9, 26.1, 22.6, 14.1. IR (ATR source): 3349, 3232 cm^{-1}. HRMS-ESI: calcd for $C_{13}H_{23}N_2^+$ $(M - CF_3SO_2^-)^+$ 207.1856, found 207.1856.

1,3-bis-3-(1-Octylpyridylium)thiourea triflate (**5**). In a 6 dram vial under argon, 3-isothiocyanato-1-octylpyridinium triflate (50 mg, 0.13 mmol) was dissolved in 1 mL of CH_2Cl_2 and 3-amino-1-octylpyridinium triflate (45 mg, 0.13 mmol) was added at room temperature. The reaction mixture was allowed to stir overnight and then concentrated under reduced pressure. The resulting residue was washed with 2 mL of pentane and

dried under vacuum to afford the product as a pale yellow oil (93 mg, 98%). ^{1}H NMR (500 MHz, acetone-d_6) δ 10.62 (s, 2H), 9.66 (s, 2H), 8.99 (d, J = 5.9 Hz, 2H), 8.74 (d, J = 8.4 Hz, 2H), 8.25 (dd, J = 5.9, 8.4 Hz, 2H), 4.85 (t, J = 7.3 Hz, 4H), 2.14 (m, 4H), 1.45 – 1.24 (m, 20H), 0.85 (t, J = 6.9 Hz, 6H). ^{13}C NMR (126 MHz, acetone-d_6) δ 181.5, 141.3, 140.5, 140.4, 128.8, 121.7 (q, $J_{C\text{-}F}$ = 322 Hz), 63.1, 32.3, 31.8, 29.6, 29.5, 26.5, 23.1, 14.2. IR (ATR source): 3446 cm^{-1}. HRMS-ESI: calcd for $C_{27}H_{43}N_4S^+$ (M – $2CF_3SO_2^-$ – H^+)$^+$ 455.3203, found 455.3203.

1-Methyl-4-(3-phenylthioureido)pyridinium iodide (**6I**). In a 6-dram vial, 60 mg (0.22 mmol) of 4-isothiocyanato-1-methylpyridinium iodide[9] was dissolved in 3 mL of CH_3CN under argon. Aniline (20 μL, 0.22 mmol) was added dropwise and the reaction mixture was allowed to stir overnight at room temperature. A minimal amount of a 1 : 1 mixture of ethyl acetate and pentane was subsequently added (~ 2 mL) and the resulting precipitate was filtered, washed with 5 mL of ethyl acetate and dried under vacuum to afford 40 mg (49%) of **6I** as a yellow solid (mp 186 – 187 ℃). ^{1}H NMR (500 MHz, DMSO-d_6) δ 11.18 (s, 1H), 11.01 (s, 1H), 8.64 (d, J = 7.4 Hz, 2H), 8.10 (d, J = 6.9 Hz, 2H), 7.53 (d, J = 7.8 Hz, 2H), 7.41 (t, J = 7.8 Hz, 2H), 7.24 (t, J = 7.8 Hz, 1H), 4.14 (s, 3H). ^{13}C NMR (126 MHz, DMSO-d_6) δ 178.4, 152.8, 145.0, 138.1, 128.9, 126.0, 123.9, 115.0, 46.1. IR (ATR source): 3339, 3242 cm^{-1}. HRMS-ESI: calc for $C_{13}H_{14}N_3S^+$ (M – I^-)$^+$ 244.0903, found 244.0900.

1-Octyl-3-(3-phenylthioureido)pyridin-1-ium triflate (**9OTf**). In a 6 dram vial, 3-isothiocyanato-1-octylpyridinium triflate[8] (50 mg, 0.13 mmol) was dissolved in 1 mL of CH_2Cl_2 and 12 mg (0.13 mmol) of aniline was added at room temperature. The reaction mixture was allowed to stir overnight before being concentrated under reduced pressure. The resulting residue was washed with 2 mL of pentane and dried under vacuum to afford 61 mg (99%) of the product as a pale yellow oil. ^{1}H NMR (500 MHz, $CDCl_3$) δ 10.21 (br s, 1H), 9.85 (s, 1H), 9.57 (br s, 1H), 8.60 (d, *J* = 8.8 Hz, 1H), 8.26 (d, *J* = 5.4 Hz, 1H), 7.75 (dd, *J* = 5.9, 8.8 Hz, 1H), 7.56 (d, *J* = 8.3 Hz, 2H), 7.36 (t, *J* = 7.8 Hz, 2H), 7.23 (t, *J* = 7.4 Hz, 1H), 4.40 (t, *J* = 7.4 Hz, 2H), 1.96 (t, *J* = 6.4 Hz, 2H), 1.37 – 1.15 (m, 10H), 0.86 (t, *J* = 6.9 Hz, 3H). ^{13}C NMR (126 MHz, $CDCl_3$) δ 179.3, 141.7, 138.0, 137.0, 136.7, 136.4, 128.9, 127.6, 126.6, 124.9, 120.4 (q, $J_{C\text{-}F}$ = 320 Hz), 62.9, 31.7, 31.2, 29.0, 28.9, 26.1, 22.6, 14.2. IR (ATR source): 3273, 3086, 2927, 1497, 1223, 1162, 1026 cm^{-1}. HRMS-ESI: calcd for $C_{20}H_{28}N_3S^+$ $(M - CF_3SO_2^-)^+$ 342.1998, found 342.1993.

General Procedure for Preparing Thiourea Catalysts 6-10. Thiourea catalysts **6-10** were prepared from their iodide or triflate salts using our previous reported general procedure.[8,9]

1-Methyl-4-(3-phenylthioureido)pyridinium tetrakis(3,5-bis(trifluoromethyl)phenyl)borate (**6**). This compound was prepared following the general procedure starting with 0.081 mmol of **6I** and was obtained in a 94% yield (85 mg) as a white solid (mp 60 – 62 ℃). ^{1}H NMR (500 MHz, acetone-d_6) δ 10.36 (br s, 1H), 8.77 (d, *J* = 6.4 Hz, 2H), 8.47 (d,

J = 6.9 Hz, 2H), 7.80 (s, 8H), 7.69 (s, 4H), 7.57 (d, *J* = 6.9 Hz, 2H), 7.44 (t, *J* = 7.4 Hz, 2H), 7.30 (t, *J* = 7.4 Hz, 1H), 4.42 (s, 3H), 3.02 (br s, 1H). ^{13}C NMR (126 MHz, acetone-d_6) δ 179.6, 162.5 (q, $^{1}J_{B\text{-}C}$ = 50.5 Hz), 154.6, 146.0, 138.7, 135.5, 130.0 (qq, $^{3}J_{B\text{-}C}$ = 3.0 Hz and $^{2}J_{F\text{-}C}$ = 32.3 Hz), 129.9, 127.5, 125.3, 125.2 (q, $^{1}J_{F\text{-}C}$ = 272 Hz), 118.4, 116.7, 47.2. IR (ATR source): 3405, 3351cm^{-1}. HRMS-ESI: calc for $C_{13}H_{14}N_3S^+$ (M – $C_{32}H_{12}BF_{24}^-$)$^+$ 244.0903, found 244.0909 and calc for $C_{32}H_{12}BF_{24}^-$ (M – $C_{27}H_{44}N_4S^+$)$^-$ 863.0654, found 863.0667.

1-Methyl-3-(3-phenylthioureido)pyridinium tetrakis(pentafluorophenyl)borate (**7**). This compound was prepared following the general procedure starting with 0.067 mmol of 1-methyl-3-(3-phenylthioureido)pyridinium iodide[8] (**3I**) and was obtained in a 96% yield (60 mg) as a white solid (mp 94 – 96 ℃). ^{1}H NMR (500 MHz, acetone-d_6) δ 9.89 (s, 2H), 9.61 (s, 1H), 8.83 (d, *J* = 5.9 Hz, 1H), 8.70 (d, *J* = 8.3 Hz, 1H), 8.16 (dd, *J* = 6.4, 8.3 Hz, 1H), 7.52 (d, *J* = 7.9 Hz, 2H), 7.43 (t, *J* = 7.4 Hz, 2H), 7.29 (t, *J* = 7.4 Hz, 1H), 4.64 (s, 3H). ^{13}C NMR (126 MHz, acetone-d_6) δ 181.4, 149.0 (d, *J* = 250 Hz), 141.6, 141.3, 140.4 (d, *J* = 194 Hz), 140.0, 138.6, 138.0, 137.0 (d, *J* = 243 Hz), 130.1, 129.8, 128.1, 127.4, 125.7 (*ipso*-C), 49.4. IR (ATR source): 3356 cm^{-1}. HRMS-ESI: calc for $C_{13}H_{14}N_3S^+$ (M – $C_{24}BF_{20}^-$)$^+$ 244.0903, found 244.0929 and calc for $C_{24}BF_{20}^-$ (M – $C_{13}H_{14}N_3S^+$)$^-$ 679.0426, found 679.0420.

1,3-bis-3-(1-Methylpyridylium)thiourea tetrakis(pentafluorophenyl)borate (**8**). This compound was prepared following the general procedure starting with 0.065 mmol of

1,3-bis-3-(1-methylpyridyl-ium)thiourea iodide[8] (**4I**) and was obtained in a 88% yield (92 mg) as a white solid (mp 115 – 117 ℃). ^{1}H NMR (500 MHz, acetone-d_6) δ 10.72 (s, 2H), 9.61 (s, 2H), 8.96 (d, J = 5.9 Hz, 2H), 8.82 (d, J = 8.3 Hz, 2H), 8.28 (dd, J = 6.4, 8.3 Hz, 2H), 4.68 (s, 6H). ^{13}C NMR (126 MHz, acetone-d_6) δ 182.2, 149.0 (d, J = 243 Hz), 141.9 (d, J = 194 Hz), 140.7, 140.2, 140.1, 140.0, 139.9, 137.0 (d, J = 247 Hz), 128.7 (*ipso*-C), 49.6. IR (ATR source): 3305 cm^{-1}. HRMS-ESI: calc for $C_{13}H_{15}N_4S^+$ (M – H – $2C_{24}BF_{20}^-$)$^+$ 259.1007, found 259.1015 and calc for $C_{24}BF_{20}^-$ (M – $C_{13}H_{15}N_4S^+$)$^-$ 679.0426, found 679.0431.

1-Octyl-3-(3-phenylthioureido)pyridin-1-ium tetrakis(3,5-bis(trifluoromethyl)phenyl)-borate (**9**). This compound was prepared following the general procedure starting with 0.17 mmol of 1-octyl-3-(3-phenylthioureido)pyridin-1-ium triflate[9] (**9-OTf**) and was obtained in a 100% yield (0.21 g) as a yellow oil. ^{1}H NMR (500 MHz, acetone-d_6) δ 9.94 (s, 1H), 9.85 (s, 1H), 9.75 (s, 1H), 8.91 (d, J = 5.9 Hz, 1H), 8.65 (d, J = 8.8 Hz, 1H), 8.20 (dd, J = 6.4, 8.3 Hz, 1H), 7.83 (s, 8H), 7.70 (s, 4H), 7.54 (d, J = 8.3 Hz, 2H), 7.44 (t, J = 7.8 Hz, 2H), 7.30 (t, J = 7.4 Hz, 1H), 4.87 (t, J = 7.4 Hz, 2H), 2.17 (m, 2H), 1.50-1.27 (m, 10H), 0.84 (t, J = 6.9 Hz, 3H). ^{13}C NMR (126 MHz, acetone-d_6) δ 181.6, 162.6 (q, $^{1}J_{B\text{-}C}$ = 50.5 Hz), 141.8, 141.2, 140.1, 139.7, 138.6, 135.5, 130.1, 130.0 (qq, $^{3}J_{B\text{-}C}$ = 3.0 Hz and $^{2}J_{F\text{-}C}$ = 32.3 Hz), 128.5, 127.4, 125.8, 125.4 (q, $^{1}J_{F\text{-}C}$ = 272 Hz), 118.4, 83.1, 32.4, 32.0, 29.7, 29.6, 26.6, 23.2, 14.2. IR (ATR source): 3415 cm^{-1}. HRMS-ESI: calc for $C_{20}H_{28}N_3S^+$ (M – $C_{32}H_{12}BF_{24}^-$)$^+$ 342.1998, found 342.2006 and calc for $C_{32}H_{12}BF_{24}^-$ (M – $C_{20}H_{28}N_3S^+$)$^-$ 863.0654, found 863.0679.

1,3-bis-3-(1-Octylpyridylium)thiourea tetrakis(3,5-bis(trifluoromethyl)phenyl)borate (**10**). This compound was prepared following the general procedure starting with 0.080 mmol of 1,3-bis-3-(1-octylpyridylium)thiourea triflate[9] (**5**) and was obtained in a 100% yield (0.17 g) as a yellow oil. ^{1}H NMR (500 MHz, acetone-d_6) δ 10.65 (s, 2H), 9.74 (s, 2H), 9.04 (d, J = 5.4 Hz, 2H), 8.74 (d, J = 8.8 Hz, 2H), 8.29 (dd, J = 5.4, 8.8 Hz, 2H), 7.80 (s, 16H), 7.66 (s, 8H), 4.89 (t, J = 6.8 Hz, 4H), 2.14 (m, 4H), 1.46-1.22 (m, 20H), 0.79 (t, J = 6.4 Hz, 6H). ^{13}C NMR (126 MHz, acetone-d_6) δ 182.8, 162.6 (q, $^{1}J_{B\text{-}C}$ = 49.4 Hz), 141.8, 141.3, 140.7, 140.7, 135.6, 130.0 (qq, $^{3}J_{B\text{-}C}$ = 3.0 Hz and $^{2}J_{F\text{-}C}$ = 31.3 Hz), 129.2, 125.4 (q, $^{1}J_{F\text{-}C}$ = 273 Hz), 118.4, 63.4, 32.4, 32.1, 30.5, 29.7, 26.7, 23.2, 14.2. IR (ATR source): 3285 cm^{-1}. HRMS-ESI: calc for $C_{27}H_{43}N_4S^+$ $(M - H^+ - 2C_{32}H_{12}BF_{24}^-)^+$ 455.3203, found 455.3194 and calc for $C_{32}H_{12}BF_{24}^-$ $(M - C_{27}H_{44}N_4S^+)^-$ 863.0654, found 863.0660.

General Procedure for Friedel–Crafts reactions. In oven-dried NMR tubes, 7.5 mg (0.050 mmol) of *trans*-β-nitrostyrene, 19 μL (0.15 mmol) of *N*-methylindole and the desired amount of catalyst were mixed in 0.6 mL of $CDCl_3$ (or an alternative solvent) at room temperature under an inert atmosphere. Proton NMR spectra were recorded to monitor reaction progress using signals for *trans*-β-nitrostyrene (8.04 ppm) and the alkylation product (5.23 ppm). A second-order integrated rate law was used to obtain rate constants and the first half-lives of *trans*-ß-nitrostyrene, the limiting reagent:

$$\ln \frac{[N\text{-methylindole}][\beta\text{-nitrostyrene}]_0}{[\beta\text{-nitrostyrene}][N\text{-methylindole}]_0} = k([N\text{-methylindole}]_0 - [\beta\text{-nitrostyrene}]_0)t$$

where $[\beta\text{-nitrostyrene}]_0$ and $[N\text{-methylindole}]_0$ indicate the initial concentrations and [β-nitrostyrene] and [*N*-methylindole] are the concentrations at given times. Reaction kinetic data are summarized in Table S1.

Computations. Calcuations were carried out with Gaussian 09[19] on computers at the Minnesota Supercomputer Institute for Advanced Computational Research. Full geometry optimizations with the B3LYP[20] and M06-2X[21] functionals and the cc-pVDZ[22] basis set were performed on a single conformer of the **S···5** complex.

Chapter 4. Synthesis of Cyclic Organic Carbonates Using Atmospheric Pressure CO_2 and Charge-Containing Thioureas Catalysts*

4.1. Introduction

Carbon dioxide (CO_2) is a problematic greenhouse gas of great concern in the Earth's atmosphere. Its atmospheric concentration has been rapidly rising over the past fifty years in large part due to human activities such as fuel combustion, and this is a major cause of global warming.[1] Reduction of unwanted CO_2 emissions and atmospheric levels, consequently is a subject of the utmost importance in the development of a modern sustainable society.[2] Carbon dioxide is also a non-toxic and renewable potential C1 feedstock in organic synthesis that could be of enormous utility in industrial and pharmaceutical applications.[3] Sustainable and efficient methods of chemical fixation of CO_2 are urgently needed, and are the focus of current research in the management strategy of this greenhouse gas.[4] One alternative approach is the incorporation of CO_2 into epoxides to afford cyclic five-membered ring organic carbonates because this chemical transformation is 100% atom economical and the resulting compounds are of broad utility. For example, they are used as aprotic polar solvents in the development of batteries and ionic liquids, and as precursors and intermediates in organic and polymer syntheses.[5,6]

---

* Fan, Y.; Tiffner, M.; Schörgenhumer, J.; Robiette, R.; Waser, M.; Kass, S. R. Synthesis of Cyclic Organic Carbonates Using Atmospheric Pressure CO_2 and Charge-Containing Thioureas Catalysts. *J. Org. Chem.* To be submitted.

Despite the global desire to readily and sustainably make use of CO_2 in chemical reactions, this has proven to be difficult due to its kinetic and thermodynamic stability. Elevated temperatures and pressures are typically required to overcome energy barriers and make use of this abundant potential C1 feedstock. The development of catalysts to exploit this reagent under milder conditions has received considerable attention in recent years. A wide range of species have been studied for carrying out cycloadditions of epoxides with CO_2 to afford cyclic carbonates with a focus on metal complexes,[7] ionic liquids[8] and combinations of the two. Halide salt additives have proven useful in these systems but the resulting processes suffer from air and/or water sensitivity, poor reactivity necessitating harsh reaction conditions, and the need for organic solvents.[9] In this context, the development of organocatalysts has emerged as an attractive new research direction.

Hydrogen bond catalysts such as alcohols,[10] polyphenols,[11] carboxylic acids[12], silandiols[13] and squaramides[14] have been reported recently and show promising results for the preparation of cyclic carbonates. Electrophilic activation of the epoxide via a hydrogen bonded complex is generally considered to facilitate its ring-opening in the presence of a halide anion in the rate determining step.[15] When compared to metal-based catalysts and ionic liquids, organic hydrogen bond donors are considered to be advantageous with respect to toxicity, sustainability, and the use of milder conditions.[16]

Thioureas are the most extensively studied hydrogen bond catalysts and of these, Schreiner's thiourea (**1**, $(3,5\text{-}(CF_3)_2C_6H_3NH)_2CS$) is commonly viewed as the most active species. We recently reported on a series of novel charge-enhanced derivatives bearing

one or two *N*-alkylpyridinium ion centers and a weakly coordinating counteranion.[17] These solid salts proved to be more active than Schreiner's thiourea by orders of magnitude in several organic transformations carried out in non-polar media. Inspired by these results, we decided to examine their ability to catalyze the cycloadditions of epoxides with CO_2. The catalytic performance of eight such derivatives (**T1**-**T8**, Figure 1) is reported herein.

4.2. Results and Discussion

To initiate our study upon the chemical fixation of CO_2 into epoxides using charged thiourea salts as catalysts, we first examined the reaction of 2-phenyloxirane (**2**) with CO_2 to afford the phenyl-substituted carbonate **3** (eq. 1). Under mild solvent free conditions at 60 ˚C with an atmospheric pressure of CO_2, 1 mol% of **T1** and a halide salt, the cyclic

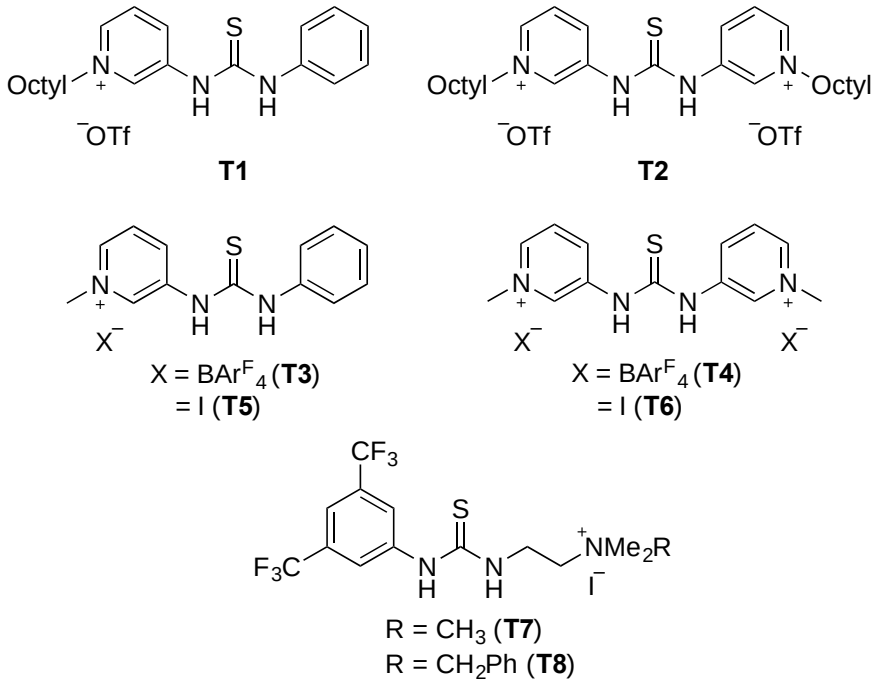

Figure 1. Charge-containing thiourea salts examined in this work.

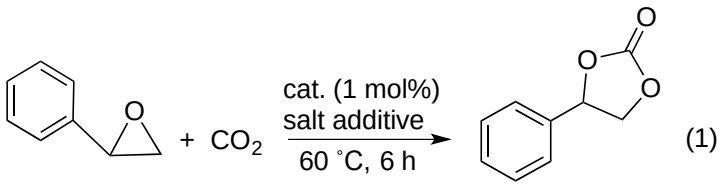

carbonate was formed with moderate conversions after 6 h (Table 1). When tetrabutylammonium iodide (TBAI) was employed, 57% of the 2-phenyloxirane was converted to **3** (entry 1) whereas progressively smaller amounts were obtained in going to the bromide and chloride salts (entries 2-3). This order is the reverse of the gas-phase proton affinities of these halide anions and their nucleophilicities in aprotic media. Use of bis(triphenylphosphine)iminium chloride (PPNCl) had little, if any, impact (entry 4) even though this salt is known to dissociate to a larger extent than TBACl in nonpolar media.[18]

Table 1. Catalytic performance of **T1** with various halide salts co-catalysts in the fixation of CO_2 into 2-phenyloxirane.[a]

entry	additive	(mol%)	conversion (%)[b]
1	$(Bu)_4NI$	1	57
2	$(Bu)_4NBr$	1	41
3	$(Bu)_4NCl$	1	20
4	$(Ph_3P)_2NCl$	1	19
5	none		0
6[c]	$(Bu)_4NI$	1	29
7[c]	$(Bu)_4NI$	2	56
8	$(Bu)_4NI$	2	74
9	$(Bu)_4NI$	3	65
10	$(Bu)_4NI$	5	66
11	$(Bu)_4NI$	10	53

12[d]	$(Bu)_4NI$	2	16

[a]Unless otherwise indicated, this reaction was carried out at 60 °C with 1 mol% of catalyst **T1** and the indicated additive under an atmospheric pressure (0.1 MPa) of CO_2. [b]Reaction conversions were obtained after 6 h by ^1H NMR. [c]No thiourea catalyst was used. [d]The reaction was carried out under 4.0 MPa of CO_2 and analyzed after 1.5 h.

Omission of the halide salt led to no observed product (entry 5) whereas when the catalyst (**T1**) was excluded but 1 mol% of TBAI was employed about half the amount of product was formed (entry 6). These results indicate that a nucleophilic anion is required for product formation and the presence of thiourea **T1** improves the efficiency of this process.

Further optimization of this transformation was carried out by varying the amount of the TBAI additive. When 2 mol% of this salt was used, a higher conversion of 74% was achieved (entry 8) and this exceeds the 56% that is obtained when **T1** was omitted from the reaction (entry 7). Further increases of TBAI were explored (3-10 mol%), but this led to smaller amounts of product (entries 9-11). We speculate that this is due to aggregation and/or a medium effect resulting in a decrease in the nucleophilicty of I^-. A reaction was also carried out at an elevated pressure of CO_2 (4.0 MPa) with 1 mol% **T1** and 2 mol% TBAI, but this did not appear to accelerate the transformation.[19] These results suggest that CO_2 is not involved in the rate-determining step, but that both the nucleophile and the hydrogen bond catalyst play an important role in this process.

Based upon these preliminary results with catalyst **T1**, a variety of catalyst structures (**T2-T8**) were examined with varying amounts of TBAI (Table 2). Incorporation of a second positively charged center into the thiourea (**T2**) leads to a less efficient catalyst

than **T1** (entries 1-2). The triflate counteranion is weakly basic but previously was shown to have a deleterious effect on the rate of a Friedel–Crafts alkylation.[20] Consequently, mono- and bis-charged thioureas **T3** and **T4** with weakly coordinating

Table 2. Catalyst and additive screening for the reaction of 2-phenyloxirane with CO_2.[a]

entry	catalyst	TBAI (mol%)	conversion (%)[b]
1	**T1**	2	74
2	**T2**	2	53
3	**T3**	0	0
4	**T3**	1	20
5	**T3**	2	52
6	**T4**	0	0
7	**T4**	2	87
8	**T5**	0	48
9	**T5**	1	61
10	**T5**	2	88
11	**T5**	3	88
12	**T5**	2[c]	79
13[d]	**T5**	2	83
14[e]	**T5**	2	71
15[f]	**T5**	2	82
16	**T6**	0	17
17	**T6**	2	54
18	**T7**	0	28
19	**T8**	0	34
20	$(PhNH)_2CS$	2	48
21	**1**	2	40

[a]These transformations were carried out for 6 h with 1 mol% of the catalyst and atmospheric pressure (0.1 MPa) CO_2 at 60 ˚C. [b]Product conversions were obtained by ^{1}H NMR. [c]Tetra-*n*-heptylammonium iodide was used instead of TBAI. [d]4-Dimethylaminopyridine (DMAP, 2 mol%) was added. [e]Acetic acid (1 mol%) was added. [f]Trifluoroacetic acid (1 mol%) was added.

tetrakis[3,5-bis(trifluoromethyl)phenyl]borate anions ($BAr^F_4^-$) were explored.[17] In the absence of a nucleophile no carbonate was produced (entries 3 and 6) and the mono-charged catalyst **T3** is not as effective as **T1** (entries 4-5), but the bis-charged derivative

T4 gave an improved result (entry 7). Bifunctional thiourea salts **T5-T8** with iodide counteranions were also examined. Unlike **T1-T4**, these species led to product formation without the need for an external iodide source and the conversions followed the order: **T6** < **T7** < **T8** < **T5** (entries 8, 16 and 18-19). Further optimization of **T5** led to our best result and an 88% conversion to product in a 6 h time period at 60 ˚C (entries 9-11); this was achieved with 2 or 3 mol% TBAI. A larger quaternary ammonium salt, tetra-*n*-heptylammonium iodide was tested too (entry 12), but it led to slightly poorer results.

Previous studies have found that organic bases can facilitate the cycloaddition of epoxides with CO_2 by activating the latter reagent.[21] When we added 2 mol% of 4-dimethylamino-pyridine (DMAP) along with **T5** and TBAI, no improvement was observed (entry 13). This is consistent with our observation that an increase in the CO_2 pressure did not accelerate the reaction. Alternatively, thioureas can be activated by Brønsted acids[22] so 1 mol% of acetic acid and trifluoroacetic acid were tested (entries 14-15). Both of these additivities, however, had a small deleterious effect. Finally, reactions were carried out with diphenylthiourea and $(3,5\text{-}(CF_3)_2C_6H_3NH)_2CS$ (**1**), and as suspected the conversions (48 and 40%, respectively) were reduced with respect to our charged analogs (entries 20-21). In fact under the employed conditions both catalysts actually function slightly as inhibitors since a 56% conversion was obtained when they are omitted.

Given the excellent performance of the binary **T5**/TBAI catalyst system,[23] the scope of this transformation was explored (eq. 2, Table 3). A series of 11 monosubstituted

aromatic and aliphatic epoxides were examined at 60 ˚C with 1 atmosphere pressure of CO_2, 1 mol% **T5** and 2 mol% TBAI, and isolated yields of ≥ 90% were obtained after

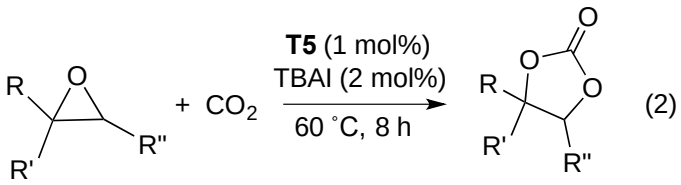

(2)

Table 3. Reaction scope with the use of the **T5**/TBAI binary catalyst system.

entry	epoxide (and carbonate **3**)	yield (%)
1	R = Ph, R', R'' = H (**2a**)	95
2	R = *p*-ClC_6H_4, R', R'' = H (**2b**)	95
3	R = *p*-FC_6H_4, R', R'' = H (**2c**)	93
4	R = *p*-$MeOC_6H_4$, R', R'' = H (**2d**)	98[a]
5	R = *p*-$O_2NC_6H_4$, R', R'' = H (**2e**)	98[b]
6	R = $PhOCH_2$, R', R'' = H (**2f**)	99
7	R = $ClCH_2$, R', R'' = H (**2g**)	98
8	R = CH_2=$CHCH_2CH_2$, R', R'' = H (**2h**)	90
9	R = CH_2=CH, R', R'' = H (**2i**)	97
10	R = $PhCH_2$, R', R'' = H (**2j**)	97
11	R = $BnOCH_2$, R', R'' = H (**2k**)	95
12	R,R'' = $(CH_2)_4$, R' = H (**2l**)	trace
13	R = Ph, R' = CH_3, R'' = H (**2m**)	trace

[a] t = 3 h. [b] t = 4 h and T = 90 ˚C.

8 h in all cases (entries 1-11); see the Appendix for the application scope of **T7** and **T8**. Disubstituted epoxides (1,1- and 1,2-), however, are not suitable substrates under the employed reaction conditions (entries 12-13). From a mechanistic standpoint, these results suggest that sterics are important.

To address the mechanism of this transformation further, (*R*)-2-phenyloxirane (**2a**, ≥ 99% ee) and (*R*)-2-(benzyloxymethyl)oxirane (**2k**, ≥ 99% ee) were reacted with **T5** as illustrated in eq. 2 and the isolated products were both obtained in 95% yields with 86%

ee for **3a** and ≥99% ee for **3k**. The absolute configuration of the major enantiomer in both cases corresponded to retention of configuration (*R*) by comparison to previously reported chiral HPLC data.[24] In accord with these findings, when enantiopure samples of **2a** were heated to 60 ˚C in the absence of CO_2 but in the presence of **T1** and TBAI (1 and 2 mol%, respectively) or **T7** (1 and 3 mol%), racemization was observed to slowly occur (eq. 3). In the former case, the epoxide had an 86% ee after 1 h and was completely

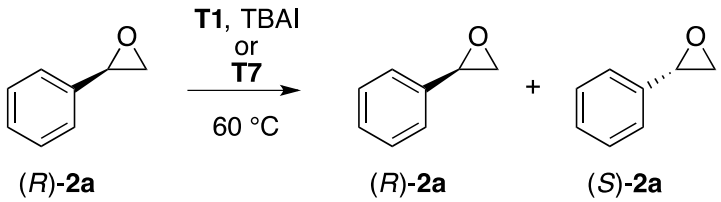

(3)

T1 (1 mol%), TBAI (2 mol%): 86% ee (*R*) (1 h), racemic (18 h)
T7: 86% ee (*R*) (1 mol%, 15 h), 55% ee (*R*) (3 mol%, 15 h)

racemized within 18 h. In the latter instance with 1 or 3 mol% of **T7**, 86% and 55% ee samples were obtained respectively after 15 h. These results reveal that a slow epimerization takes place when a stabilized benzylic cation can form when starting from **2a**, but not when a secondary alkyl carbenium ion would be produced using epoxide **2k**. These acid-catalyzed processes presumably are catalytically off-cycle events (i.e., they are unrelated to the mechanism for formation of the cyclic carbonate) given that alkyl substituted epoxides are good substrates, 1,1-disubstituted derivative **2l** is unreactive, and a competition study showed that the reaction of 2-(*p*-nitrophenyl)oxirane (**2e**) takes place more rapidly than the parent compound, 2-phenyloxirane (**2a**). That is, a 1:1 mixture of **2e** and **2a** at 60 ˚C with 1 mol% **T5** and 2 mol% TBAI led to 54% and 32% conversions to their respective carbonates after 2 h.

Electrophilic activation of the monosubstituted epoxide by coordination to the thiourea catalyst via hydrogen bond formation would be expected to preferentially activate the internal position due to a larger build-up of positive charge at this site.[17] To probe this latter mechanistic detail, kinetic isotope effects were measured using 2-deuterio-2-phenyloxirane (**2a**-d_1, >99% D) and 3,3-dideuterio-2-phenyloxirane (**2a**-d_2, 85% D_2) at 45 ˚C with 1 mol% **T5** and 2 mol% TBAI (eq. 4). Surprisingly, k_H/k_D = 1.0 for the monodeuterio compound and 1.56 for the dideuterio species were observed (see Table S4 in the supporting information for additional details). The latter

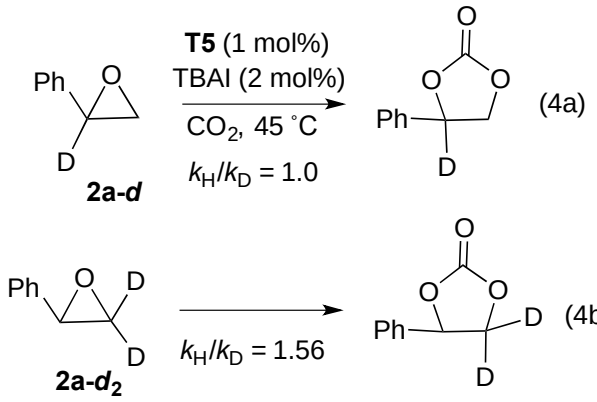

secondary isotope effect is large, and taken together these results indicate that nucleophilic attack occurs at the terminal methylene carbon of 2-phenyloxirane. Additionally, when the reaction of **2a** with **T7** was monitored by ^{1}H NMR, a small amount of an intermediate was observed. This species (**4**) was subsequently isolated and characterized, and is the product resulting from nucleophilic attack of the epoxide by the thiourea. Submission of this compound to the reaction conditions led to the formation of the cyclic carbonate product in a kinetically competent fashion and led us to propose the novel mechanism illustrated in Scheme 1.

Thiourea-catalyed pathways:

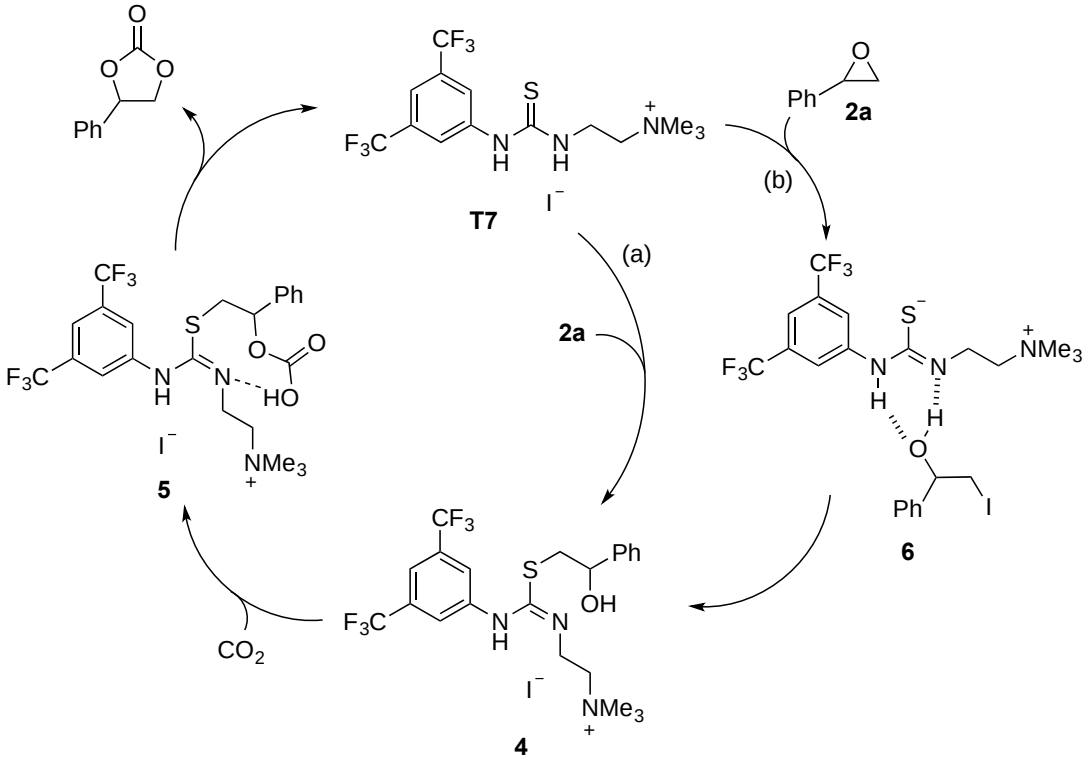

TBAI-catalyed route in the absence of **T7**:

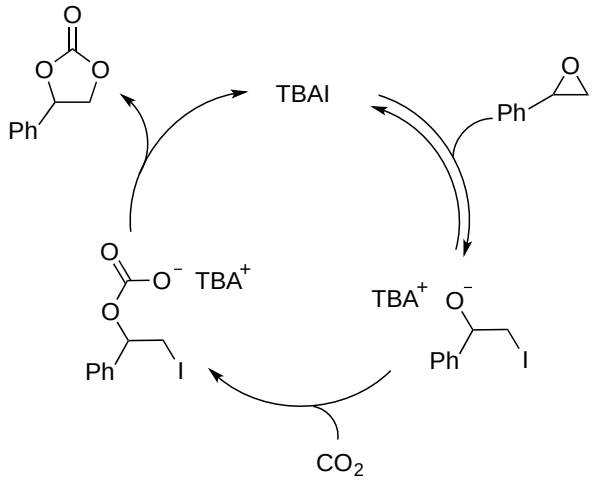

Scheme 1. Proposed mechanism for the cycloaddition of 2-phenyloxirane with CO_2 in the presence of a charge-containing thiourea/TBAI binary catalyst system (top), and an alternative route in the absence of the thiourea (bottom).

In our proposed mechanism, the charge-containing thiourea catalyst acts as a nucleophile in an S_N2 ring opening of the epoxide at the less hindered methylene carbon to yield **4** via pathway a. Alternatively, iodide may serve as the initial nucleophile to afford **6** as shown in route b. An ensuing displacement of I^- by the sulfur atom of the thiourea would lead to **4** by a two step process. Both pathways account for the formation of this intermediate and the observed secondary kinetic isotope effect, and are consistent with 1,1- and 1,2-disubstituted epoxides being poor reaction partners due to increased steric effects. Subsequent trapping of CO_2 to give **5** followed by cyclization via an intramolecular substitution reaction affords the carbonate product and regenerates the thiourea catalyst. Putative intermediate **6** also could react with CO_2 (pathway c, not shown) in a similar manner to the TBAI-catalyzed process that takes place in the absence of a thiourea. If this is the case, then the conversion of **6** to **4** would need to be reversible.

To address these mechanistic alternatives further, B3LYP calculations were carried out on different structural arrangements of hydrogen bonded complexes between **T7** and **2a** (see Appendix for additional details). Low energy structures that are well positioned to use the sulfur or iodine atom as the nucleophile was located (Figure 2, **7** and **8**, respectively).

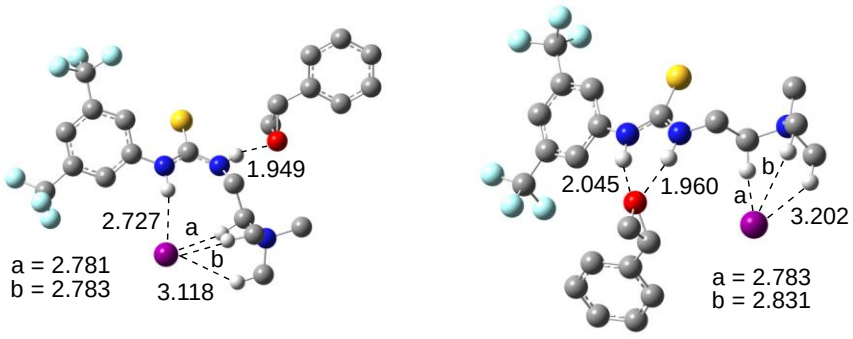

7 **8**

Figure 2. Fully optimized B3LYP/aug-cc-pVDZ/6-311G(d) structures, where the second all electron basis set was used for iodine. Distances are given in Å and most of the hydrogen atoms attached to carbon are omitted for clarity sake.

The covalently bound complex between the thiourea catalyst and 2-phenyloxirane (i.e., **4**) is more stable than **6** by 13.3 kcal mol^{-1}, but the reaction barrier for formation of the latter is much more favorable than the one for direct formation of **4**. That is, nucleophilic attack of the epoxide by I^- has a computed barrier of 25.5 kcal mol^{-1} whereas that for the sulfur atom of the catalyst is 46.8 kcal mol^{-1} (Figure 3).[25] These results suggest that pathway b is the favored process,[26] but given the computational complexity of this system, additional experimental data would be useful for further differentiating the various reaction pathways.

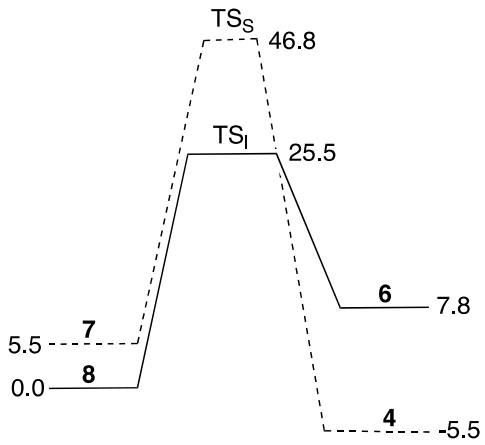

Figure 3. Computed B3LYP/aug-cc-pVDZ/6-311+G(d) single point free energy reaction diagrams for the **T7** catalyzed ring opening of 2-phenyloxirane. Relative free energies are given in kcal mol^{-1} at 298 K.

4.3. Conclusion

A series of metal-free electrostatically enhanced thiourea catalysts **T1-T8** were explored and found to induce CO_2 fixation at atmospheric pressure into monosubstituted epoxides with low loadings (1 mol%) and the addition of a small amount (2 mol%) of tetrabutylammonium iodide. High yields of ≥ 90% were obtained at modest temperatures for 11 different substrates in 8 h or less. These species are more active than the only other thiourea catalyst previously reported, an ionic liquid containing a remote imidizolium ion,[7g] in that lower temperatures (60 vs 130 ˚C) and pressures (1 vs 15 atm.) were employed in this work. Mechanistic studies suggest that this cycloaddition reaction occurs via a novel pathway in which the thiourea acts as a nucleophile to either open the

epoxide directly at the less hindered position or to replace the iodine in 2-iodo-1-phenylethanol. In either case, the resulting covalently bound thiourea **4** was spectroscopically observed, isolated, and found to react with CO_2 in a kinetically competent manner to afford the cyclic carbonate product along with the regenerated thiourea catalyst.

4.4. Experimental

General. All chemicals and reagents were obtained from Sigma Aldrich and Alfa Aesar except for deuterated solvents which came from Cambridge Isotope Laboratories. Reactions were carried out in oven-dried glassware (i.e., flasks, vials and NMR tubes) under an argon or CO_2 atmosphere. NMR spectra were recorded on 300, 500 and 700 MHz instruments. The ^{1}H and ^{13}C chemical shifts are given in ppm and were referenced respectively as follows: 7.26 and 77.2 ($CDCl_3$); 2.05 and 29.8 (acetone-d_6). IR spectra were obtained with a Nicolet iS5 FT-IR with an ATR iD5 source. A Bruker ESI BioTOF instrument was used to obtain high resolution mass spectrometry data using methanolic solutions containing polyethylene glycol as an internal standard. Enantiomeric ratios were measured with an Agilent 1260 HPLC and a 25 cm x 4.6 mm (5 μm) RegisPack™ and Chiracel OD-H chiral columns. Synthesis and characterization data for T1-T6 have been reported in previous work.[17,20]

General procedure for the cycloaddition reactions of 2-phenyloxirane (2) with CO_2. A 3-dram vial was purged with gaseous CO_2 for 5 min and then charged with 2-phenyloxirane (57 μL, 0.5 mmol), TBAI (3.7 mg, 10 μmol) and **T5** (1.9 mg, 5 μmol). The vial was then sealed with a septum which was connected to a balloon filled with CO_2 and heated at 60 ˚C for 6 h. Reaction conversions were obtained by ^{1}H NMR in $CDCl_3$ using integrations for the signals of **2** at δ 3.84 and **3** at δ 4.32 ppm.

Preparation of 3,3-dideuterio-2-phenyloxirane (2a-*d*$_2$).

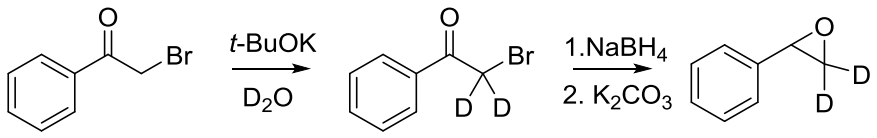

A solution of 2-bromo acetophenone (1999 mg, 10 mmol) in 5 mL $CDCl_3$ was cooled to 0 ℃. Carefully, *t*-BuOK (842 mg, 7.5 mmol) was added in small portions while the reaction mixture was strongly stirred. After 1 hour of stirring at 0 ℃, 3 ml D_2O were slowly added. A ^{1}H NMR sample of the $CDCl_3$ phase was recorded which showed a degree of deuteration of only 33%. Additional *t*-BuOK (562 mg, 5.0 mmol) was then carefully added to the strongly stirred biphasic mixture, which was then stirred for 2 hours while allowing it to warm to room temperature. The two phases were then separated and the aqueous solution was extracted with $CDCl_3$ (2 x 2 mL). The combined organic material was dried with Na_2SO_4 and the solvent was removed by rotatory evaporation. Purification of the crude product was then carried out by column chromatography (silica gel, heptanes/EtOAc, 50:1 → 30:1) and 1.42 g (62%) was

obtained as white orange solid containing 90% of the fully deuterated product at the acidic α-position. Analytical data are in accordance with those reported in literature.[27] ^{1}H NMR (300 MHz, $CDCl_3$) δ 8.02 – 7.95 (m, 2H), 7.65 – 7.56 (m, 1H), 7.54 – 7.45 (m, 2H), 4.47 – 4.42 (m, 0.21 H). ^{13}C NMR (75 MHz, $CDCl_3$) δ 191.3, 133.9, 133.8, 128.8, 128.7, 30.3 (quintet, J = 22.5 Hz).

2-Bromo-1-phenylethan-1-one-2,2-d_2 (1400 mg, 7 mmol) was put into a Schlenk flask which was then evacuated and refilled three times with argon before adding 15 mL of MeOH. This suspension was then cooled to 0 ℃ using an ice-salt/water bath. Sodium borohydride (294 mg, 7.7 mmol) was added portionwise and the reaction mixture was stirred for 3 h while letting it warm up to room temperature. Subsequently, K_2CO_3 (968 mg, 7 mmol) was added in one portion and stirring was continued for 15 h. The MeOH was removed by rotatory evaporation, 50 mL of H_2O was added and the aqueous phase was extracted with CH_2Cl_2 (3 x 50 mL). The combined organic material was washed with brine (50 mL), dried over Na_2SO_4 and the solvent was removed by rotatory evaporation. This afforded pure product (720 mg, 84%) as a colorless liquid. Analytical data are in accordance with those reported in literature.[28] ^{1}H NMR (300 MHz, $CDCl_3$) δ 7.40 – 7.25 (m, 5H), 3.86 (s, 1H), 3.18 – 3.12 (m, 0.15H), 2.83 – 2.78 (m, 0.15H). ^{13}C NMR (75 MHz, $CDCl_3$) δ 137, 128.4, 128.1, 125.4, 52.1, 51.5 (quintet, J = 26 Hz).

Preparation of 2-deuterio-2-phenyloxirane (2a-*d*).

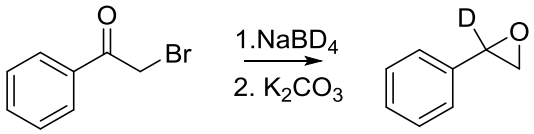

2-Bromo acetophenone (1000 mg, 5 mmol) was put into a Schlenk flask which was then evacuated and refilled with argon (3x) before adding 12 mL of MeOH. This suspension was then cooled to 0 ℃ using an ice-salt/water bath. Sodium borodeuteride (210 mg, 5.5 mmol) was added portionwise and the reaction mixture was stirred for 3 h while letting it warm up to room temperature. Then K_2CO_3 (691 mg, 5 mmol) was added in one portion and stirring was continued for 20 h. The reaction mixture was then filtered through a plug of Na_2SO_4 and the solvent was removed by rotatory evaporation. Purification of the crude product by column chromatography (silica gel, heptanes/EtOAc, 100:1 → 50:1) afforded 545 mg (91%) of the desired oxirane as a colourless liquid. Analytical data are in accordance with those reported in the literature.[24] ^{1}H NMR (300 MHz, $CDCl_3$) δ 7.41 – 7.26 (m, 5H), 3.17 (d, *J* = 5.5 Hz, 1H), 2.84 (d, *J* = 5.5 Hz, 1H). ^{13}C NMR (75 MHz, $CDCl_3$) δ 137.4, 128.4, 128.1, 125.4, 51.9 (t, 27 Hz), 51.0.

T7. To a suspension of 2-(aminoethyl)trimethylammonium iodide (1 g, 2.81 mmol)[30] in 10 mL of dry CH_2Cl_2 was added triethylamine (392 µL, 2.81 mmol) at room temperature. This mixture turned clear and subsequently 3,5-bis(trifluoromethylphenyl)isothiocyanate (517 µl, 3.09 mmol) was added. Stirring was continued for 15 h before filtering the reaction mixture through a plug of Na_2SO_4. Removal of the solvent by rotatory evaporation afforded the crude product which was

purified by column chromatography on silica gel with CH_2Cl_2/MeOH (50:1 → 10:1) to afford 1.35 mg (96%) of **T7** as a white solid; analytical data in accordance to the previously reported chloride salt[31]. ^{1}H NMR (300 MHz, $CDCl_3$) δ 9.79 (s, 1H) ppm, 8.49 (t, *J* = 5.8 Hz, 1H), 8.24 (s, 2H), 7.60 (s, 1H), 4.38 – 4.28 (m, 2H), 3.98 – 3.91 (m, 2H), 3.45 (s, 9H). ^{13}C NMR (75 MHz, $CDCl_3$) δ 181.7, 140.3, 131.4 (q, *J* = 34 Hz), 123.1 (q, *J* = 274 Hz), 123.0, 118.0, 64.9, 54.8, 38.3. ^{19}F NMR (282 MHz, D_2O) δ -64.5. HRMS-ESI): calcd for $C_{14}H_{18}F_6N_3S^+$ $(M)^+$ 374.1120, found: 374.1125.

T8. To a solution of 3,5-bis(trifluoromethyl)phenyl isothiocyanate (0.336 mL, 1.84 mmol) in toluene (2 mL) was added *N*,*N*-dimethylethylenediamine (0.201 mL, 1.84 mmol). After stirring for 14 h at room temperature the reaction mixture was directly subjected to column chromatography on silica gel with CH_2Cl_2/MeOH (20:1) to afford 625 mg (95%) of the known thiourea intermediate.[32] A mixture of this compound (100 mg, 0.278 mmol) and benzylbromide (95 mg, 0.556 mmol) was stirred in 2 mL of CH_3CN for 15 h at room temperature. The reaction mixture was directly subjected to column chromatography on silica gel with CH_2Cl_2/MeOH (10:1) to yield 148 mg (92%) of catalyst **T8** as a white solid. ^{1}H NMR (300 MHz, $CDCl_3$) δ 9.83 (s, 1H), 8.74 (t, *J* = 5.7 Hz, 1H), 8.24 (s, 2H), 7.42 – 7.60 (m, 6H), 4.83 (s, 2H), 4.37 – 4.48 (m, 2H), 3.99 (t, *J* = 5.8 Hz, 2H), 3.29 (s, 6H). ^{13}C NMR (75 MHz, $CDCl_3$) δ 181.8, 140.4, 133.0, 131.4 (q, *J* = 34 Hz), 131.4, 129.6, 126.0, 123.1 (q, *J* = 274 Hz), 123.0, 118.0, 68.9, 63.6, 50.7, 38.3. HRMS-ESI): calcd for $C_{20}H_{22}F_6N_3S^+$ $(M)^+$ 450.1433, found 450.1439.

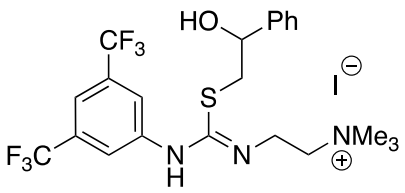

4

Intermediate 4. This compound can be obtained by heating the ammonium salt **T7** with 48 mg (10 equivalents) of 2-phenyloxirane in a pressure Schlenk vessel until the ammonium salt is dissolved, allowing the organic material to cool to room temperature and then performing a purification by silica gel column chromatography with CH_2Cl_2/MeOH (20:1) as the eluent. ^{1}H NMR (700 MHz, MeOD) δ 7.51 (s, 1H), 7.39 (s, 2H), 7.37 – 7.34 (m, 2H), 7.34 – 7.30 (m, 2H), 7.28 – 7.25 (m, 1H), 4.83 (dd, *J* = 8.4 and 3.7 Hz, 1H), 3.88 (t, *J* = 6.4 Hz, 2H), 3.66 (t, *J* = 6.6 Hz, 2H), 3.26 (s, 9H), 3.24 – 3.21 (m, 2H), 3.14 (dd, *J* = 14.4 and 3.4 Hz, 1H). ^{13}C NMR (175 MHz, MeOD) δ 155.6, 152.0, 143.0, 131.7 (q, *J* = 33 Hz), 128.2, 127.7, 125.8, 123.8 (q, *J* = 273 Hz), 123.0, 115.2, 73.5, 64.2, 52.9, 39.6, 36.6. HRMS-ESI: calcd for $C_{22}H_{26}F_6N_3OS^+$ $(M)^+$ 494.1695, found: 494.1699.

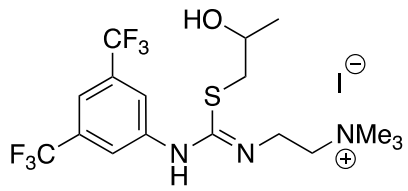

4'

Intermediate 4'. This compound was obtained when heating 0.04 mmol (20 mg) of the ammonium salt **T7** with 23 mg (10 equivalents) of methyloxirane in a pressure Schlenk vessel until the ammonium salt is dissolved, allowing the organic material to cool to room temperature and then performing a purification by silica gel column chromatography with CH_2Cl_2/MeOH (20:1) as the eluent. This afforded 7 mg (31%) of **4'** as a colorless oil. ^{1}H NMR (300 MHz, MeOD) δ 7.53 (s, 1H), 7.45 (s, 2H), 3.96 – 3.89 (m, 2H), 3.72 (t, *J* = 6.5 Hz, 2H), 3.30 (s, 9H), 3.15 – 2.93 (m, 2H), 1.26 (d, *J* = 6.2 Hz, 3H). ^{13}C NMR (75 MHz, MeOD) δ 155.7, 151.9,

131.6 (q, J = 33 Hz), 123.5 (q, J = 273 Hz), 122.9, 115.0, 66.9, 64.1, 52.9, 39.2, 36.5, 21.3.[33] HRMS-ESI calcd for $C_{17}H_{24}F_6N_3OS^+$ $(M)^+$ 432.1539, found 432.1539.

Analytical Data for Carbonates 3.

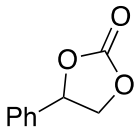

3a

4-Phenyl-1,3-dioxolan-2-one (**3a**). This material (311 mg) was formed in a 95% yield and the analytical data are in accord with those reported in the literature.[34] ^{1}H NMR (300 MHz, $CDCl_3$) δ 7.48 – 7.39 (m, 3H), 7.38 – 7.33 (m, 2H), 5.67 (t, J = 8 Hz, 1H), 4.79 (t, J = 8.4 Hz, 1H), 4.34 (dd, J = 8.6 and 7.9 Hz, 1H). ^{13}C NMR (75 MHz, $CDCl_3$) δ 154.7, 135.7, 129.5, 129.0, 125.7, 77.8, 71.0. HRMS-ESI: calcd for $C_9H_8NaO_3$ $(M + Na)^+$ 187.0371, found 187.0367. Enantiomer separation was accomplished with a Chiracel OD-H column using hexanes/*i*-PrOH = 70:30) and a flow rate of 1 mL min^{-1} to give retention times of 8.8 (*R*) and 10.0 (*S*) min.[24] When (*R*)-**2a** was used, (*R*)-**3a** was observed as the major enantiomer.

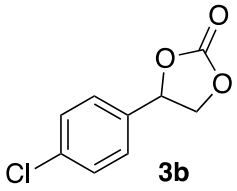

3b

4-(4-Chlorophenyl)-1,3-dioxolan-2-one (**3b**). This material (378 mg) was formed in a 95% yield and the analytical data are in accord with those reported in the literature.[34] ^{1}H NMR (300 MHz, $CDCl_3$) δ 7.42 – 7.34 (d, 2H, 8.5 Hz), 7.33 – 7.26 (d, 2H, 8.5 Hz), 5.65 (t, J = 8 Hz, 1H), 4.79 (t, J = 8.5 Hz, 1H), 4.28 (dd, J = 8.6 Hz and 7.8 Hz, 1H). ^{13}C NMR (75 MHz, $CDCl_3$) δ 154.5, 135.4, 134.2, 129.2, 127.2, 77.1, 71.8. HRMS-ESI: calcd for $C_9H_7ClNaO_3$ $(M + Na)^+$ 220.9981, found 220.9978.

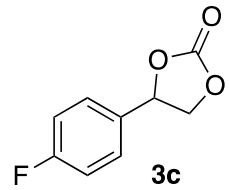

3c

4-(4-Fluorophenyl)-1,3-dioxolan-2-one (**3c**). This material (341 mg) was formed in a 93% yield and the analytical data are in accord with those reported in the literature.[34] ^{1}H NMR (300 MHz, $CDCl_3$) δ 7.41 – 7.30 (m, 2H), 7.17 – 7.06 (m, 2H), 5.66 (t, *J* = 8 Hz, 1H), 4.79 (t, *J* = 8.5 Hz, 1H), 4.31 (dd, *J* = 8.6 and 7.8 Hz, 1H). ^{13}C NMR (75 MHz, $CDCl_3$) δ 163.2 (d, *J* = 249 Hz), 154.6, 131.5 (d, *J* = 3.3 Hz), 127.9 (d, *J* = 8.5 Hz), 116.2 (d, *J* = 22.1 Hz), 77.4, 71.0. ^{19}F NMR (282 MHz, $CDCl_3$) δ -111.1. HRMS-ESI: calcd for $C_9H_7FNaO_3$ $(M + Na)^+$ 205.0277, found: 205.0271.

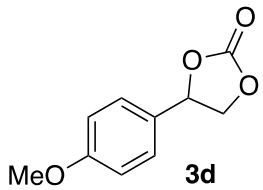

3d

4-(4-Methoxyphenyl)-1,3-dioxolan-2-one (**3d**). This material (380 mg) was formed in a 98% yield and the analytical data are in accord with those reported in the literature.[35] The product decomposed upon column chromatography. ^{1}H NMR (300 MHz, $CDCl_3$) δ 7.30 (d, *J* = 8.7 Hz, 2H), 6.96 (d, *J* = 8.7 Hz, 2H), 5.62 (t, *J* = 8.0 Hz, 1H), 4.75, (t, *J* = 8.4 Hz), 4.34 (t, *J* = 8.4 Hz, 1H), 3.83 (s, 3H).

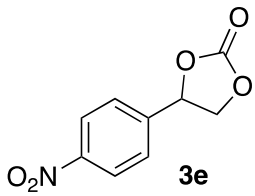

3e

4-(4-Nitrophenyl)-1,3-dioxolan-2-one (**3e**). This material (409 mg) was formed in a 98% yield and the analytical data are in accord with those reported in the literature.[36] ^{1}H NMR (300 MHz, $CDCl_3$) δ 8.28 (d, *J* = 8.4 Hz, 2H), 7.57 (d, *J* = 8.4 Hz, 2H), 5.83 (t, *J* = 7.9 Hz, 1H), 4.91, (t, *J* = 8.5 Hz), 4.32 (t, *J* = 8.2 Hz, 1H). ^{13}C NMR (75 MHz, $CDCl_3$) δ 154.1, 148.4, 142.7, 126.5, 124.3, 76.3, 70.6.

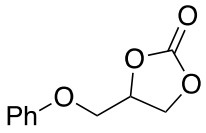

3f

4-(Phenoxymethyl)-1,3-dioxolan-2-one (**3f**). This material (384 mg) was formed in a 99% yield and the analytical data are in accord with those reported in the literature.[34] ^{1}H NMR (300 MHz, $CDCl_3$) δ 7.31 (t, *J* = 7.8 Hz, 2H), 7.02 (t, *J* = 7.4 Hz, 1H), 6.91 (d, *J* = 8.1 Hz), 5.09 – 4.96 (m, 1H), 4.60 (t, *J* = 8.5 Hz, 1H), 4.51 (dd, *J* = 6.0 and 8.4 Hz, 1H), 4.24 (dd, *J* = 10.5 and 3.8 Hz, 1H), 4.12 (dd, *J* = 10.5 and 3.8 Hz, 1H). ^{13}C NMR (75 MHz, $CDCl_3$) δ 157.7, 154.7, 129.5, 121.8, 114.5, 74.1, 66.7, 66.1. HRMS-ESI: calcd for $C_{10}H_{10}NaO_4$ $(M+Na)^+$ 217.0477, found 217.0475.

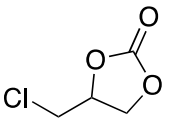

3g

4-(Chloromethyl)-1,3-dioxolan-2-one (**3g**). This material (267 mg) was formed in a 98% yield and the analytical data are in accord with those reported in the literature.[11d] ^{1}H NMR (300 MHz, $CDCl_3$) δ 5.04 – 4.91 (m, 1H), 4.59 (t, *J* = 8.2 Hz, 1H), 4.41 (dd, *J* = 5.5 and 8.0 Hz, 1H), 3.83 – 3.68 (m, 2H). ^{13}C NMR (75 MHz, $CDCl_3$) δ 154.3, 74.3, 66.7, 44.1. HRMS-ESI: calcd for $C_4H_5ClNaO_3$ $(M+Na)^+$ 158.9825, found: 158.9821.

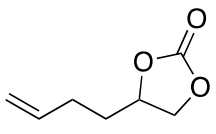

3h

4-(But-3-en-1-yl)-1,3-dioxolan-2-one (**3h**). This material (256 mg) was formed in a 90% yield and the analytical data are in accord with those reported in the literature.[34] ^{1}H NMR (300 MHz, $CDCl_3$) δ 5.84 – 5.66 (m, 1H), 5.10 – 4.96 (m, 2H), 4.77 – 4.63 (m, 1H), 4.50 (t, *J* = 8.1 Hz, 1H), 4.05 (t, *J* = 7.8 Hz, 1H), 2.32 – 2.05 (m, 2H), 1.98 – 1.81 (m, 1H), 1.81 – 1.65 (m, 1H). ^{13}C NMR

(75 MHz, $CDCl_3$) δ 154.9, 136.0, 116.1, 76.2, 69.2, 32.8, 28.4. HRMS-ESI: calcd for $C_7H_{10}NaO_3$ $(M+Na)^+$ 165.0528, found 165.0526.

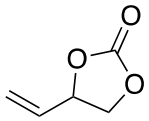

3i

4-Vinyl-1,3-dioxolan-2-one (**3i**). This material (222 mg) was formed in a 97% yield and the analytical data are in accord with those reported in the literature.[34] ^1H NMR (300 MHz, $CDCl_3$) δ 4.92 – 4.78 (m, 1H), 5.50 – 5.33 (m, 2H), 5.09 (q, *J* = 7.4 Hz, 1H), 4.56 (t, *J* = 8.3 Hz, 1H), 4.10 (t, *J* = 8 Hz, 1H). ^{13}C NMR (75 MHz, $CDCl_3$) δ 154.7, 132.0, 120.9, 77.2, 68.9. HRMS-ESI: calcd for $C_5H_6NaO_3$ $(M + Na)^+$ 137.0215, found: 137.0211.

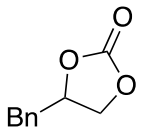

3j

4-Benzyl-1,3-dioxolan-2-one (**3j**). This material (345 mg) was formed in a 97% yield and the analytical data are in accord with those reported in the literature.[37] ^1H NMR (300 MHz, $CDCl_3$) δ 7.40 – 7.28 (m, 3H), 7.26 – 7.21 (m, 2H), 5.01 – 4.91 (m, 1H), 4.46 (t, *J* = 8.2 Hz, 1H), 4.18 (dd, *J* = 8.6 and 6.9 Hz, 1H), 3.16 (dd, *J* = 14.2 and 6.3 Hz, 1H), 3.01 (dd, *J* = 14.1 and 6.1 Hz, 1H). ^{13}C NMR (75 MHz, $CDCl_3$) δ 154.7, 133.8, 129.2, 128.8, 127.4, 76.7, 68.4, 39.4. MS-ESI: calcd for $C_{10}H_{14}NO_3$ $(M + NH_4)^+$ 196.1, found 196.1.

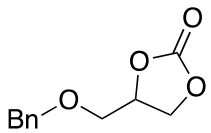

3k

4-((Benzyloxy)methyl)-1,3-dioxolan-2-one (**3k**). This material (396 mg) was formed in a 95% yield and the analytical data are in accord with those reported in the literature.[38] ^1H NMR (300 MHz, $CDCl_3$) δ 7.40 – 7.27 (m, 5H), 4.85 – 4.75 (m, 1H), 4.58 (dd, *J* = 17.5 and 12.0 Hz, 2H), 4.45 (t, *J* = 8.4 Hz, 1H), 4.35 (dd, *J* = 8.4 and 6.0 Hz, 1H), 3.70 (dd, *J* = 11.0 and 3.7 Hz, 1H)

3.59 (dd, J = 11.1 and 3.7 Hz, 1H). ^{13}C NMR (75 MHz, $CDCl_3$) δ 154.9, 137.0, 128.3, 127.8, 127.5, 74.9, 73.4, 68.7, 66.1. MS-ESI: calcd for $C_{11}H_{12}NaO_4$ $(M + Na)^+$ 231.1, found: 231.1. Enantiomer separation was achieved on a Chiracel OD-H column using hexanes/*i*-PrOH = 80 : 20 and a flow rate of 1.0 mL/min to give retention times of 22.0 and 32.4 min. When the (*R*)-enantiomer of **2k** was used only the stereoisomer of **3k** eluting at 22.0 min was observed.

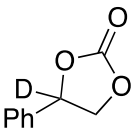

3a-D

4-Phenyl-1,3-dioxolan-2-one-4-d (**3a-D**). ^{1}H NMR (300 MHz, $CDCl_3$) δ 7.46 – 7.25 (m, 5H), 4.79 (d, J = 8.6 Hz, 1H), 4.33 (d, J = 8.6 Hz, 1H). ^{13}C NMR (75 MHz, $CDCl_3$) δ 154.9, 135.7, 129.6, 129.4, 125.9, 77.5 (t, J = 24 Hz), 71.1. MS -ESI: calc for $C_9H_7DNaO_3$ $(M + Na)^+$ 188.0, found 188.0.

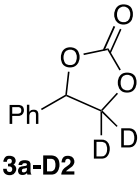

3a-D2

4-Phenyl-1,3-dioxolan-2-one-5,5-d_2 (**3a-D_2**). Isolated yield: 614 mg (94%). ^{1}H NMR (300 MHz, $CDCl_3$) δ 7.48 – 7.40 (m, 3H), 7.38 – 7.30 (m, 2H), 5.70 (s, 1H), 4.80 (m, 0.14H), 4.35 (m, 0.14H). ^{13}C NMR (75 MHz, $CDCl_3$) δ 154.8, 135.8, 129.8, 129.3, 125.9, 77.8, 70.8 (quintet, J = 24 Hz). MS-ESI: calc for $C_9H_6D_2NaO_3$ $(M + Na)^+$ 189.1, found 189.1.

Computations. Different orientations of hydrogen bonded complexes between **T7** and **2a** were fully optimized with Spartan 14[39] using B3LYP[40] and the 6-31G(d,p) basis set except for iodine, which was treated with the LANL2DZ pseudopotential.[41] Subsequent structures for **4**, **6**, and transition states leading to their formation were also located. Single point energies, reoptimizations and vibrational frequencies for select species were computed with Gaussian 09[42] using the aug-cc-pVDZ[43] and 6-311G(d) all electron basis set for iodine.[44] Thereafter, B3LYP/aug-cc-pVDZ/6-311+G(d) single point energies were computed.

Chapter 5. Enantioselective Friedel–Crafts Alkylation between Nitroalkenes and Indoles Catalyzed by Charge Activated Thiourea Organocatalysts*

5.1. Introduction

Small molecule metal-free organocatalysts are commonly exploited in carrying out a wide variety of chemical transformations.[1] Over the past two decades asymmetric control of these reactions has emerged as one of the most vibrant and challenging research areas in organic synthesis.[2] Hydrogen bond interactions are commonly used in this regard and play a key role in lowering activation barriers and organizing three-dimensional transition state geometries.[3] Thioureas with their two N–H hydrogen bond donating sites have proven to be a particularly successful functional group motif and continue to be extensively investigated.[4]

Reaction rates often correlate with organocatalyst acidities. That is, faster transformations typically occur with more acidic species of a given structural type.[5] Electron withdrawing groups are routinely employed because of this, and no substituent has been exploited more than a 3,5-bis(trifluoromethyl)phenyl ring. Doubly activated *N*,*N*′-bis(3,5-bis(trifluoromethyl)phenyl)-thiourea [$(3,5\text{-}(CF_3)_2C_6H_3NH)_2CS$, **1**] is commonly referred to as Schreiner's thiourea and represents a milestone in the

*Fan, Y.; Kass, S. R. Enantioselective Friedel–Crafts Alkylation between Nitroalkenes and Indoles Catalyzed by Charge Activated Thiourea Organocatalysts. *J. Org. Chem.* **2017**, *82*, 13288-13296. Copyright ACS. Reproduced with permission.

development of hydrogen bond donating organocatalysts.[6] Its greater catalytic ability leads to faster transformations and has been attributed to an enhanced acidity due to the presence of four electron withdrawing trifluoromethyl groups and two weak intramolecular C−H···S hydrogen bonds. The incorporation of the CF_3 groups also stabilize the reactive *Z,Z*-conformer, increase the structural rigidity and enhance the solubility of the thiourea in non-polar solvents.[7] Replacement of one of the 3,5-bis(trifluoromethyl)phenyl rings with a chiral moiety leads to a versatile platform for catalyst design and extensive efforts have been reported in this regard.[8]

Inspired by the many remarkable studies carried out with thiourea catalysts, we recently communicated the synthesis and reactivity of charge-containing derivatives with one or two cationic *N*-methylpyridinium ion centers and an appropriate noncoordinating anionic counterion (**2** and **3**, Figure 1).[9] These achiral compounds were found to lead to rate enhancements of one to three orders of magnitude relative to Schreiner's thiourea in

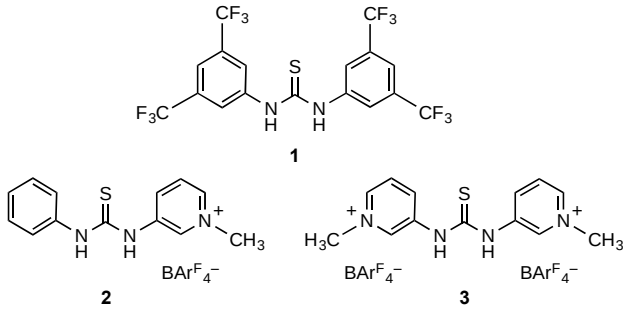

Figure 1. Schreiner's thiourea (**1**) and previously studied pyridinium ion containing analogs (**2** and **3**), where $BAr^F{}_4^- = (3,5\text{-}(CF_3)_2C_6H_3)_4B^-$.

several organic transformations without altering the binding motif or introducing an additional N–H or O–H hydrogen bond donating site.[10,11] For example, the reaction of *trans*-β-nitrostyrene with *N*-methylindole (eq. 1) was found to have a half-life of 29 hours when 10 mol% of **1** was used as the catalyst whereas this was reduced to 4.5 hours and 4.3 minutes with **2** and **3**, respectively. Given that the incorporation of a single charged center outperformed the presence of four trifluoromethyl groups, it seemed worthwhile to explore chiral variants of **2** (Scheme 1).

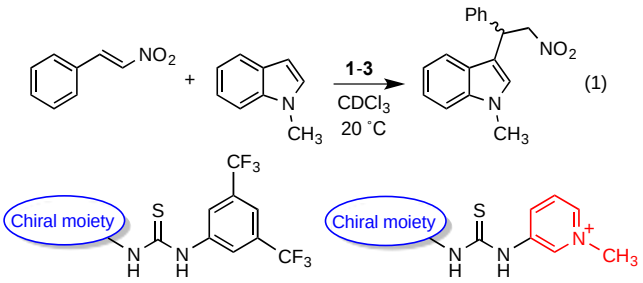

Scheme 1. New chiral design strategy for introducing a charged substituent to enhance the acidity and reactivity of a thiourea catalyst in nonpolar media.

A wealth of chiral thioureas with a 3,5-bis(trifluoromethyl)phenyl substituent have been developed but relatively few have an acidic group on the chiral moiety.[12] As these bifunctional species are expected to be compatible with the strategy illustrated in Scheme 1 (i.e., more acidic thioureas), we focused our attention on (1*S*, 2*R*)-1-amino-2-indanol derivatives (**4**, Scheme 2). The enantioselective Friedel-Crafts alkylation of indoles with *trans*-β-nitroalkenes was chosen as the test platform because it is a fundamental transformation that leads to increased molecular complexity via the formation of a new

carbon-carbon bond. This reaction is also a perfectly atom economical process that affords valuable pharmaceutical and biology-based intermediates.[13,14] Moreover, this transformation has been frequently used to test new Brønsted acids and hydrogen bond catalysts, and was employed by both Herrera et al.[8a,15] and Ganesh and Seidel[11f] to investigate **5-7**.

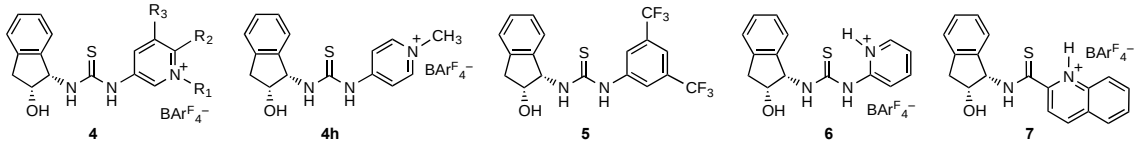

a: $R_1 = CH_3$, R_2, R_3 = H
b: R_1 = 1-C_8H_{17}, R_2, R_3 = H
c: $R_1 = CH_3$, R_2, R_3 = CH=CHCH=CH
d: R_1 = 1-C_8H_{17}, R_2, R_3 = CH=CHCH=CH
e: $R_1 = CH_3$, R_2 = H, R_3 = Ph
f: R_1 = 1-C_8H_{17}, R_2 = H, R_3 = Ph
g: $R_1 = CH_3$, R_2 = H, R_3 = 4-*t*-BuPh

Scheme 2. Chiral thioureas examined in this work (**4-5**) and previously reported (**6-7**).

5.2. Results and Discussion

A series of chiral thiourea hydrogen bond catalysts **4a–4h** bearing an *N*-alkylpyridinium ion center and a 2-indanol substituent were synthesized starting from commercially available 3- or 4-aminopyridines. These compounds were formed in a similar fashion as illustrated for **4a** in Scheme 3 by first converting the aminopyridine to its corresponding isothiocyanate. Alkylation with methyl iodide or octyl triflate was then followed by reaction with (1*S*, 2*R*)-1-amino-2-indanol to afford the thiourea precatalyst (i.e., the iodide or triflate salt). Substitution of the counterion to the weakly coordinating tetrakis(3,5-bis(trifluoromethyl)phenyl)borate anion ($BAr^F_4{}^-$) was carried out to give the

desired thiourea catalysts except in one instance when a tetrakis(pentafluorophenyl)borate ($B(C_6F_5)_4^-$) salt **4a'** was formed; this compound differs from **4a** only in the tetrakis(aryl)borate counterion.

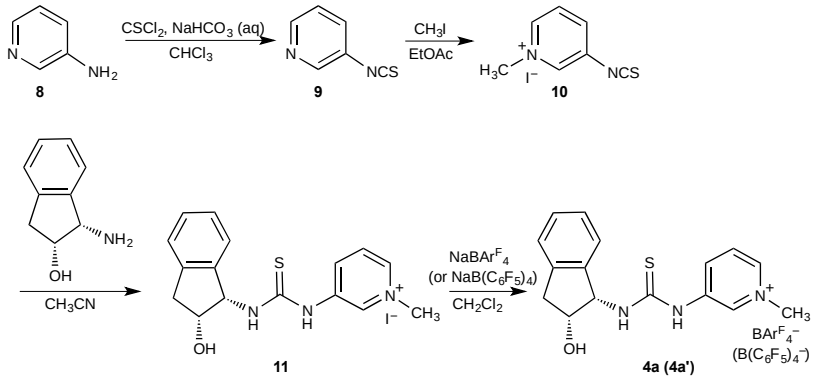

Scheme 3. Synthetic route for the formation of charge-containing thiourea catalysts **4a** and **4a'**.

To assess the catalytic performance of these charged thiourea salts, the Friedel–Crafts alkylation of indole with *trans*-β-nitrostyrene and 10 mol% of **4a** was initially examined under various conditions (Table 1). At room temperature in chloroform-*d* this transformation went to completion over the course of two days with a modest enantiomeric ratio (*er*) of 75 : 25 (entry 1).[16]

Table 1. Evaluation of **4a** under various conditions.[a]

entry	cat. loading (mol%)	solvent	temp. (˚C)	t (h)	Conversion (%)[b]	*er*[c]
1	10	$CDCl_3$	20	49	100	75 : 25
2	10	CD_2Cl_2	20	44	81	74 : 26
3	10	$C_6D_5CD_3$	20	45	66	70 : 30
4	10	$CDCl_3$	0	43	93	86 : 14

5	10	$CDCl_3$	-20	48	91	89 : 11
6	10	$CDCl_3$	-35	48	76	91 : 9
7	10	$CDCl_3$	-45	48	37	92 : 8
8	10	CD_3CN	-35	48	4	-
9[d]	10	$CDCl_3$	-35	425	38	85 : 15
10[e]	10	$CDCl_3$	-35	48	52	88 : 12
11[f]	10	$CDCl_3$	-35	48	49	90 : 10
12[g]	10	$CDCl_3$	-35	48	trace	-
13[h]	10	$CDCl_3$	-35	48	59	91 : 9
14[i]	10	$CDCl_3$	-35	48	52 (54)	87 : 13 (77 : 23)
15	20	$CDCl_3$	-35	29	91	90 : 10
16	5	$CDCl_3$	-35	51	42	89 : 11
17	1	$CDCl_3$	-35	72	23	90 : 10

[a]Unless otherwise indicated, these reactions were carried out with 0.05 mmol of *trans*-β-nitrostyrene and 3 equivalents of indole with the specified amount of catalyst in 0.6 mL of solvent. [b]Conversions were determined by ^{1}H NMR analysis of crude reaction mixtures. [c]Enantiomeric ratios were determined by chiral HPLC. [d]This reaction was carried out with 0.017 mmol of *trans*-β-nitrostyrene (i.e., ~3 x more dilute than in entries 1-8). [e]1.5 equivalents of indole were used. [f]$Bu_4NBAr^F_4$ (5 mol%) was added. [g]*p*-Toluenesulfonic acid (10 mol%) was added. [h]$Et_3NHBAr^F_4$ (10 mol%) was added. [i]1.5 mg of 3 or 4 Å molecular sieves were utilized; the latter values are given in parentheses.

Dichloromethane-d_2 and toluene-d_8 were also used (entries 2 and 3) but this led to lower product conversions and small decreases in the observed selectivities. Improved *er*s up to 92 : 8 were obtained by lowering the temperature to –45 °C (entries 4-7), but since nearly the same selectivity was observed at –35 ˚C (i.e., 91 : 9) and the reaction is noticeably faster (i.e., 37% vs 76% at t = 48 h), the higher temperature was adopted for our standard conditions. A change in the solvent to acetonitrile-d_3 led to a conversion of < 5% (entry 8), and this can be attributed to the polar nature of CD_3CN and its ability to serve as a hydrogen bond acceptor with the thiourea catalyst. Concentrations and the *trans*-β-

nitrostyrene/indole ratio were also varied (entries 9 and 10) but this slowed down the transformation without improving the stereoselectivity.

Several additives influence on the reaction were examined as well (entries 11-14). Added salt in the form of $Bu_4NBAr^F_4$ (5 mol%) reduced the amount of product formed over a 48 h reaction time period but had little, if any, effect on the *er*. External acids can activate thioureas as reported by Herrera et al.,[15] but in this case the addition of 10 mol% *p*-toluenesulfonic acid had the opposite effect and only a trace of product was observed. We attribute this catalyst deactivation to protonation of the thiourea or indole and coordination of the resulting tosylate anion with **4a** (i.e., hydrogen bonding to OTs^- is detrimental). The use of 3 and 4 Å molecular sieves to remove adventitious water are also disadvantageous with regard to yield and stereoselectivity.[17] Here too, hydrogen bonding between the oxygen atoms of the molecular sieves (i.e., an aluminosilicate) and the thiourea catalyst is apt to be the cause. Finally, triethylammonium tetrakis(3,5-bis(trifluoromethyl)phenyl)borate has no effect on the *er* but does lower the yield from 76% to 59%.

Catalytic loadings from 1–20 mol% were examined (entries 6 and 15-17) but have no notice-able impact on the enantioselectivity of the Friedel–Crafts reaction. Kinetic studies revealed second-order behavior, first-order in both indole and *trans*-β-nitrostyrene as one might expect.[18] Rate constants and the first half-life's of the limiting reagent (*trans*-β-nitrostyrene) are given in Table 2. The latter values decrease with the amount of catalyst added and span from 140 to 7.0 hours at –35 ˚C in going from 1 to 20 mol% of **4a**. A plot of the second-order rate constants versus the square of the catalyst mol% is linear

Table 2. Reaction rate constants and half-life's as a function of catalyst loading.[a]

entry	cat. loading (mol%)	k ($M^{-1}h^{-1}$)	$t_{1/2}$ (h)
1	1	0.022	140
2	5	0.059	52
3	10	0.15	21
4	20	0.44	7.0

[a]Standard reaction conditions of ~0.083 M *trans*-β-nitrostyrene, 0.25 M indole and the indicated amount of catalyst (**4a)** in $CDCl_3$ at −35 ˚C were employed. The first half-life ($t_{1/2}$) of the limiting reagent (i.e., the styrene) is given since this value changes as the reaction proceeds.

(Figure 2), consistent with previous findings and suggests that the active catalytic species of the thiourea is dimeric.[9,19] To assess this further, the ^{1}H NMR spectra of **4a** were recorded from 5.0 to 20.0 mM and both NH signals were found to move downfield linearly with increasing concentration (Table 3). This is consistent with a rapidly occurring monomer/dimer equilibrium and suggests that the association constant is small and the resting state for the catalyst is largely monomeric. It also led us to propose the catalytic cycle illustrated in Scheme 4.[20]

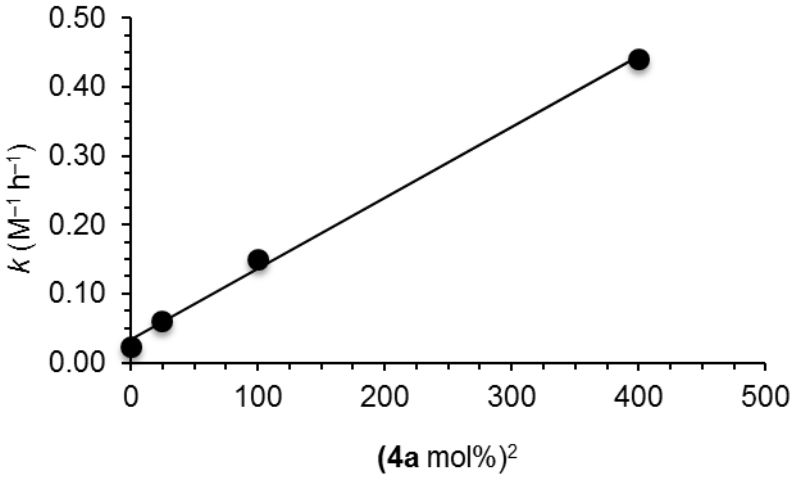

Figure 2. A plot of second-order Friedel–Crafts alkylation rate constants versus the square of the catalyst mol%; a least squares fit of the data affords: k (M^{-1} h^{-1}) = 0.00103 x (**4a** mol%)^2 + 0.33, r^2 = 0.997.

Table 3. Dilution ^{1}H NMR data for **4a** at room temperature in $CDCl_3$.[a]

[**4a**] mM	δNH_1 (ppm)	δNH_2 (ppm)	$\Delta\delta NH_2$(ppm)
5.0	10.15	9.01	0.29
6.7	10.15	9.07	0.23
10	10.17	9.14	0.16
20	10.18	9.30	0.00

[a]Presumably NH_1 and NH_2 in **4a** are attached to the pyridinium and indanol rings, respectively. A plot of NH_2 vs [**4a**] is linear; NH_2 (ppm) = -0.0185 [**4a**] + 0.363, r^2 = 0.982.

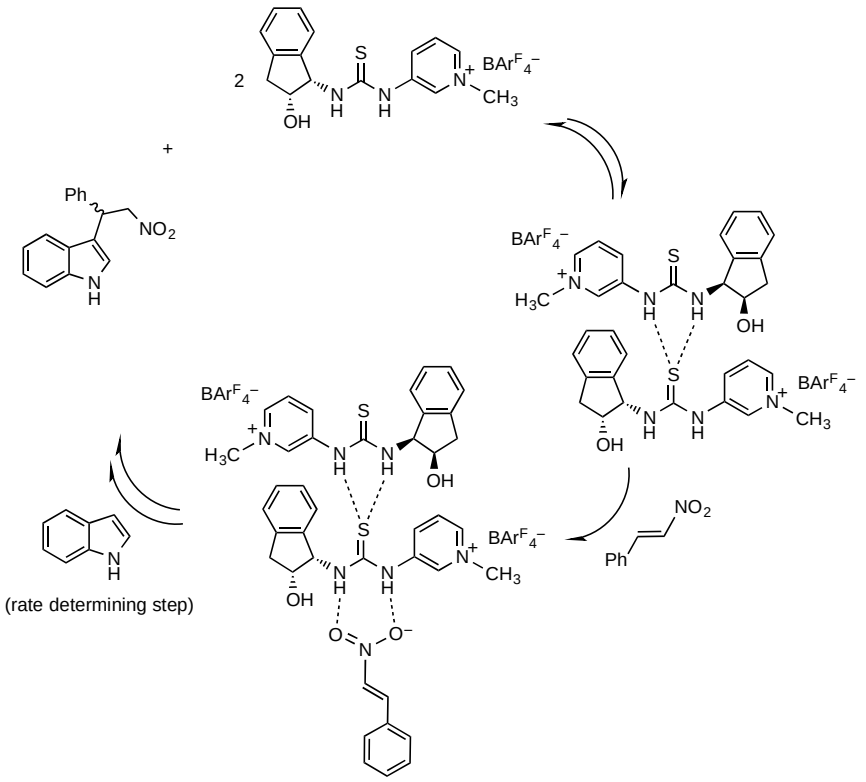

Scheme 4. Proposed catalytic cycle for the Friedel–Crafts alkylation of indole with *trans*-β-nitrostyrene.

To try and gain a better understanding of the structure-reactivity and selectivity correlation in this enantioseletive Friedel–Crafts alkylation,[21] a series of modified catalyst structures **4a**-**4h** and **4a'** were examined.[22] Variations in the achiral positively charged ring structure, the alkyl group attached to the aromatic nitrogen atom, and the weakly coordinating counterion were explored. Screening results for these thiourea catalysts at –35 ˚C with a 10 mol% catalyst loading in $CDCl_3$ are summarized in Table 4. The reaction conversions were found to vary widely (i.e., 23% (71 h) to 91% (50 h)) whereas the stereoselectivies spanned a narrow range with *er*s of 88 : 12 to 93 : 7. For the pyridinium

ions, substitution of a methyl group with a larger and more flexible 1-octyl chain at the formally charged nitrogen center led to a small increase in the *er*s from 91 : 9 to 93 : 7 (entries 1 vs 2 and 5 vs 6) but larger decreases in the reaction rates. Methylated quinolinium ion **4c** (entry 3) with an expanded π-system and a larger ring system behaved similarly to the octylated pyridinium ion **4b**, but a combination of these two design

Table 4. Screening results for the Friedel–Crafts alkylation of *trans*-β-nitrostyrene with indole using catalysts **4a-h**, **4a'**, and **5**.[a]

entry	catalyst	*t* (h)	conversion (%)[b]	*er*[c]
1	**4a**	48	76	91 : 9
2	**4b**	48	41	93 : 7
3	**4c**	49	48	93 : 7
4	**4d**	71	23	88 : 12
5	**4e**	48	83	91 : 9
6	**4f**	46	70	93 : 7
7	**4g**	46	41	91 : 9
8	**4h**	50	91	89 : 11
9	**4a'**	45	61	89 : 11
10	**5**	48	trace	–

[a]Standard reaction conditions of ~0.083 M *trans*-β-nitrostyrene and 0.25 M indole were employed. [b]Conversions were determined by ^{1}H NMR on crude reaction mixtures. [c]Enantiomeric ratios were determined by chiral HPLC.

features (i.e., the larger quinoline ring and an octyl substituent) in **4d** led to the smallest reaction conversion and stereoselectivity (entry 4). Incorporation of a phenyl substituent at the 5-position of the pyridinium ion ring in **4a** and **4b** to afford **4e** and **4f**, interestingly, improved the reaction rate without affecting the stereoselectivity (entries 5 and 6). If the

para hydrogen on the phenyl ring of **4e** is replaced by a *tert*-butyl group to afford **4g**, then the reaction conversion is reduced significantly but the *er* is unaffected (entry 7). The catalyst **4h** with a *para*-pyridinium ion center proved to be the most efficient catalyst tested but among the least selective (*er* = 89 : 11, entry 8). Conjugation of the formally charged center with one of the thiourea NH groups presumably makes this derivative the most acidic one studied and accounts for its enhanced reactivity. Finally, replacing the weakly coordinating $BAr^{F}{}_{4}^{-}$ counterion in **4a** with $(C_6F_5)_4B^-$ to afford **4a'** led to a lower product conversion and *er* value (entry 9).

All of the *N*-alkylated positively charged catalysts noted above can be compared to the performance of **5**, an analogous non-charged thiourea with a privileged 3,5-bis(trifluoromethyl)-phenyl substituent. This latter catalyst is at least one to two orders of magnitude less effective than **4a-4h** and **4a'** under the employed reaction conditions as only a trace (< 5%) of the product was observed. Excellent results with catalyst **5** previously have been reported[8a&d] but these reactions were carried out at a higher temperature (–25 vs –35 ˚C) with a larger catalyst loading (20 vs 10 mol%) and at significantly higher reaction concentrations (0.08 vs 0.0083 M catalyst, 0.40 vs 0.083 M *trans*-β-nitrostyrene and 0.60 vs 0.25 M indole). It is not surprising, consequently, that little product conversion with **5** was observed under our reaction conditions. Similar results to ours were obtained by Ganesh and Seidel with **6** (a protonated 2-pyridine containing thiourea) and somewhat greater stereoselectivities were observed with **7**, a related quinolinium thioamide catalyst.[11f] All of these findings reveal the advantage of

charged catalysts, and are in accord with our earlier reports on achiral thioureas and phosphoric acids.[9,10]

To try and further improve the reaction efficiency, several increased reactant concentrations and altered relative ratios were examined with **4b**, **4c**, and **4f**, the three most selective catalysts previously identified (Table 5). This was done in part because we worried that by varying the substrate concentrations the overall polarity of the medium

Table 5. Results for catalyzed Friedel–Crafts alkylations at –35 ˚C using **4b**, **4c** or **4f** and varying substrate concentrations after 48 h.[a]

entry	Concentration (M^{-1})		catalyst (10 mol%)		
	[βNS][b]	[indole]	**4b**	**4c**	**4f**
1	0.083	0.25	41 (93 : 7)[c]	48 (93 : 7)	70 (93 : 7)[d]
2	0.17	0.25	56 (90 : 10)	45 (92 : 8)	73 (92 : 8)
3	0.25	0.375	60 (95 : 5)	58 (92 : 8)	81 (92 : 8)
4	0.25	0.75	99 (92 : 8)[e]	88 (91 : 9)	91 (92 : 8)

[a]Reactant conversions were determined by ^{1}H NMR of the crude reaction mixtures and the enantiomeric ratios were measured by chiral HPLC. [b]βNS = *trans*-β-nitrostyrene. [c]*t*= 49 h. [d]*t*= 46 h. [e]*t*= 72 h.

would be perturbed since $CDCl_3$ is a low-polarity solvent, and the stereoselectivity might be negatively impacted. This concern was not born out in that all three catalysts gave good enantiomeric ratios and there is little variation with substrate concentration over the range that was examined. Since **4b** led to the highest *er* (95 : 5), this catalyst and the reactant concentrations that led to this result were adopted for examining the scope of this transformation.

Friedel–Crafts alkylations of a series of substituted *trans*-β-nitroalkenes and indoles (eq. 2) were found to afford high yields and good enantioselectivities (Table 6). Substituents on the aromatic ring of the nitrostyrene had relatively little impact upon the reaction rate or the *er* whereas incorporation of an electron donating methoxy group or

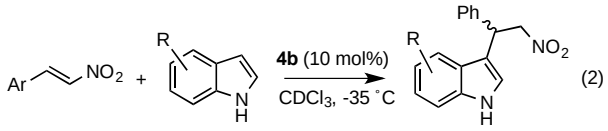

(2)

Table 6. Reaction scope for Friedel–Crafts alkylations catalyzed by **4b** at –35 ˚C using substituted *trans*-β-nitroalkenes and indoles as illustrated in eq. 2.[a]

entry	Ar	R	*t* (h)	Yield[b]	*er*[c]
1	Ph	H	71	76	93 : 7
2	Ph	5-OMe	70	99	91 : 9
3	Ph	6-OMe	70 (5 d)	99 (99)	95 : 5 (92 : 8)[d]
4	Ph	5-Cl	72	35	92 : 8
5	Ph	6-Cl	72	32	89 : 11
6	4-MeC_6H_4	H	70	83	92 : 8
7	2-ClC_6H_4	H	72	91	89 : 11
8	3-BrC_6H_4	H	72	85	92 : 8

[a]Standard conditions of 10 mol% catalyst, 0.083 M *trans*-β-nitrostyrene and 0.25 M indole were used. [b]Determined by ^{1}H NMR of the crude reaction mixtures. [c]Measurements were carried out using chiral HPLC. [d]Parenthetical values are for a larger scale reaction with 1.5 mmol of *trans*-β-nitrostyrene (220 mg), 2.25 mmol of 6-methoxyindole (330 mg), 10 mol% **4b** and 0.075 mmol (12 mg) of hexamethylbenzene as an internal standard in 6.0 mL of $CHCl_3$ at –35 ˚C. Recycled catalyst on ~1/3 of this larger reaction scale gave an 85% yield after 47 h with a 91 : 9 *er*.

an electron withdrawing chlorine atom on to the indole enhanced and retarded the reactivity, respectively. The stereoselectivity, however, was only slightly perturbed and gave good results in each case. A 30 times larger scale reaction under similar conditions was also carried out and gave similar results (parenthetical values in entry 3). The catalyst can also be recovered and reused with little or no falloff in activity and selectivity.

5.3. Conclusion

Asymmetric Friedel–Crafts alkylations of *trans*-β-nitrostyrenes with indoles are promoted by non-protonated positively charged thiourea catalysts (i.e., **4**). These atom economical transformations add molecular complexity via carbon-carbon bond formation in good yields and enantioselectivities. Mechanistic studies reveal a first-order dependence on both reactants and second-order behavior of the catalyst under the employed reaction conditions. These results are consistent with the dimer of the thiourea being the active catalyst and lead to some sensitivity to sterics in **4** on the yield, whereas the enantiomeric ratios are relatively constant. Incorporation of a charged center and the use of salts with non-interactive counteranions as a means of activating catalysts without introducing new N–H or O–H hydrogen bond donating sites offers a promising avenue for catalyst development. It also suggests a method for improving existing catalytic platforms by replacing the privileged 3,5-bis(trifluoromethyl)phenyl substituent with a charged group.

5.4. Experimental

General. Commercially obtained chemicals were used as received from Sigma Aldrich and Alfa Aesar except for tetrakis(3,5-bis(trifluoromethyl)phenyl)borate ($NaBAr^F_4$) and deuterated solvents. These latter materials came from Matrix Scientific and Cambridge Isotope Laboratories, respectively. Oven-dried glassware (i.e., flasks, vials and NMR tubes) was employed for all transformations under an inert atmosphere of argon unless specified otherwise. Thin-layer chromatography was carried out using precoated 250 mm silica gel 60 Å plates and the separated compounds were visualized with a hand held UV lamp. A medium pressure liquid chromatography system with silica gel columns (60 Å, 40-75 μm) was used for purification purposes. Melting points were obtained with a Uni-Melt apparatus in unsealed tubes and are uncorrected. NMR spectra were obtained with a 500 MHz instrument and the respective ^1H and ^{13}C chemical shifts were referenced in ppm as follows: δ 8.03 and 34.9 (DMF-d_7); 7.26 and 77.2 ($CDCl_3$); 5.32 and 53.8 (CD_2Cl_2); 3.31 and 49.0 (CD_3OD); 2.50 and 39.5 (DMSO-d_6); 2.05 and 29.8 (acetone-d_6); 1.94 and 1.3 (CD_3CN); 2.08 (toluene-d_8). A FT-IR with an ATR source was used to obtain IR spectra. High resolution mass spectrometry data were obtained with an ESI TOF instrument using aqueous methanolic and acetonitrile solutions containing polyethylene glycol as an internal standard. Enantiomeric ratios (*er*) were measured with a HPLC and a 25 cm x 4.6 mm (5 μm) RegisCell™ chiral column. Thiourea **5** was prepared as previously described.[8a]

5-(4-tert-Butyl)phenylpyridin-3-amine (**8g**). A mixture of 5-bromopyridin-3-amine (248 mg, 1.43 mmol), $Pd(PPh_3)_4$ (50.4 mg, 43.6 μmol), toluene (3 mL), aqueous sodium carbonate (2 M, 3 mL, 6 mmol), and 4-*tert*-butylphenylboronic acid (285 mg, 1.60 mmol) dissolved in ethanol (3 mL) was heated at 90 ℃ overnight. The reaction mixture was then allowed to cool to ambient temperature and extracted with EtOAc (20 mL × 2). The combined organic material was washed with brine, dried over magnesium sulfate, filtered and concentrated in vacuo. Purification of the residue by column chromatography (10% EtOAc/hexanes to 10% methanol/EtOAc) afforded 255 mg (79%) of **8g** as a white solid (R_f = 0.10 in 33% EtOAc/hexanes, mp 145 – 146 ℃). ^{1}H NMR (500 MHz, $CDCl_3$) δ 8.27 (s, 1H), 8.06 (s, 1H), 7.50 (d, *J* = 8.3 Hz, 4H), 7.14 (s, 1H), 3.84 (br s, 2H), 1.36 (s, 9H). ^{13}C NMR (126 MHz, $CDCl_3$) δ 151.2, 142.6, 138.8, 136.9, 136.2, 135.2, 126.9, 126.0, 119.8, 34.7, 31.4. IR (ATR source): 3427, 3314 cm^{-1}. HRMS-ESI: calcd for $C_{15}H_{19}N_2$ $(M + H)^+$ 227.1543, found 227.1542.

3-Isothiocyanatoisoquinoline (**9c**).[23] Thiophosgene (0.58 mL, 7.6 mmol) was slowly added to a mixture of isoquinolin-3-amine (1.0 g, 6.9 mmol) in water (25 mL) over a period of 5 min at 0 ℃ and the mixture was subsequently stirred at room temperature for 2 h before being diluted with water and extracted with EtOAc (25 mL × 3). The combined organic solution was dried over Na_2SO_4 and concentrated under reduced pressure with a rotary evaporator. Medium pressure liquid chromatography of the residue (10 – 20% EtOAc/hexanes) afforded 0.83 g (64%) of **9c** as a white solid (R_f = 0.30 in 10% EtOAc/hexanes, mp 64 – 65 ℃). ^{1}H NMR (500 MHz, CD_2Cl_2) δ 8.78 (s, 1H), 8.08

(d, *J* = 8.8 Hz, 1H), 7.98 (s, 1H), 7.81 (d, *J* = 8.3 Hz, 1H), 7.74 (t, *J* = 8.3 Hz, 1H), 7.61 (t, *J* = 8.8 Hz, 1H). ^{13}C NMR (126 MHz, CD_2Cl_2) δ 148.0, 146.3, 138.7, 130.4, 130.2, 129.7, 128.1, 127.7, 127.6, 126.0. IR (ATR source): 2021 cm^{-1}. HRMS-ESI: calcd for $C_{10}H_7N_2S$ $(M + H)^+$ 187.0324, found 187.0342.

3-Isothiocyanato-5-phenylpyridine (**9e**). To a solution of 0.90 g (5.3 mmol) of 3-amino-5-phenylpyridine[24] dissolved in 15 mL of chloroform was added an equal volume of saturated aqueous $NaHCO_3$ at room temperature. The resulting solution was stirred and 0.50 mL (6.5 mmol) of thiophosgene in 5 mL of $CHCl_3$ was added dropwise. After 2 h, the reaction mixture was filtered and the aqueous layer was extracted with CH_2Cl_2 (25 mL × 2). The combined organic material was dried over $MgSO_4$ and concentrated under reduced pressure with a rotary evaporator. Medium pressure liquid chromatography of the residue (5% EtOAc/hexanes) afforded 0.68 g (61%) of **9e** as a yellow solid (R_f = 0.15 in 10% EtOAc /hexanes, mp 51 – 52 ℃). ^{1}H NMR (500 MHz, $CDCl_3$) δ 8.72 (d, *J* = 2.0 Hz, 1H), 8.50 (d, *J* = 2.5 Hz, 1H), 7.70 (dd, *J* = 2.0, 2.5 Hz, 1H), 7.56 (d, *J* = 7.4 Hz, 2H), 7.50 (t, *J* = 6.9 Hz, 2H), 7.45 (t, *J* = 6.9 Hz, 1H). ^{13}C NMR (126 MHz, $CDCl_3$) δ 146.2, 145.4, 139.5, 137.5, 136.1, 130.6, 129.7, 129.4, 128.9, 127.2. IR (ATR source): 2039 cm^{-1}. HRMS-ESI: calcd for $C_{12}H_9N_2S$ $(M + H)^+$ 213.0481, found 213.0494.

5-(4-tert-Butyl)phenyl-3-isothiocyanatopyridine (**9g**). To a solution of 0.25 g (1.1 mmol) of **8g** dissolved in 2.5 mL of chloroform was added an equal volume of saturated aqueous $NaHCO_3$ at room temperature. The resulting solution was stirred and 0.11 mL (1.4 mmol)

of thiophosgene in 1 mL of $CHCl_3$ was added dropwise. After 2 h, the reaction mixture was filtered and the aqueous layer was extracted with CH_2Cl_2 (10 mL × 2). The combined organic material was dried over $MgSO_4$ and concentrated under reduced pressure. Medium pressure liquid chromatography of the residue (5 – 30% EtOAc/hexanes) afforded 0.17 g (57%) of **9g** as a yellow solid (R_f = 0.10 in 33% EtOAc/hexanes, mp 113 – 114 ℃). ^{1}H NMR (500 MHz, $CDCl_3$) δ 8.71 (s, 1H), 8.47 (s, 1H), 7.67 (s, 1H), 7.52 (d, *J* = 8.3 Hz, 2H), 7.50 (d, *J* = 8.8 Hz, 2H), 1.37 (s, 9H). ^{13}C NMR (126 MHz, $CDCl_3$) δ 152.3, 146.1, 145.2, 139.4, 137.4, 133.2, 130.4, 129.7, 126.9, 126.4, 34.8, 31.4. IR (ATR source): 2067 cm^{-1}. HRMS-ESI: calcd for $C_{16}H_{17}N_2S$ $(M + H)^+$ 269.1107, found 269.1086.

3-Isothiocyanato-1-methylisoquinolinium iodide (**10c**). In a 6 dram vial, 40 mg (0.22 mmol) of **9c** was dissolved in 1 mL of EtOAc and 0.23 mL (3.7 mmol) of methyl iodide was added at 40 ^{o}C under argon. The reaction mixture was allowed to stir for 72 h and the resulting precipitate was filtered, washed with 1 mL of hexanes and dried under vacuum to afford 30 mg (42%) of **10c** as a yellow solid (mp decomposed over 200 ℃). ^{1}H NMR (500 MHz, DMSO-d_6) δ 9.89 (s, 1H), 9.36 (s, 1H), 8.51 (d, *J* = 8.8 Hz, 1H), 8.40 (d, *J* = 7.8 Hz, 1H), 8.27 (dd, *J* = 7.3, 8.8 Hz, 1H), 8.08 (dd, *J* = 7.3, 7.8 Hz, 1H), 4.63 (s, 3H). ^{13}C NMR (126 MHz, DMSO-d_6) δ 148.9, 141.2, 140.8, 136.4, 135.5, 130.7, 129.9, 128.6, 125.8, 119.2, 45.6. IR (ATR source): 2000 cm^{-1}. HRMS-ESI: calcd for $C_{11}H_9N_2S$ $(M – I)^+$ 201.0481, found 201.0459.

General procedure for preparing 3-isothiocyanato-*N*-octylpyridinium ions 10b, 10d and 10f. In a 6 dram vial, 0.73 mmol of a 3-isothiocyanatopyridine derivative (**9a**,[25] **9c** or **9e**) was dissolved in 1 mL of CH_2Cl_2 and 0.39 g (1.47 mmol) of 1-octyl triflate[26] was added at room temperature under argon. The reaction mixture was allowed to stir overnight and concentrated under reduced pressure. The resulting residue was washed with 2 mL of pentane and dried under vacuum to afford the corresponding product.

3-Isothiocyanato-1-(1-octyl)pyridinium triflate (**10b**). An 86% yield (0.25 g) of this product was obtained as a yellow oil. ^{1}H NMR (500 MHz, $CDCl_3$) δ 8.87 (d, J = 6.3 Hz, 1H), 8.68 (s, 1H), 8.22 (d, J = 8.3 Hz, 1H), 8.07 (dd, J = 6.3, 8.3 Hz, 1H), 4.70 (t, J = 7.3 Hz, 2H), 2.00 (m, 2H), 1.20 - 1.40 (m, 10H), 0.87 (t, J = 6.9 Hz, 3H). ^{13}C NMR (126 MHz, $CDCl_3$) δ 145.3, 142.5, 141.7, 141.2, 134.9, 129.4, 120.5 (q, $J_{C\text{-}F}$ = 315 Hz), 63.0, 31.64, 31.58, 29.0, 28.9, 26.0, 22.6, 14.1. IR (ATR source): 2003 cm^{-1}. HRMS-ESI: calcd for $C_{14}H_{21}N_2S$ $(M - CF_3SO_2)^+$ 249.1420, found 249.1403.

3-Isothiocyanato-1-(1-octyl)isoquinolinium triflate (**10d**). This product was obtained in a 93% yield (0.30 g) as a yellow solid (mp 50 – 52 ℃). ^{1}H NMR (500 MHz, $CDCl_3$) δ 9.38 (s, 1H), 8.87 (s, 1H), 8.32 (d, J = 8.3 Hz, 1H), 8.30 (d, J = 8.3 Hz, 1H), 8.17 (t, J = 8.3 Hz, 1H), 7.93 (t, J = 8.3 Hz, 1H), 5.08 (t, J = 7.8 Hz, 2H), 2.02 (m, 2H), 1.01-1.49 (m, 10H), 0.80 (t, J = 6.4 Hz, 3H). ^{13}C NMR (126 MHz, $CDCl_3$) δ 146.7, 144.0, 141.9, 136.5, 136.0, 131.4, 130.8, 130.2, 128.2, 120.7 (q, $^1J_{F\text{-}C}$ = 321 Hz), 118.6, 59.2, 31.7, 30.3, 29.0,

26.4, 22.6, 14.8, 14.1. IR (ATR source): 1992 cm^{-1}. HRMS-ESI: calcd for $C_{18}H_{23}N_2S$ (M – CF_3SO_2)$^+$ 299.1576, found 299.1569.

3-Isothiocyanato-5-phenyl-1-(1-octyl)pyridinium triflate (**10f**). This product was obtained quantitatively (0.36 g) as a yellow oil. ^{1}H NMR (500 MHz, $CDCl_3$) δ 9.04 (s, 1H), 8.76 (s, 1H), 8.22 (s, 1H), 7.72 (m, 2H), 7.52 (m, 3H), 4.77 (t, *J* = 7.8 Hz, 2H), 1.98 (pentet, *J* = 7.4 Hz, 2H), 1.38-1.12 (m, 10H), 0.83 (t, *J* = 6.9 Hz, 3H). ^{13}C NMR (126 MHz, $CDCl_3$) δ 145.5, 142.8, 140.4, 139.1, 138.3, 135.0, 131.9, 131.3, 130.1, 127.7, 120.8 (q, *J* = 322 Hz), 63.4, 32.0, 31.8, 29.1, 26.1, 22.7, 14.8, 14.2. IR (ATR source): 2010 cm^{-1}. HRMS-ESI: calcd for $C_{20}H_{25}N_2S$ (M – CF_3SO_2)$^+$ 325.1733, found 325.1740.

General procedure for preparing 3-isothiocyanato-*N*-methylpyridinium ions 10e, 10g and 10h. In a 6 dram vial, 0.47 mmol of a 3-isothiocyanatopyridine derivative (**9e**, **9g** or **9h**)[27] was dissolved in 1 mL of EtOAc and 90 μL (1.4 mmol) of iodomethane was added at room temperature under argon. The reaction mixture was allowed to stir overnight and the resulting precipitate was filtered, washed with 2 mL of EtOAc and dried under vacuum to afford the corresponding product.

3-Isothiocyanato-1-methyl-5-phenylpyridinium iodide (**10e**). This product was obtained in a 60% yield (0.10 g) as a pale yellow solid (mp 154 – 155 ℃). ^{1}H NMR (500 MHz, DMSO-d_6) δ 9.36 (s, 1H), 9.26 (s, 1H), 9.01 (s, 1H), 7.92 (d, *J* = 6.9 Hz, 2H), 7.62 (m, 3H), 4.37 (s, 3H). ^{13}C NMR (126 MHz, DMSO-d_6) δ 141.8, 141.4, 141.1, 139.4, 138.7,

132.2, 131.7, 130.5, 129.4, 127.5, 48.4. IR (ATR source): 2035 cm^{-1}. HRMS-ESI: calcd for $C_{13}H_{11}N_2S$ $(M - I)^+$ 227.0637, found 227.0643.

3-Isothiocyanato-1-methyl-5-(4-tert-butyl)phenylpyridinium iodide (**10g**). This product was obtained in a 77% yield (0.15 g) as a yellow solid (mp 205 – 207 ℃). ^1H NMR (500 MHz, DMSO-d_6) δ 9.33 (s, 1H), 9.23 (s, 1H), 8.97 (s, 1H), 7.85 (d, J = 8.8 Hz, 2H), 7.64 (d, J = 8.8 Hz, 2H), 4.36 (s, 3H), 1.33 (s, 9H). ^{13}C NMR (126 MHz, DMSO-d_6) δ 153.4, 141.6, 141.2, 140.9, 139.3, 138.3, 131.7, 129.4, 127.3, 126.3, 48.4, 34.6, 30.9. IR (ATR source): 1989 cm^{-1}. HRMS-ESI: calcd for $C_{17}H_{19}N_2S$ $(M - I)^+$ 283.1263, found 283.1282.

4-Isothiocyanato-1-methylpyridinium iodide (**10h**). This product was obtained in a 66% yield (86 mg) as a yellow solid (mp 152 – 154 ℃). ^1H NMR (500 MHz, CD_3CN) δ 8.60 (d, J = 5.9 Hz, 2H), 7.74 (d, J = 5.9 Hz, 2H), 4.23 (s, 3H). ^{13}C NMR (126 MHz, DMF-d_7) δ 149.6, 145.6, 126.7, 126.1, 66.3. IR (ATR source): 2017 cm^{-1}. HRMS-ESI: calcd for $C_7H_7N_2S$ $(M - I)^+$ 151.0324, found 151.0335; **(**$M - I)^+$ 201.0481, found 201.0459.

General procedure for preparing thiourea catalyst precursors 11a-h. In a 6 dram vial, 0.18 mmol of a 3-isothiocyanato-1-alkylpyridinium ion (**10a-h**) was dissolved in 2 mL of CH_3CN or CH_2Cl_2 and (1*S*,2*R*)-*cis*-1-amino-2-indanol (27 mg, 0.18 mmol) was added at room temperature under argon. The reaction mixture was allowed to stir overnight and was then either (a) concentrated under reduced pressure if no precipitate was present, or (b) filtered if precipitate was present. In the latter case the resulting

residue was washed with 2 mL of pentane and dried under vacuum to afford the corresponding product.

3-(3-((1S,2R)-2-Hydroxy-2,3-dihydro-1H-inden-1-yl)thioureido)-1-methylpyridinium iodide **(11a)**. This compound was obtained in a 90% yield (70 mg) as a pale yellow solid (mp 175 – 178 ℃). ^{1}H NMR (500 MHz, DMSO-d_6) δ 9.47 (s, 1H), 8.70 (d, J = 5.9 Hz, 1H), 8.64 (d, J = 8.8 Hz, 1H), 8.62 (br s, 1H), 8.06 (dd, J = 5.9, 8.8 Hz, 1H), 7.10 - 7.35 (m, 4H), 5.80 (d, J = 3.9 Hz, 1H), 5.52 (d, J = 3.9 Hz, 1H), 4.57 (t, J = 4.4 Hz, 1H), 4.37 (s, 3H), 3.14 (dd, J = 4.4, 16.1 Hz, 1H), 2.87 (d, J = 16.1 Hz, 1H). ^{13}C NMR (126 MHz, DMSO-d_6) δ 180.6, 141.2, 140.6, 139.73, 139.68, 138.3, 136.9, 127.6, 127.0, 126.2, 125.1, 124.1, 71.7, 71.6, 61.5, 48.3. IR (ATR source): 3370, 3329, 3265 cm^{-1}. HRMS-ESI: calcd for $C_{16}H_{18}N_3OS$ $(M - I)^+$ 300.1165, found 300.1167.

3-(3-((1S,2R)-2-Hydroxy-2,3-dihydro-1H-inden-1-yl)thioureido)-1-(1-octyl)pyridinium triflate (**11b**). A 72% yield (71 mg) of **11b** was obtained as a pale yellow solid (mp 53 – 55 °C). ^{1}H NMR (500 MHz, $CDCl_3$) δ 9.98 (s, 1H), 9.69 (s, 1H), 8.38 (d, J = 8.3 Hz, 1H), 8.13 (d, J = 5.9 Hz, 1H), 7.96 (d, J = 8.3 Hz, 1H), 7.59 (dd, J = 5.9, 8.8 Hz, 1H), 7.37 (d, J = 6.4 Hz, 1H), 7.17 (m, 3H), 5.85 (dd, J = 4.4, 7.3 Hz, 1H), 4.75 (t, J = 4.4 Hz, 1H), 4.31 (t, J = 7.4 Hz, 2H), 3.11 (dd, J = 4.9, 16.6 Hz, 1H), 2.92 (d, J = 16.6 Hz, 1H), 1.91 (m, 2H), 1.27 (m, 10H), 0.86 (t, J = 4.9 Hz, 3H). ^{13}C NMR (126 MHz, $CDCl_3$) δ 181.2, 141.4, 140.5, 140.2, 137.0, 136.8, 136.4, 128.3, 127.5, 127.1, 125.4, 124.8, 120.3 (q, $J_{C\text{-}F}$ = 320 Hz), 73.3, 62.8, 39.8, 31.8, 31.2, 29.1, 29.0, 26.1, 24.3, 22.7, 14.2. IR (ATR

source): 3372, 3266 cm^{-1}. HRMS-ESI: calcd for $C_{23}H_{32}N_3OS$ $(M - CF_3SO_2)^+$ 398.2261, found 398.2259.

3-(3-((1S,2R)-2-Hydroxy-2,3-dihydro-1H-inden-1-yl)thioureido)-1-methylisoquinolinium iodide (**11c**). This product was obtained in a 67% yield (58 mg) as a yellow solid (mp 157 – 159 ℃). ^{1}H NMR (500 MHz, CD_3OD) δ 10.03 (s, 1H), 9.00 (s, 1H), 8.41 (d, *J* = 8.8 Hz, 1H), 8.31 (d, *J* = 8.3 Hz, 1H), 8.16 (dd, *J* = 7.3, 8.3 Hz, 1H), 7.98 (dd, *J* = 7.3, 8.8 Hz, 1H), 7.44 (d, *J* = 5.4 Hz, 1H), 7.26 (d, *J* = 5.4 Hz, 1H), 7.20 (m, 2H), 5.97 (d, *J* = 4.4 Hz, 1H), 4.74 (dd, *J* = 4.4, 4.9 Hz, 1H), 4.68 (s, 3H), 3.20 (dd, *J* = 4.9, 16.1 Hz, 1H), 2.98 (d, *J* = 16.1 Hz, 1H). ^{13}C NMR (126 MHz, CD_3OD) δ 184.2, 149.1, 142.1, 141.8, 138.2, 137.0, 136.1, 135.4, 131.5, 131.1, 131.0, 129.2, 127.9, 126.5, 125.6, 119.8, 66.9, 64.0, 46.7, 41.0. IR (ATR source): 3372, 3329, 3266 cm^{-1}. HRMS-ESI: calcd for $C_{20}H_{20}N_3OS$ $(M - I)^+$ 350.1322, found 350.1327.

3-(3-((1S,2R)-2-Hydroxy-2,3-dihydro-1H-inden-1-yl)thioureido)-1-(1-octyl)isoquinolinium triflate (**11d**). This product was obtained in a 64% yield (69 mg) as a yellow solid (mp 50 – 52 ℃). ^{1}H NMR (500 MHz, CD_2Cl_2) δ 10.16 (s, 1H), 9.91 (s, 1H), 8.46 (s, 1H), 8.02 – 8.10 (m, 3H), 7.99 (d, *J* = 7.3 Hz, 1H), 7.87 (t, , *J* = 6.9 Hz, 1H), 7.42 (d, *J* = 7.8 Hz, 1H), 7.02 (d, *J* = 7.3 Hz, 1H), 6.84 (t, *J* = 7.4 Hz, 1H), 6.64 (t, *J* = 7.4 Hz, 1H), 5.73 (t, *J* = 6.4 Hz, 1H), 4.94 (t, *J* = 4.4 Hz, 1H), 4.86 (m, 1H), 4.74 (m, 1H), 3.12 (dd, *J* = 3.9, 16.6 Hz, 1H), 2.97 (d, *J* = 16.6 Hz, 1H), 2.10 (m, 2H), 1.52 (m, 2H), 1.19 – 1.44 (m, 8H), 0.87 (t, *J* = 6.4 Hz, 3H). ^{13}C NMR (126 MHz, CD_2Cl_2) δ 182.8, 147.2, 140.4, 140.1,

135.8, 134.9, 133.7, 130.4, 130.0, 129.8, 127.6, 126.5, 124.8, 124.6, 124.5, 120.5 (q, $^{1}J_{F\text{-}C}$ = 321 Hz), 116.3, 73.1, 63.0, 58.5, 39.9, 31.7, 29.8, 29.0, 26.6, 22.6, 18.6, 13.8. IR (ATR source): 3372, 3329, 3266 cm^{-1}. HRMS-ESI: calcd for $C_{27}H_{34}N_3OS$ $(M - CF_3SO_2)^+$ 448.2417, found 448.2396.

3-(3-((1S,2R)-2-Hydroxy-2,3-dihydro-1H-inden-1-yl)thioureido)-1-methyl-5-phenylpyridinium iodide (**11e**). This product was obtained in a 97% yield (88 mg) as a pale yellow solid (mp 160 – 162 ℃). ^{1}H NMR (500 MHz, CD_3OD) δ 9.48 (s, 1H), 8.91 (s, 1H), 8.89 (s, 1H), 7.80 (d, *J* = 7.8 Hz, 2H), 7.60 – 7.45 (m, 3H), 7.40 (d, *J* = 7.3 Hz, 1H), 7.28 – 7.11 (m, 3H), 5.94 (d, 1H), 4.71 (t, *J* = 4.4 Hz, 1H), 4.43 (s, 3H), 3.16 (dd, *J* = 4.4, 16.6 Hz, 1H), 2.95 (d, *J* = 16.7 Hz, 1H). ^{13}C NMR (126 MHz, CD_3OD) δ 182.6, 141.9, 141.8, 141.7, 141.4, 138.6, 137.3, 134.9, 134.6, 131.4, 130.7, 129.0, 128.5, 127.7, 126.3, 125.4, 73.6, 63.5, 49.7, 40.9. IR (ATR source): 3329, 3253 cm^{-1}. HRMS-ESI: calcd for $C_{22}H_{22}N_3OS$ $(M - I)^+$ 376.1478, found 376.1491.

3-(3-((1S,2R)-2-Hydroxy-2,3-dihydro-1H-inden-1-yl)thioureido)-1-(1-octyl)-5-phenylpyridinium triflate (**11f**). This product was obtained in a 85% yield (95 mg) as a pale yellow solid (mp 73 – 76 ℃). ^{1}H NMR (500 MHz, $CDCl_3$) δ 9.97 (s, 1H), 9.46 (s, 1H), 8.78 (s, 1H), 8.37 (s, 1H), 8.02 (d, *J* = 8.3 Hz, 1H), 7.63 (d, *J* = 5.4 Hz, 2H), 7.48 (m, 3H), 7.39 (d, *J* = 6.8 Hz, 1H), 7.20-7.10 (m, 3H), 5.89 (dd, *J* = 4.9, 6.9 Hz, 1H), 4.79 (t, *J* = 4.7 Hz, 1H), 4.39 (m, 2H), 3.97 (d, *J* = 5.9 Hz, 1H), 3.11 (dd, *J* = 4.9, 16.6 Hz, 1H), 2.88 (d, *J* = 16.6 Hz, 1H), 1.95 (t, *J* = 6.4 Hz, 2H), 1.40-1.11 (m, 10H), 0.87 (t, *J* =

6.4 Hz, 3H). ^{13}C NMR (126 MHz, $CDCl_3$) δ 181.4, 141.4, 140.9, 140.3, 139.8, 135.4, 134.8, 134.2, 132.8, 130.7, 129.9, 128.3, 127.4, 127.1, 125.3, 124.8, 120.3 (q, *J* = 320 Hz), 73.5, 63.0, 57.6, 39.5, 31.8, 31.4, 29.1, 26.1, 22.7, 14.8, 14.2. IR (ATR source): 3315 cm^{-1}. HRMS-ESI: calcd for $C_{29}H_{36}N_3OS$ $(M - CF_3SO_2)^+$ 474.2574, found 474.2558.

5-(4-tert-Butyl)phenyl-3-(3-((1S,2R)-2-hydroxy-2,3-dihydro-1H-inden-1-yl)thioureido)-1-methylpyridinium iodide (**11g**). This product was obtained in 75% (82 mg) as a pale yellow solid (mp 145 – 148 ℃). ^{1}H NMR (500 MHz, $CDCl_3$) δ 9.51 (s, 1H), 9.09 (s, 1H), 8.35 (s, 1H), 8.32 (d, *J* = 7.8 Hz, 1H), 7.63 (d, *J* = 7.8 Hz, 2H), 7.54 (d, *J* = 7.8 Hz, 2H), 7.50 (d, *J* = 7.8 Hz, 1H), 7.21 – 7.10 (m, 4H), 5.86 (t, *J* = 4.9 Hz, 1H), 4.84 (t, *J* = 4.9 Hz, 1H), 4.23 (d, *J* = 5.9 Hz, 1H), 4.20 (s, 3H), 3.14 (dd, *J* = 4.9, 16.6 Hz, 1H), 3.00 (d, *J* = 16.6 Hz, 1H), 1.35 (s, 9H). ^{13}C NMR (126 MHz, acetone-d_6) δ 181.9, 154.3, 141.8, 141.6, 140.1, 137.9, 135.6, 133.0, 131.4, 128.5, 127.9, 127.4, 127.2, 125.9, 125.4, 111.0, 73.4, 63.2, 49.8, 40.5, 35.4, 31.4. IR (ATR source): 3242 cm^{-1}. HRMS-ESI: calcd for $C_{26}H_{30}N_3OS$ $(M - I)^+$ 432.2104, found 432.2128.

4-(3-((1S,2R)-2-Hydroxy-2,3-dihydro-1H-inden-1-yl)thioureido)-1-methylpyridinium iodide (**11h**). This product was obtained in a 65% (50 mg) yield as a yellow solid (mp 138 – 140 ℃). ^{1}H NMR (500 MHz, CD_3CN) δ 10.95 (s, 1H), 8.59 (d, *J* = 6.9 Hz, 2H), 8.56 (s, 1H), 8.26 (d, *J* = 7.3 Hz, 2H), 7.67 (d, *J* = 9.8 Hz, 1H), 7.41 (d, *J* = 7.3 Hz, 1H), 7.28 (t, *J* = 7.3 Hz, 1H), 7.22 (t, *J* = 7.3 Hz, 1H), 5.90 (dd, *J* = 4.9, 8.3 Hz, 1H), 4.71 (t, *J* = 4.9 Hz, 1H), 4.06 (s, 3H), 3.45 (s, 1H), 3.19 (dd, *J* = 4.9, 16.7 Hz, 1H), 2.94 (d, *J* = 16.6

Hz, 1H). ^{13}C NMR (126 MHz, DMSO-d_6) δ 179.4, 152.5, 145.1, 140.8, 140.7, 127.8, 126.3, 125.2, 124.2, 114.5, 71.6, 61.5, 46.0, 39.9. IR (ATR source): 3375, 3329, 3268 cm^{-1}. HRMS-ESI: calcd for $C_{16}H_{18}N_3OS$ $(M - I)^+$ 300.1165, found 300.1183.

General procedure for preparing thiourea catalysts 4a-h and 4a'. To a 6 dram vial, 21 mg (24 μmol) of sodium tetrakis(3,5-bis(trifluoromethyl)phenyl)borate or 17 mg (24 μmol) of potassium tetrakis(pentafluorophenyl)borate, 24 μmol of a thiourea catalyst precursor (**11a, c-h**) and 1 mL of CH_2Cl_2 were added. This mixture was stirred at room temperature under an argon atmosphere until the solid material was totally dissolved and a cloudy suspension formed. Stirring was then stopped and the solution was left undisturbed until a white solid precipitated and a clear solution formed. The reaction mixture was then filtered and concentrated under reduced pressure. The resulting residue was washed with 2 mL of pentane and dried under vacuum to afford the corresponding product.

3-(3-((1S,2R)-2-Hydroxy-2,3-dihydro-1H-inden-1-yl)thioureido)-1-methylpyridinium tetrakis(3,5-bis(trifluoromethyl)phenyl)borate (**4a**). The title compound was obtained in an 86% yield (24 mg) as a pale yellow solid (mp 70 – 73 °C). ^{1}H NMR (500 MHz, CD_2Cl_2) δ 10.00 (s, 1H), 8.14 (s, 1H), 8.02 (d, J = 5.9 Hz, 1H), 7.75 (s, 8H), 7. 80 – 7.45 (m, 3H), 7.59 (s, 4H), 7.38 (d, J = 7.4 Hz, 1H), 7.28 (m, 3H), 5.96 (s, 1H), 4.78 (d, J =4.9 Hz, 1H), 4.31 (s, 3H), 3.26 (dd, J = 4.9, 16.7 Hz, 1H), 2.95 (d, J = 16.2 Hz, 1H) ^{13}C NMR (126 MHz, CD_2Cl_2) δ 180.8, 162.1 (q, $^1J_{B\text{-}C}$ = 49.5 Hz), 141.6, 140.1, 139.7, 137.9, 137.7,

136.8, 135.2 (q, $^{2}J_{B\text{-}C}$ = 31.3 Hz), 129.3 (qq, $^{3}J_{B\text{-}C}$ = 3.0 Hz and $^{2}J_{F\text{-}C}$ = 31.3 Hz), 128.4, 127.8, 127.7, 125.0, 124.9 (q, $^{1}J_{F\text{-}C}$ = 272 Hz), 124.7, 117.9 (q, $^{3}J_{F\text{-}C}$ = 2.0 Hz), 67.5, 62.9, 49.8, 40.4. IR (ATR source): 3334 cm^{-1}. HRMS-ESI: calcd for $C_{16}H_{18}N_3OS$ (M – $C_{32}H_{12}BF_{24})^{+}$ 300.1165, found 300.1181.

3-(3-((1S,2R)-2-Hydroxy-2,3-dihydro-1H-inden-1-yl)thioureido)-1-(1-octyl)pyridinium tetrakis (3, 5-bis(trifluoromethyl)phenyl)borate **(4b)**. This catalyst was obtained in an 81% yield (25 mg) as a pale yellow solid (mp 51 – 53 °C). ^{1}H NMR (500 MHz, CD_2Cl_2) δ 10.23 (s, 1H), 8.93 (s, 1H), 7.80 (d, *J* = 5.9 Hz, 1H), 7.72 (s, 8H), 7.69 (s, 1H), 7.54 (s, 4H), 7.50 (m, 1H), 7.41 (dd, *J* = 5.9, 8.3 Hz, 1H), 7.36 (d, *J* = 7.4 Hz, 1H), 7.20 – 7.33 (m, 3H), 5.95 (s, 1H), 4.81 (s, 1H), 4.35 (t, *J* = 6.8 Hz, 2H), 3.29 (d, *J* = 16.1 Hz, 1H), 2.98 (d, *J* = 16.0 Hz, 1H), 2.18 (br s, 1H), 2.02 (m, 2H), 1.10 – 1.40 (m, 10H), 0.88 (t, *J* = 6.4 Hz, 3H). ^{13}C NMR (126 MHz, CD_2Cl_2) δ 181.0, 162.2 (q, $^{1}J_{B\text{-}C}$ = 49.1 Hz), 141.8, 140.1, 137.3, 136.9, 136.7, 136.6, 136.5, 136.3, 135.3 (q, $^{2}J_{B\text{-}C}$ = 35.3 Hz), 129.3 (qq, ^{3}JB-C = 3.0 Hz and ^{2}JF-C = 31.3 Hz), 128.4, 128.1, 125.9, 125.0 (q, $^{1}J_{F\text{-}C}$ = 273 Hz), 117.9 (q, $^{3}J_{F\text{-}C}$ = 2.0 Hz), 74.2, 63.9, 40.4, 31.9, 31.6, 29.2, 29.1, 26.3, 22.9, 22.8, 14.2. IR (ATR source): 3427, 3300 cm^{-1}. HRMS-ESI: calcd for $C_{23}H_{32}N_3OS$ (M – $C_{32}H_{12}BF_{24})^{+}$ 398.2261, found 398.2251.

3-(3-((1S,2R)-2-Hydroxy-2,3-dihydro-1H-inden-1-yl)thioureido)-1-methylisoquinolinium tetrakis(3,5-bis(trifluoromethyl)phenyl)borate (**4c**). This product was obtained in an 86% yield (25 mg) as a yellow solid (mp 75 – 77 ℃). ^{1}H NMR (500 MHz, CD_2Cl_2) δ 9.95 (s,

1H), 9.35 (s, 1H), 8.74 (s, 1H), 8.00 – 8.15 (m, 3H), 7.92 (t, *J* = 6.9 Hz, 1H), 7.80 (s, 1H), 7.75 (s, 8H), 7.57 (s, 4H), 7.42 (d, *J* = 7.4 Hz, 1H), 7.00 – 7.24 (m, 3H), 5.97 (s, 1H), 4.79 (s, 1H), 4.52 (s, 3H), 3.23 (dd, *J* = 4.4, 16.6 Hz, 1H), 2.94 (d, *J* = 16.1 Hz, 1H), 2.92 (br s, 1H). ^{13}C NMR (126 MHz, CD_2Cl_2) δ 182.4, 162.1 (q, $^1J_{B\text{-}C}$ = 49.1 Hz), 146.1, 140.2, 137.3, 135.7, 135.2 (q, $^2J_{B\text{-}C}$ = 32.7 Hz), 134.6, 131.5, 131.3, 130.5, 130.3, 129.8, 129.2 (qq, $^3J_{B\text{-}C}$ = 3.0 Hz and $^2J_{F\text{-}C}$ = 32.8 Hz), 127.6, 127.5, 125.8, 125.1 (q, $^1J_{F\text{-}C}$ = 276 Hz), 125.0, 124.7, 117.9 (q, $^3J_{F\text{-}C}$ = 2.0 Hz), 74.3, 68.3, 46.3, 40.2. IR (ATR source): 3411, 3317 cm^{-1}. HRMS-ESI: calcd for $C_{20}H_{20}N_3OS$ $(M - C_{32}H_{12}BF_{24})^+$ 350.1322, found 350.1298.

3-(3-((1S,2R)-2-Hydroxy-2,3-dihydro-1H-inden-1-yl)thioureido)-1-(1-octyl)isoquino-linium tetra-kis(3,5-bis(trifluoromethyl)phenyl)borate (**4d**). This product was obtained in a 67% yield (21 mg) as a yellow solid (mp 56 – 58 ℃). ^{1}H NMR (500 MHz, CD_3OD) δ 10.14 (s, 1H), 8.80 (s, 1H), 8.41 (d, *J* = 8.8 Hz, 1H), 8.24 (d, *J* = 7.9 Hz, 1H), 8.09 (t, *J* = 7.4 Hz, 1H), 7.88 (t, *J* = 7.8 Hz, 1H), 7.64 (s, 8H), 7.60 (s, 4H), 7.42 (s, 1H), 7.31 - 7.00 (m, 4H), 5.98 (s, 1H), 5.04 (t, *J* = 6.8 Hz, 2H), 4.74 (d, *J* = 4.9 Hz, 1H), 3.19 (dd, *J* = 4.4, 16.1 Hz, 1H), 2.99 (d, *J* = 16.1 Hz, 1H), 2.12 (m, 2H), 2.01 (br s, 1H), 1.52 (m, 2H), 1.42 – 1.14 (m, 8H), 0.82 (t, *J* = 6.4 Hz, 3H). ^{13}C NMR (126 MHz, CD_3OD) δ 184.4, 163.0 (q, $^1J_{B\text{-}C}$ = 50.5, Hz) 148.8, 142.1, 141.8, 138.1, 136.4, 136.0, 135.4, 131.6, 131.4, 130.6 (qq, $^3J_{B\text{-}C}$ = 3.0 Hz and $^2J_{F\text{-}C}$ = 33.3 Hz), 129.2, 128.0, 127.9, 126.6, 126.5, 125.9 (q, $^1J_{F\text{-}C}$ = 273 Hz), 125.5, 119.6, 118.6 (q, $^1J_{F\text{-}C}$ = 3.0 Hz), 73.9, 64.1, 59.6, 41.0, 32.9, 31.1, 30.8,

30.3, 27.7, 23.7, 14.5. IR (ATR source): 3287 cm^{-1}. HRMS-ESI: calcd for $C_{27}H_{34}N_3OS$ $(M - C_{32}H_{12}BF_{24})^+$ 448.2417, found 448.2427.

3-(3-((1S,2R)-2-Hydroxy-2,3-dihydro-1H-inden-1-yl)thioureido)-1-methyl-5-phenylpyridinium tetrakis(3,5-bis(trifluoromethyl)phenyl)borate (**4e**). This product was obtained in an 89% yield (26 mg) as a yellow solid (mp 68 – 71 ℃). ^{1}H NMR (500 MHz, $CDCl_3$) δ 9.63 (s, 1H), 9.24 (s, 1H), 8.49 (s, 1H), 8.10 (s, 1H), 7.71 (s, 8H), 7.65 (s, 1H), 7.56 – 7.41 (m, 5H), 7.53 (s, 4H), 7.32 (d, *J* = 6.9 Hz, 1H), 7.28 – 7.13 (m, 3H), 5.93 (s, 1H), 4.76 (s, 1H), 4.19 (s, 3H), 3.22 (d, *J* = 16.2 Hz, 1H), 2.87 (d, *J* = 15.6 Hz, 1H), 2.53 (s, 1H). ^{13}C NMR (126 MHz, CD_2Cl_2) δ 180.7, 161.8 (q, $^1J_{B\text{-}C}$ = 50.5, Hz), 142.4, 141.3, 139.8, 139.4, 135.4, 135.3, 134.8 (q, $^2J_{B\text{-}C}$ = 31.3 Hz), 134.3, 132.1, 131.5, 131.1, 130.3, 129.9, 128.9 (qq, $^3J_{B\text{-}C}$ = 3.0 Hz and $^2J_{F\text{-}C}$ = 33.3 Hz), 127.3, 126.9, 124.6 (q, $^1J_{F\text{-}C}$ = 273 Hz), 124.5, 117.5 (q, $^3J_{F\text{-}C}$ = 3.0 Hz), 74.0, 62.6, 49.5, 40.1. IR (ATR source): 3336 cm^{-1}. HRMS-ESI: calcd for $C_{22}H_{22}N_3OS$ $(M - C_{32}H_{12}BF_{24})^+$ 376.1478, found 376.1479.

3-(3-((1S,2R)-2-Hydroxy-2,3-dihydro-1H-inden-1-yl)thioureido)-1-(1-octyl)-5-phenylpyridinium tetrakis(3,5-bis(trifluoromethyl)phenyl)borate (**4f**). This product was obtained in an 87% yield (28 mg) as a yellow solid (mp 58 – 61 ℃). ^{1}H NMR (500 MHz, $CDCl_3$) δ 9.95 (s, 1H), 9.28 (s, 1H), 8.25 (s, 1H), 8.17 (s, 1H), 7.71 (s, 9H), 7.51 (s, 4H), 7.55-7.40 (m, 5H), 7.36 (d, *J* = 7.4 Hz, 1H), 7.32-7.20 (m, 3H), 5.98 (s, 1H), 4.79 (s, 1H), 4.44 (t, *J* = 6.9 Hz, 2H), 3.27 (d, *J* = 15.6 Hz, 1H), 2.94 (d, *J* = 15.6 Hz, 1H), 2.68 (br s, 1H), 2.08 (t, *J* = 7.3 Hz, 2H), 1.44-1.18 (m, 10H), 0.87 (t, *J* = 4.9 Hz, 3H). ^{13}C NMR (126

MHz, CD_3OD) δ 183.0, 162.9 (q, $^1J_{B\text{-}C}$ = 50.5, Hz), 142.4, 142.3, 141.7, 137.5, 137.2, 135.8, 135.3, 134.7, 131.5, 130.8, 130.4 (qq, $^3J_{B\text{-}C}$ = 3.0 Hz and $^2J_{F\text{-}C}$ = 32.3 Hz), 129.1, 128.5, 127.7, 126.4, 126.0, 125.8 (q, $^1J_{F\text{-}C}$ = 272 Hz), 125.4, 118.5 (q, $^3J_{F\text{-}C}$ = 3.0 Hz), 73.6, 63.6, 47.9, 40.9, 32.8, 32.4, 30.1, 30.0, 27.2, 23.6, 14.3. IR (ATR source): 3340, 3163 cm^{-1}. HRMS-ESI: calcd for $C_{29}H_{36}N_3OS$ $(M - C_{32}H_{12}BF_{24})^+$ 474.2574, found 474.2572.

3-(3-((1S,2R)-2-Hydroxy-2,3-dihydro-1H-inden-1-yl)thioureido)-1-methyl-5-(4-tert-butyl)-phenylpyridinium tetrakis(3,5-bis(trifluoromethyl)phenyl)borate (**4g**). This product was obtained in an 88% yield (27 mg) as a yellow solid (mp 70 – 72 ℃). ^{1}H NMR (500 MHz, acetone-d_6) δ 10.22 (s, 1H), 9.72 (s, 1H), 9.15 (s, 1H), 8.94 (s, 1H), 8.27 (s, 1H), 7.81 (s, 8H), 7.77-7.62 (m, 4H), 7.69 (s, 4H), 7.43 (d, *J* = 6.9 Hz, 1H), 7.29-7.19 (m, 3H), 6.02 (s, 1H), 4.79 (t, *J* = 5.4 Hz, 1H), 4.71 (s, 3H), 4.55 (s, 1H), 3.25 (dd, *J* = 4.4, 16.6 Hz, 1H), 2.99 (d, *J* = 16.6 Hz, 1H), 1.37 (s, 9H). ^{13}C NMR (126 MHz, acetone-d_6) δ 182.3, 162.6 (q, $^1J_{B\text{-}C}$ = 49.5, Hz), 154.7, 141.7, 141.6, 141.0, 138.7, 137.4, 135.5, 135.0, 131.5, 130.0 (qq, $^3J_{B\text{-}C}$ = 3.0 Hz and $^2J_{F\text{-}C}$ = 31.3 Hz), 128.7, 128.0, 127.6, 127.4, 127.3, 126.1, 125.4 (q, $^1J_{F\text{-}C}$ = 273 Hz), 125.3, 118.5 (q, $^3J_{F\text{-}C}$ = 3.0 Hz), 73.4, 63.2, 49.7, 44.0, 41.0, 31.3. IR (ATR source): 3325, 3163 cm^{-1}. HRMS-ESI: calcd for $C_{26}H_{30}N_3OS$ $(M - C_{32}H_{12}BF_{24})^+$ 432.2104, found 432.2107.

4-(3-((1R,2S)-2-Hydroxy-2,3-dihydro-1H-inden-1-yl)thioureido)-1-methylpyridinium tetrakis(3,5-bis(trifluoromethyl)phenyl)borate (**4h**). This product was obtained in a 73%

yield (20 mg) as a pale yellow solid (mp 109 – 111 ℃). ^{1}H NMR (500 MHz, CD_3OD) δ 8.49 (d, *J* = 6.9 Hz, 2H), 8.43 (d, *J* = 7.4 Hz, 2H), 7.60 (s, 12H), 7.37 (d, *J* = 7.3 Hz, 1H), 7.29-7.06 (m, 3H), 5.96 (d, *J* = 4.9 Hz, 1H), 4.74 (t, *J* = 4.9 Hz, 1H), 4.16 (s, 3H), 3.22 (dd, *J* = 4.9, 16.6 Hz, 1H), 2.98 (d, *J* = 16.6 Hz, 1H). ^{13}C NMR (126 MHz, CD_3OD) δ 181.4, 162.9 (q, $^{1}J_{B\text{-}C}$ = 49.4, Hz), 155.1, 145.8, 141.8, 141.5, 135.8, 130.4 (qq, $^{3}J_{B\text{-}C}$ = 3.0 Hz and $^{2}J_{F\text{-}C}$ = 31.3 Hz), 129.2, 127.8, 126.4, 125.8 (q, $^{1}J_{F\text{-}C}$ = 272 Hz), 125.3, 118.5 (q, $^{3}J_{F\text{-}C}$ = 3.0 Hz), 115.9, 73.5, 63.3, 46.6, 41.0. IR (ATR source): 3229 cm^{-1}. HRMS-ESI: calcd for $C_{16}H_{18}N_3OS$ $(M - C_{32}H_{12}BF_{24})^{+}$ 300.1165, found 300.1176.

3-(3-((1S,2R)-2-Hydroxy-2,3-dihydro-1H-inden-1-yl)thioureido)-1-methylpyridinium tetrakis(pentafluorophenyl)borate (**4a'**). This product was obtained in an 87% yield (20 mg) as a pale yellow solid (mp 74 – 77 ℃). ^{1}H NMR (500 MHz, acetone-d_6) δ 10.16 (br s, 1H), 9.89 (s, 1H), 8.80 (d, *J* = 6.4 Hz, 1H), 8.73 (d, *J* = 8.3 Hz, 1H), 8.22 (s, 1H), 8.16 (dd, *J* = 5.9, 8.4 Hz, 1H), 7.40 (d, *J* = 7.4 Hz, 1H), 7.30-7.09 (m, 3H), 5.98 (s, 1H), 4.77 (t, *J* = 4.9 Hz, 1H), 4.65 (s, 3H), 4.57 (s, 1H), 3.23 (dd, *J* = 4.9, 16.6 Hz, 1H), 2.98 (*J* = 16.6 Hz, 1H). ^{13}C NMR (126 MHz, CD_2Cl_2) δ 180.9, 148.4 (d, $J_{o\text{-}FC}$ = 241 Hz), 140.9 (d, $J_{p\text{-}FC}$ = 196 Hz), 139.5, 137.3, 136.6 (d, $J_{m\text{-}FC}$ = 242 Hz), 136.3, 136.2, 128.9, 128.2, 127.9, 127.6, 125.9, 124.9, 124.7 (*ipso*-C), 124.0, 74.6, 62.9, 49.6, 40.2. IR (ATR source): 3331 cm^{-1}. HRMS-ESI: calcd for $C_{16}H_{18}N_3OS$ $(M - C_{24}BF_{20})^{+}$ 300.1165, found 300.1185.

Representative procedure for the catalytic enantioselective Friedel–Crafts alkylation of *trans*-β-nitroalkenes with indoles (see eq. 2). Oven-dried NMR tubes were charged with 0.050 mmol of a trans-β-nitroalkene, 0.15 mmol of the desired indole and 0.005 mmol (10 mol%) of the catalyst in 0.6 mL of $CDCl_3$ at –35 ˚C under an inert atmosphere. Reaction conversions were obtained at different times by ^1H NMR using the indole and the alkylation product resonances as indicated in Table S1. Second-order rates constants were obtained using the integrated rate law (i.e., $\ln([\text{indole}][\beta\text{-nitrostyrene}]_0/[\beta\text{-nitrostyrene}][\text{indole}]_0) = k([\text{indole}]_0 - [\beta\text{-nitrostyrene}]_0)t$) where $[\beta\text{-nitrostyrene}]_0$ and $[\text{indole}]_0$ are the initial concentrations and [β-nitrostyrene] and [indole] are the concentrations at different times. The resulting kinetic data are given in Table S2. The catalyst can be recovered by normal phase MPLC using CH_2Cl_2/MeOH (95 : 5).

Bibliography

References for Chapter 1

1. Taylor, M. S.; Jacobsen, E. N. *Angew. Chem. Int. Ed.* **2006**, *45*, 1520-1543.

2. (a) Arunan, E.; Desiraju, G. R.; Klein, R. A.; Sadlej, J.; Scheiner, S.; Alkorta, I.; Clary, D. C.; Crabtree, R. H.; Dannenberg, J. J.; Hobza, P.; Kjaergaard, H. G.; Legon, A. C.; Mennucci, B.; Nesbitt, D. J. *Pure Appl. Chem.* **2011**, *83*, 1637-1641; (b) Perrin, C. L.; Nielson, J. B. *Annu. Rev. Phys. Chem.* **1997**, *48*, 511-544.

3. Miller, C. *Nature* **2006**, *440*, 484.

4. (a) Etter, M. C. *Acc. Chem. Res.* **1990**, *23*, 120-126; (b) Etter, M. C. *J. Phys. Chem.* **1991**, *95*, 4601-4610.

5. Wilcox, C. S.; Adrian, J. C.; Webb, T. H.; Zawacki, F. J. *J. Am. Chem. Soc.* **1992**, *114*, 10189-10197.

6. (a) Wharton, C. W. *Comprehensive Biological Catalysis*. Acad. Press: London, 1998; Vol. 1, pp 345-379; (b) Zhang, X.; Houk, K. N. *Acc. Chem. Res.* **2005**, *38*, 379-385.

7. Lee, A. Y.; Stewart, J. D.; Clardy, J.; Ganem, B. *Chemistry & biology* **1995**, *2*, 195-203.

8. Wong, C.-H.; Halcomb, R. L.; Ichikawa, Y.; Kajimoto, T. *Angew. Chem. Int. Ed.* **1995**, *34*, 521-546.

9. Hine, J.; Linden, S. M.; Kanagasabapathy, V. M. *J. Org. Chem.* **1985**, *50*, 5096-5099.

10. (a) Schreiner, P. R. *Chem. Soc. Rev.* **2003**, *32*, 289-296; (b) Akiyama, T.; Itoh, J.; Fuchibe, K. *Adv. Synth. Catal.* **2006**, *348*, 999-1010; (c) Akiyama, T. *Chem. Rev.* **2007**, *107*, 5744-5758; (d) Doyle, A. G.; Jacobsen, E. N. *Chem. Rev.* **2007**, *107*, 5713-5743; (e) Pihko, P. Introduction. In *Hydrogen Bonding in Organic Synthesis*, Wiley-VCH Verlag GmbH & Co. KGaA: 2009; pp 1-4; (f) Sohtome, Y.; Nagasawa, K. *Synlett* **2010**, *2010*, 1-22; (g) Schenker, S.; Zamfir, A.; Freund, M.; Tsogoeva, S. B. *Eur. J. Org. Chem.* **2011**, 2209-2222; (h) Giacalone, F.; Gruttadauria, M.; Agrigento, P.; Noto, R. *Chem. Soc. Rev.* **2012**, *41*, 2406-2447; (i) Phipps, R. J.; Hamilton, G. L.; Toste, F. D. *Nature Chemistry* **2012**, *4*, 603; (j) Wende, R. C.; Schreiner, P. R. *Green Chem.* **2012**, *14*, 1821-1849; (k) Auvil, T. J.; Schafer, A. G.; Mattson, A. E. *Eur. J. Org. Chem.* **2014**, *2014*, 2633-2646.

11. Etzenbach-Effers, K.; Berkessel, A. Noncovalent Organocatalysis Based on Hydrogen Bonding: Elucidation of Reaction Paths by Computational Methods. In *Asymmetric Organocatalysis*, List, B., Ed. Springer Berlin Heidelberg: Berlin, Heidelberg, 2009; pp 38-69.

12. (a) Rodriguez, A. A.; Yoo, H.; Ziller, J. W.; Shea, K. J. *Tetrahedron Letters* **2009**, *50*, 6830-6833. (b) Beletskiy, E. V.; Schmidt, J.; Wang, X.-B.; Kass, S. R. *J. Am. Chem. Soc.* **2012**, *134*, 18534-18537.

13. (a) Dalko, P. I.; Moisan, L. *Angew. Chem. Int. Ed.* **2001**, *40*, 3726-3748; (b) List, B.; Yang, J. W. *Science* **2006**, *313*, 1584-1586; (c) Yamamoto, H. *Tetrahedron* **2007**, *63*, 8377-8412.

14. Huang, Y.; Unni, A. K.; Thadani, A. N.; Rawal, V. H. *Nature* **2003**, *424*, 146.

15. McDougal, N. T.; Schaus, S. E. *J. Am. Chem. Soc.* **2003**, *125*, 12094-12095.

16. Christ, P.; Lindsay, A. G.; Vormittag, S. S.; Neudörfl, J.-M.; Berkessel, A.; O'Donoghue, A. C. *Chem. Eur. J.* **2011**, *17*, 8524-8528.

17. Connon, S. J. *Angew. Chem. Int. Ed.* **2006**, *45*, 3909-3912.

18. Akiyama, T.; Itoh, J.; Yokota, K.; Fuchibe, K. *Angew. Chem. Int. Ed.* **2004**, *43*, 1566-1568.

19. Uraguchi, D.; Terada, M. *J. Am. Chem. Soc.* **2004**, *126*, 5356-5357.

20. Malerich, J. P.; Hagihara, K.; Rawal, V. H. *J. Am. Chem. Soc.* **2008**, *130*, 14416-14417.

21. Qian, Y.; Ma, G.; Lv, A.; Zhu, H.-L.; Zhao, J.; Rawal, V. H. *Chem. Commun.* **2010**, *46*, 3004-3006.

22. Kondo, S.-i.; Harada, T.; Tanaka, R.; Unno, M. *Org. Lett.* **2006**, *8*, 4621-4624.

23. Schafer, A. G.; Wieting, J. M.; Mattson, A. E. *Org. Lett.* **2011**, *13*, 5228-5231.

24. Tran, N. T.; Wilson, S. O.; Franz, A. K. *Org. Lett.* **2012**, *14*, 186-189.

25. (a) Whiting, A. K.; Peticolas, W. L. *Biochemistry* **1994**, *33*, 552-561; (b) Zhang, Y.; Kua, J.; McCammon, J. A. *J. Am. Chem. Soc.* **2002**, *124*, 10572-10577; (c) Sigala, P. A.; Kraut, D. A.; Caaveiro, J. M. M.; Pybus, B.; Ruben, E. A.; Ringe, D.; Petsko, G. A.; Herschlag, D. *J. Am. Chem. Soc.* **2008**, *130*, 13696-13708; (d) Simón, L.; Goodman, J. M. *J. Org. Chem.* **2010**, *75*, 1831-1840; (e) Childs, W.; Boxer, S. G. *Biochemistry* **2010**, *49*, 2725-2731.

26. (a) Shan, S.-o.; Loh, S.; Herschlag, D. *Science* **1996**, *272*, 97-101; (b) Shan, S.-o.; Herschlag, D. *J. Am. Chem. Soc.* **1996**, *118*, 5515-5518; (c) Shan, S.-o.; Herschlag, D.

Proc. Natl. Acad. Sci. U.S.A. **1996**, *93*, 14474-14479; (d) Shan, S. O.; Herschlag, D. *Methods Enzymol.* **1999**, *308*, 246-276.

27. (a) Tian, Z.; Fattahi, A.; Lis, L.; Kass, S. R. *J. Am. Chem. Soc.* **2009**, *131*, 16984-16988; (b) Shokri, A.; Abedin, A.; Fattahi, A.; Kass, S. R. *J. Am. Chem. Soc.* **2012**, *134*, 10646-10650; (c) Shokri, A.; Schmidt, J.; Wang, X.-B.; Kass, S. R. *J. Am. Chem. Soc.* **2012**, *134*, 2094-2099; (d) Shokri, A.; Schmidt, J.; Wang, X.-B.; Kass, S. R. *J. Am. Chem. Soc.* **2012**, *134*, 16944-16947.

28. Bordwell, F. G. *Acc. Chem. Res.* **1988**, *21*, 456-463.

29. Shokri, A.; Wang, X.-B.; Kass, S. R. *J. Am. Chem. Soc.* **2013**, *135*, 9525-9530.

30. (a) Samet, M.; Danesh-Yazdi, M.; Fattahi, A.; Kass, S. R. *J. Org. Chem.* **2015**, *80*, 1130-1135; (b) Samet, M.; Fattahi, A.; Kass, S. R. *Org. Biomol. Chem.* **2015**, *13*, 2170-2176; (c) Samet, M.; Kass, S. R. *J. Org. Chem.* **2015**, *80*, 7727-7731; (d) Samet, M.; Wang, X. B.; Kass, S. R. *J. Phys. Chem. A* **2014**, *118*, 5989-5993.

31. Jakab, G.; Tancon, C.; Zhang, Z.; Lippert, K. M.; Schreiner, P. R. *Org. Lett.* **2012**, *14*, 1724-1727.

32. (a) Takemoto, Y. *Org. Biomol. Chem.* **2005**, *3*, 4299-4306; (b) Connon, S. J. *Chem. Eur. J.* **2006**, *12*, 5418-5427; (c) Connon, S. J. *Chem. Commun.* **2008**, 2499-2510; (d) Connon, S. J. *Synlett* **2009**, 354-376; (e) Zhang, Z.; Schreiner, P. R. *Chem. Soc. Rev.* **2009**, *38*, 1187-1198; (f) Serdyuk, O. V.; Heckel, C. M.; Tsogoeva, S. B. *Org. Biomol. Chem.* **2013**, *11*, 7051-7071; (g) Fang, X.; Wang, C.-J. *Chem. Commun.* **2015**, *51*, 1185-1197.

33. (a) Etter, M. C.; Panunto, T. W. *J. Am. Chem. Soc.* **1988,** *110*, 5896-5897; (b) Etter, M. C.; Urbanczyk-Lipkowska, Z.; Zia-Ebrahimi, M.; Panunto, T. W. *J. Am. Chem. Soc.* **1990**, *112*, 8415-8426.

34. Curran, D. P.; Kuo, L. H. *Tetrahedron Lett.* **1995**, *36*, 6647-6650.

35. Wilcox, C. S.; Kim, E.-i.; Romano, D.; Kuo, L. H.; Burt, A. L.; Curran, D. P., *Tetrahedron* **1995**, *51*, 621-634.

36. (a) Schreiner, P. R.; Wittkopp, A. *Org. Lett.* **2002**, *4*, 217-220; (b) Wittkopp, A.; Schreiner, P. R. *Chem. Eur. J.* **2003**, *9*, 407-414.

37. Sigman, M. S.; Jacobsen, E. N. *J. Am. Chem. Soc.* **1998**, *120*, 4901-4902.

38. Vachal, P.; Jacobsen, E. N. *J. Am. Chem. Soc.* **2002**, *124*, 10012-10014.

39. Zuend, S. J.; Jacobsen, E. N. *J. Am. Chem. Soc.* **2009**, *131*, 15358-15374.

40. Joly, G. D.; Jacobsen, E. N. *J. Am. Chem. Soc.* **2004**, *126*, 4102-4103.

41. (a) Wenzel, A. G.; Jacobsen, E. N. *J. Am. Chem. Soc.* **2002**, *124*, 12964-12965; (b) Wenzel, A. G.; Lalonde, M. P.; Jacobsen, E. N. *Synlett* **2003**, *2003*, 1919-1922.

42. Taylor, M. S.; Jacobsen, E. N. *J. Am. Chem. Soc.* **2004**, *126*, 10558-10559.

43. Yoon, T. P.; Jacobsen, E. N. *Angew. Chem. Int. Ed.* **2005**, *44*, 466-468.

44. (a) Okino, T.; Hoashi, Y.; Takemoto, Y. *J. Am. Chem. Soc.* **2003**, *125*, 12672-12673; (b) Okino, T.; Hoashi, Y.; Furukawa, T.; Xu, X.; Takemoto, Y. *J. Am. Chem. Soc.* **2005**, *127*, 119-125.

45. Hamza, A.; Schubert, G.; Soós, T.; Pápai, I. *J. Am. Chem. Soc.* **2006**, *128*, 13151-13160.

46. (a) Takemoto, Y. *J. Synth. Org. Chem Jpn.* **2006**, *64*, 1139-1147; (b) Takemoto, Y. *Chem. Pharm. Bull.* **2010**, *58*, 593-601.

47. (a) Okino, T.; Nakamura, S.; Furukawa, T.; Takemoto, Y. *Org. Lett.* **2004**, *6*, 625-627; (b) Xu, X.; Furukawa, T.; Okino, T.; Miyabe, H.; Takemoto, Y. *Chem. Eur. J.* **2006**, *12*, 466-476.

48. Hideto, M.; Yoshiji, T. *Bull. Chem. Soc. Jpn.* **2008**, *81*, 785-795.

49. Brown, A. R.; Kuo, W.-H.; Jacobsen, E. N. *J. Am. Chem. Soc.* **2010**, *132*, 9286-9288.

50. Samet, M.; Buhle, J.; Zhou, Y.; Kass, S. R. *J. Am. Chem. Soc.* **2015**, *137*, 4678-4680.

51. (a) Corey, E. J.; Grogan, M. J. *Org. Lett.* **1999**, *1*, 157-160; (b) Schuster, T.; Kurz, M.; Göbel, M. W. *J. Org. Chem.* **2000**, *65*, 1697-1701; (c) Huang, J.; Corey, E. J. *Org. Lett.* **2004**, *6*, 5027-5029; (d) Nugent, B. M.; Yoder, R. A.; Johnston, J. N. *J. Am. Chem. Soc.* **2004**, *126*, 3418-3419; (e) Takenaka, N.; Sarangthem, R. S.; Seerla, S. K. *Org. Lett.* **2007**, *9*, 2819-2822; (f) Ganesh, M.; Seidel, D. *J. Am. Chem. Soc.* **2008**, *130*, 16464-16465.

52. Ma, J.; Kass, S. R. *Org. Lett.* **2016**, *18*, 5812-5815.

References for Chapter 2

1. (a) Doyle, A. G.; Jacobsen, E. N. *Chem. Rev*. **2007**, *107*, 5713. (b) Giacalone, F.; Gruttadauria, M.; Agrigento, P.; Noto, R. *Chem. Soc. Rev*. **2012**, *41*, 2406. (c) Wende, R. C.; Schreiner, P. R. *Green Chem*. **2012**, *14*, 1821. (d) Phipps, R. J.; Hamilton, G. L.;

Toste, F. D. *Nat. Chem*. **2012**, *4*, 603. (e) Auvil, T. J.; Schafer, A. G.; Mattson, A. E. *Eur. J. Org. Chem.* **2014**, 2633.

2. (a) Yu, S.; Pu, L. *Tetrahedron* **2015**, *71*, 745. (b) Li, G.; Liu, F.; Wu, M. *ARKIVOC* **2015**, *6*, 140.

3. (a) Tran, N. T.; Wilson, S. O.; Franz, A. K. *Org. Lett.* **2012**, *14*, 186. (b) Schafer, A. G.; Wieting, J. M.; Fisher, T. J.; Mattson, A. E. *Angew. Chem. Int. Ed.* **2013**, *52*, 11321. (c) Wieting, J. M.; Fisher, T. J.; Schafer, A. G.; Visco, M. D.; Gallucci, J. C.; Mattson, A. E. *Eur. J. Org. Chem.* **2015**, 525.

4. (a) Wurm, F. R.; Klok, H.-A. *Chem. Soc. Rev*. **2013**, *42*, 8220. (b) Tsakos, M.; Kokotos, C. G. *Tetrahedron* **2013**, *69*, 10199. (c) Chauhan, P.; Mahajan, S.; Kaya, U.; Hack, D.; Enders, D. *Adv. Synth. Catal.* **2015**, *357*, 253.

5. (a) Seebach, D.; Beck, A. K.; Heckel, A. *Angew. Chem. Int. Ed.* **2001**, *40*, 92. (b) Pellissier, H. *Tetrahedron* **2008**, *64*, 10279. (c) Gratzer, K.; Gururaja, G. N.; Waser, M. *Eur. J. Org. Chem*. **2013**, 4471.

6. (a) Zhang, Z.; Schreiner, P. R. *Chem. Soc. Rev*. **2009**, *38*, 1187. (b) Kotke, M.; Schreiner, P. R. In *Hydrogen Bonding in Organic Synthesis*; Pihko, P. M., Ed.; Wiley; New York, 2009; 141. (c) Hof, K.; Lippert, M.; Schreiner, P. R. In *Asymmetric Organocatalysis, Science of Synthesis;* Maruoka, K., Ed.; Thieme; Stuttgart, Germany, 2012; 2, 297. (d) Takemoto, Y.; Inokuma, T. In *Asymmetric Synthesis II*; Christmann, M.; Bräse, S., Eds.; Wiley; New York, 2012; 233. (e) Serdyuk, O. V.; Heckel, C. M.; Tsogoeva, S. B. *Org. & Biomol. Chem*. **2013**, *11*, 7051. (f) Jakab, G.; Schreiner, P. R. In *Comprehensive Enantioselective Organocatalysis;* Dalko, P. I., Ed.; Wiley; New York,

2013; 2, 315. (g) Jiang, J.; Gong, L.-Z. In *Catalytic Cascade Reactions*; Xu, P.-F.; Wang, W., Eds.; Wiley; New York, 2014; 53. (h) Fang, X.; Wang, C.-J. *Chem. Commun*. **2015**, *51*, 1185.

7. (a) Schreiner, P. R.; Wittkopp, A. *Org. Lett.* **2002**, *4*, 217. (b) Wittkopp, A.; Schreiner, P. R. *Chem. Eur. J.* **2003**, *9*, 407. (c) Lippert, K. M.; Hof, K.; Gerbig, D.; Ley, D.; Hausmann, H.; Guenter, S.; Schreiner, P. R. *Eur. J. Org. Chem.* **2012**, 5919.

8. Jakab, G.; Tancon, C.; Zhang, Z.; Lippert, K. M.; Schreiner, P. R. *Org. Lett.* **2012**, *14*, 1724.

9. (a) Schuster, T.; Kurz, M.; Göbel, M. W. *J. Org. Chem.* **2000**, *65*, 1697. (b) Akalay, D.; Dürner, G.; Bats, J. W.; Bolte, M.; Göbel, M. W. *J. Org. Chem*. **2007**, *72*, 5618.

10. Huang, J.; Corey, E. J. *Org. Lett.* **2004**, *6*, 5027.

11. (a) Corey, E. J.; Grogan, M. J. *Org. Lett.* **1999**, *1*, 157. (b) Terada, M.; Ube, H.; Yaguchi, Y. *J. Am. Chem. Soc*. **2006**, *128*, 1454. (c) Terada, M.; Nakano, M.; Ube, H. *J. Am. Chem. Soc.* **2006**, *128*, 16044. (d) Uyeda, C.; Jacobsen, E. N. *J. Am. Chem. Soc*. **2008**, *130*, 9228. (e) Leow, D.; Tan, C.-H. *Synlett*. **2010**, *11*, 1589. (f) Uyeda, C.; Jacobsen, E. N. *J. Am. Chem. Soc*. **2011**, *133*, 5062. (g) Selig, P. *Synthesis* **2013**, *45*, 703.

12. (a) Takenaka, N.; Sarangthem, R. S.; Seeria, S. K. *Org. Lett.* **2007**, *9*, 2819. (b) Takenaka, N.; Chen, J.; Captain, B.; Sarangthem, R. S.; Chandrakumar, A. *J. Am. Chem. Soc*. **2010**, *132*, 4536.

13. (a) B. M. Nugent, R. A. Yoder, J. N. Johnston, *J. Am. Chem. Soc.* **2004**, *126*, 3418-3419; (b) Singh, A.; Yoder, R. A.; Shen, B.; Johnston, J. N. *J. Am. Chem. Soc.* **2007**, *129*,

3466. (c) Singh, A.; Johnston, J. N. *J. Am. Chem. Soc.* **2008**, *130*, 5866. (d) Ganesh, M.; Seidel, D. *J. Am. Chem. Soc.* **2008**, *130*, 16464.

14. Bolm, C.; Rantanen, T.; Schiffers, I.; Zani, L. *Angew. Chem. Int. Ed.* **2005**, *44*, 1758.

15. Berkessel, A.; Das, S.; Pekel, D.; Neudörfl, J.-M. *Angew. Chem. Int. Ed.* **2014**, *53*, 11660.

16. Samet, M.; Buhle, J.; Zhou, Y.; Kass, S. R. *J. Am. Chem. Soc.* **2015**, *137*, 4678.

17. For a related organometallic example, see: (a) Scherer, A.; Mukherjee, T.; Hampel, F.; Gladysz, J. A. *Organometallics* **2014**, *33*, 6709. (b) Mukherjee, T.; Ganzmann, C.; Bhuvanesh, N.; Gladysz, J. A. *Organometallics* **2014**, *33*, 6723.

18 Fan, Y.; Samet, M.; Kass, S. R. U. S. provisional patent serial no. 62/169,371, filed 6/15/15.

19. Luo, R.; Laitinen, T.; Teng, L.; Nevalainen, T.; Lahtela-Kakkonen, M.; Zheng, B.; Wang, H.; Poso, A.; Zhang, X. *Lett. Drug Des. Discov*ery **2013**, *10*, 640.

20. Huang, S.; Wong, J. C. S.; Leung, A. K. C.; Chan, Y. M.; Wong, L.; Fernendez, M. R.; Miller, A. K.; Wu, W. *Tetrahedron Lett*. **2009**, *50*, 5018.

21. Shokri, A.; Wang, X.-B.; Kass, S. R. *J. Am. Chem. Soc.* **2013**, *135*, 9525.

22. Samet, M.; Kass, S. R. *J. Org. Chem.* **2015**, *80*, 7727.

23. Rho, H. S.;S Oh, S. H.; Lee, J. W.; Lee, J. Y.; Chin, J.; Song, C. E. *Chem. Commun*. **2008**, 1208.

24. (Piperidinomethyl)polystyrene deprotonates **4** in $CDCl_3$ but the presence of an acid impurity being the active catalyst was addressed. Control experiments with acetic acid

(ref. 21) and *p*-TsOH reveal that these Brønsted acids are not as active as **4**. In the latter case, 0.1 mol % leads to a 34% conversion in 0.5 h.

25. Bordwell, F. G. et al. University of Wisconsin Madison Bordwell pK_a table (http://www.chem.wisc.edu/areas/reich/pkatable).

26. Bordwell, F. G.; Cheng, J. P. *J. Am. Chem. Soc.* **1991**, *113*, 1736.

27. This value was obtained by solving the following equation: 1.3/2.4 = x/5.5 and subtracting the result from the acidity of **2** (i.e., 13.4 as given in ref. 8).

28. Given the differences in activity between **3** and **4**, it seems unlikely that their methyl groups are serving as activating hydrogen bond donors in the reactions that were examined. Carbon-hydrogen bond donors acting as catalysts, however, recently were reported in a noteworthy contribution. See: Shirakawa, S.; Liu, S.; Kaneko, S.; Kumatabara, Y.; Fukuda, A.; Omagari, Y.; Maruoka, K. *Angew. Chem. Int. Ed.* **2015**, *54*, 15767.

29. Enhanced selectivities also often correlate with reactivity. For example, see: (a) Jensen, K. H.; Sigman, M. S. *Angew. Chem. Int. Ed.* **2007**, *46*, 4748. (b) Jensen, K. H.; Sigman, M. S. *J. Org. Chem.* **2010**, *75*, 7194. (c) Li, X.; Deng, H.; Zhang, B.; Li, J.; Zhang, L.; Luo, S.; Cheng, J.-P. *Chem. Eur. J.* **2010**, *16*, 450.

References for Chapter 3

1. (a) Wharton, C. W. *Comprehensive Biological Catalysis*. Acad. Press: London, 1998; Vol. 1, pp 345-379. (b) Wong, C.-H.; Halcomb, R. H.; Ichikawa, Y.; Kajimoto, T. *Angew. Chem. Int. Ed.* **1995**, *34*, 412-432.

2. For recent reviews on hydrogen bonding catalysis, see: (a) Schreiner, P. R. *Chem. Soc. Rev.* **2003**, *32*, 289-296. (b) Akiyama, T.; Itoh, J.; Fuchibe, K., *Adv. Synth. Catal.* **2006**, *348*, 999-1010. (c) Akiyama, T. *Chem. Rev.* **2007**, *107*, 5744-5758. (d) Doyle, A. G.; Jacobsen, E. N. *Chem. Rev.* **2007**, *107*, 5713-5743. (e) Giacalone, F.; Gruttadauria, M.; Agrigento, P.; Noto, R. *Chem. Soc. Rev.* **2012**, *41*, 2406-2447. (f) Phipps, R. J.; Hamilton, G. L.; Toste, F. D. *Nature Chemistry* **2012**, *4*, 603-614. (g) Wende, R. C.; Schreiner, P. R. *Green Chem.* **2012**, *14*, 1821-1849. (h) Auvil, T. J.; Schafer, A. G.; Mattson, A. E. *Eur. J. Org. Chem.* **2014**, *2014*, 2633-2646.

3. Knowles, R. R.; Jacobsen, E. N. *Proc. Natl. Acad. Sci. U. S. A.* **2010**, *107*, 20678-20685.

4. For recent reviews on thiourea organocatalysis, see: (a) Takemoto, Y. *Org. Biomol. Chem.* **2005**, *3*, 4299-4306. (b) Connon, S. J. *Chem. Eur. J.* **2006**, *12*, 5418-5427. (c) Taylor, M. S.; Jacobsen, E. N. *Angew. Chem. Int. Ed.* **2006**, *45*, 1520-1543. (d) Connon, S. J. *Synlett* **2009**, *2009*, 354-376. (e) Zhang, Z.; Schreiner, P. R. *Chem. Soc. Rev.* **2009**, *38*, 1187-1198. (f) Serdyuk, O. V.; Heckel, C. M.; Tsogoeva, S. B. *Org. Biomol. Chem.* **2013**, *11*, 7051-7071.

5. Schreiner, P. R.; Wittkopp, A. *Org. Lett.* **2002**, *4*, 217-220.

6. (a) Wittkopp, A.; Schreiner, P. R. *Chem. Eur. J.* **2003**, *9*, 407-414. (b) Lippert, K. M.; Hof, K.; Gerbig, D.; Ley, D.; Hausmann, H.; Guenther, S.; Schreiner, P. R. *Eur. J. Org.*

Chem. **2012**, *2012*, 5919-5927. (c) Zhang, Z.; Bao, Z.; Xing, H. *Org. Biomol. Chem.* **2014**, *12*, 3151-3162. (d) Supady, A.; Hecht, S.; Baldauf, C. *Org. Lett.* **2017**, *19*, 4199-4202.

7. For selected examples of asymmetric thiourea organocatalysts bearing a 3,5-bis(trifluoromethyl)phenyl group, see: (a) Okino, T.; Hoashi, Y.; Takemoto, Y. *J. Am. Chem. Soc.* **2003**, *125*, 12672-12673. (b) Herrera, R. P.; Sgarzani, V.; Bernardi, L.; Ricci, A. *Angew. Chem. Int. Ed.* **2005**, *44*, 6576-6579. (c) Ganesh, M.; Seidel, D. *J. Am. Chem. Soc.* **2008**, *130*, 16464-16465. (d) Klausen, R. S.; Jacobsen, E. N. *Org. Lett.* **2009**, *11*, 887-890. (e) Zhang, Z.; Lippert, K. M.; Hausmann, H.; Kotke, M.; Schreiner, P. R. *J. Org. Chem.* **2011**, *76*, 9764-9776.

8. Fan, Y.; Kass, S. R. *Org. Lett.* **2016**, *18*, 188-191.

9. Fan, Y.; Kass, S. R. *J. Org. Chem.* **2017**, *82*, 13288-13296.

10. For a list of reports on pK_a measurement of hydrogen bonding catalysts and Brønsted acids, see: (a) Gilli, P.; Pretto, L.; Bertolasi, V.; Gilli, G. *Acc. Chem. Res.* **2009**, *42*, 33-44. (b) Kütt, A.; Rodima, T.; Saame, J.; Raamat, E.; Mäemets, V.; Kaljurand, I.; Koppel, I. A.; Garlyauskayte, R. Y.; Yagupolskii, Y. L.; Yagupolskii, L. M.; Bernhardt, E.; Willner, H.; Leito, I. *J. Org. Chem.* **2011**, *76*, 391-395. (c) Jakab, G.; Tancon, C.; Zhang, Z.; Lippert, K. M.; Schreiner, P. R. *Org. Lett.* **2012**, *14*, 1724-1727. (d) Ni, X.; Li, X.; Wang, Z.; Cheng, J.-P. *Org. Lett.* **2014**, *16*, 1786-1789. (e) Li, Z.; Li, X.; Ni, X.; Cheng, J.-P. *Org. Lett.* **2015**, *17*, 1196-1199. (f) Li, Z.; Li, X.; Cheng, J.-P. *J. Org. Chem.* **2017**, *82*, 9675-9681.

11. Juhasz, M.; Hoffmann, S.; Stoyanov, E.; Kim, K. C.; Reed, C. A. *Angew. Chem., Int. Ed.* **2004**, *43*, 5352-5355.

12. Samet, M.; Buhle, J.; Zhou, Y.; Kass, S. R. *J. Am. Chem. Soc.* **2015**, *137*, 4678-4680.

13. (a) Huynh, P. N. H.; Walvoord, R. R.; Kozlowski, M. C. *J. Am. Chem. Soc.* **2012**, *134*, 15621-15623. (b) Walvoord, R. R.; Huynh, P. N. H.; Kozlowski, M. C. *J. Am. Chem. Soc.* **2014**, *136*, 16055-16065.

14. Ma, J.; Kass, S. R. *Org. Lett.* **2016**, *18*, 5812-5815.

15. (a) Shokri, A.; Wang, X.-B.; Kass, S. R. *J. Am. Chem. Soc.* **2013**, *135*, 9525-9530. (b) Samet, M.; Kass, S. R. *J. Org. Chem.* **2015**, *80*, 7727-7731.

16. Dessole, G.; Herrera, R. P.; Ricci, A. *Synlett* **2004**, *13*, 2374-2378.

17. For reports on observations of thiourea aggregation, see: (a) Rho, H. S.; Oh, S. H.; Lee, J. W.; Lee, J. Y.; Chin, J.; Song, C. E. *Chem. Commun.* **2008,** 1208-1210. (b) Gimeno, M. C.; Herrera, R. P. *Crystal Growth & Design* **2016**, *16*, 5091-5099 and ref. 8.

18. Kyasa, S.; Meier, R.; Pardini, R.; Truttmann, T.; Kuwata, K.; Dussault, P. *J. Org. Chem.* **2015**, *80*, 12100-12114.

19. Frisch, M. J.; Trucks, G. W.; Schlegel, H. B.; Scuseria, G. E.; Robb, M. A., *et al*. Gaussian 09. Gaussian, Inc., Wallingford CT, 2009.

20. (a) Becke, A. D. *J. Chem. Phys.* **1993**, *98*, 5648-5652. (b) Lee, C.; Yang, W.; Parr, R. G. *Phys. Rev. B* **1988**, *37*, 785-789.

21. (a) Zhao, Y.; Truhlar, D. G. *J. Phys. Chem. A* **2008**, *112*, 1095–1099. (b) Zhao, Y.; Truhlar, D. G. *Theor. Chem. Acc.* **2008**, *120*, 215-241. (c) Zhao, Y.; Truhlar, D. G. *Acc. Chem. Res.* **2008**, *41*, 157-167.

22. Dunning, Jr., T. H. *J. Chem. Phys*. **1989**, *90*, 1007-1023.

References for Chapter 4

1. Tans, P., NOAA/ESRL (www.esrl.noaa.gov/gmd/ccgg/trends/) and Keeling, R., Scripps Institution of Oceanography (scrippsco2.ucsd.edu/).

2. (a) Trogler, W. C. *J. Chem. Educ.* **1995**, *72*, 973-976. (b) Quadrelli, E. A.; Centi, G.; Duplan, J.-L.; Perathoner, S. *ChemSusChem* **2011**, *4*, 1194-1215. (c) Martín, R.; Kleij, A. W. *ChemSusChem* **2011**, *4*, 1259-1263. (d) Centi, G.; Iaquaniello, G.; Perathoner, S. *ChemSusChem* **2011**, *4*, 1265-1273. (e) Aresta, M.; Dibenedetto, A.; Angelini, A. *Chem. Rev*. **2014**, *114*, 1709-1742.

3. (a) Leitner, W. *Acc. Chem. Res.* **2002**, *35*, 746-756. (b) Omae, I. *Catal. Today* **2006**, *115*, 33-52. (c) Aresta, M.; Dibenedetto, A. *Dalton Trans.* **2007**, 2975-2992. (d) D'Alessandro, D. M.; Smit, B.; Long, J. R. *Angew. Chem. Int. Ed.* **2010**, *49*, 6058-6082. (e) Riduan, S.N.; Zhang, Y. *Dalton Trans.* **2010**, *39*, 3347-3357. (f) Cokoja, M.; Bruckmeier, C.; Rieger, B.; Herrmann, W. A.; Kühn, F. E. *Angew. Chem. Int. Ed.* **2011**, *50*, 8510-8537.

4. (a) Jessop, P. G.; Ikariya, T.; Noyori, R. *Chem. Rev.* **1995**, *95*, 259-272. (b) Gibson, D. H. *Chem. Rev.* **1996**, *96*, 2063-2096. (c) Tundo, P.; Selva, M. *Acc. Chem. Res.* **2002**, *35*, 706-716. (d) Sakakura, T.; Choi, J. C.; Yasuda, H. *Chem. Rev.* **2007**, *107*, 2365-2387. (e) North, M.; Pasquale, R.; Young, C. *Green Chem.* **2010**, *12*, 1514-1539.

5. (a) Shaikh, A.-A. G.; Sivaram, S. *Chem. Rev.* **1996**, *96*, 951-976. (b) Fukuoka, S.; Kawamura, M.; Komiya, K.; Tojo, M.; Hachiya, H.; Hasegawa, K.; Aminaka, M.; Okamoto, H.; Fukawa, I.; Konno, S. Green Chem. **2003**, *5*, 497-507. (c) Ochiai, B.; Endo, T. *Prog. Polym. Sci.* **2005**, *30*, 183-215. (d) Schäffner, B.; Schäffner, F.; Verevkin, S. P.; Börner, A. *Chem. Rev.* **2010**, *110*, 4554-4581. (e) Balaraman, E.; Gunanathan, C.; Zhang, J.; Shimon, L. J. W.; Milstein, D. *Nat. Chem.* **2011**, *3*, 609-614.

6. (a) Nicolaou, K. C.; Yang, Z.; Liu, J. J.; Ueno, H.; Nantermet, P. G.; Guy, R. K.; Claiborne, C. F.; Renaud, J.; Couladouros, E. A.; Paulvannan, K.; Sorensen, E. J. *Nature* **1994**, *367*, 630-634. (b) Chang, H. T.; Sharpless, K. B. *Tetrahedron Lett.* **1996**, *37*, 3219-3222. (c) Takata, T.; Furusho, Y.; Murakawa, K.; Endo, T.; Matsuoka, H.; Hirasa, T.; Matsuo, J.; Sisido, M. *J. Am. Chem. Soc.* **1998**, *120*, 4530-4531; (d) Bayardon, J.; Holz, J.; Schäffner, B.; Andrushko, V.; Verevkin, S.; Preetz, A.; Börner, A. *Angew. Chem. Int. Ed.* **2007**, *46*, 5971-5974. (e) Yu, K. M. K.; Curcic, I.; Gabriel, J.; Tsang, S. C. E. *ChemSusChem* **2008**, *1*, 893-899. (f) Sakakura, T.; Kohno, K. *Chem. Commun.* **2009**, 1312-1330.

7. (a) Lu, X.; Liang, B.; Zhang, Y.; Tian, Y.; Wang, Y.; Bai, C.; Wang, H.; Zhang, R. *J. Am. Chem. Soc.* **2004**, *126*, 3732-3733. (b) Jing, H.; Nguyen, S. T. *J. Mol. Catal. A* **2007**, *261*, 12-15. (c) Zhang, X.; Jia, Y.; Lu, X.; Li, B.; Wang, H.; Sun, L. *Tetrahedron Lett.* **2008**, *49*, 6589-6592. (d) Ren, Y.; Shi, Y.; Chen, J.; Yang, S.; Qi, C.; Jiang, H. *RSC Adv.* **2013**, *3*, 2167-2170. (e) Whiteoak, C. J.; Kielland, N.; Laserna, V.; Adán, E. C. E.; Martin, E.; Kleij, A. W. *J. Am. Chem. Soc.* **2013**, *135*, 1228-1231. (f) Maeda, C.;

Taniguchi, T.; Ogawa, K.; Ema, T. *Angew. Chem. Int. Ed.* **2015**, *54*, 134-138. (g) Xu, F.; Cheng, W.; Yao, X.; Sun, J.; Sun, W.; Zhang, S. *Catal. Lett.* **2017**, *147*, 1654-1664.

8. (a) Peng, J.; Deng, Y. *New. J. Chem.* **2001**, *25*, 639-641. (b) Kawanami, H.; Sasaki, A.; Matsui, K. Ikushima, Y. *Chem. Commun.* **2003**, *39*, 896-897. (c) He, L.; Yasuda, H.; Sakakura, T. *Green Chem.* **2003**, *5*, 92-94. (d) Xie, H.; Li, S.; Zhang, S. *J. Mol. Catal. A: Chem.* **2006**, *250*, 30-34. (e) Sun, J.; Wang, L.; Zhang, S.; Li, Z.; Zhang, X.; Dai, W.; Mori, R. *J. Mol. Catal. A: Chem.* **2006**, *256*, 295-300. (f) Lee, J. K.; Kim, Y. J.; Choi, Y. S.; Lee, H.; Lee, J. S.; Hong, J.; Jeong, E.-K.; Kim, H. S.; Cheong, M. *Appl. Catal., B* **2012**, *111-112*, 621-627. (g) Song, Y.; Cheng, C.; Jing, H. *Chem. Eur. J.* **2014**, *20*, 12894-12900. (h) Jiang, X.; Gou, F.; Fu, X.; Jing, H. *J. CO2 Util.* **2016**, *16*, 264-271.

9. Sun, J.; Han, L.; Cheng, W.; Wang, J.; Zhang, X.; Zhang, S. *ChemSusChem* **2011**, *4*, 502-507.

10. (a) Shen, Y.; Duan, W.; Shi, M. *Eur. J. Org. Chem.* **2004**, 3080-3089. (b) Whiteoak, C. J.; Nova, A.; Maseras, F.; Kleij, A. W. *ChemSusChem*, **2012**, *5*, 2032-2038. (c) Whiteoak, C. J.; Henseler, A. H.; Ayats, C.; Kleij, A. W.; Pericàs, M. A. *Green Chem.* **2014**, *16*, 1552-1559. (d) Sopeña, S.; Fiorani, G.; Martín, C.; Kleij, A. W. *ChemSusChem* **2015**, *8*, 3248-3254. (e) Okada, M.; Nishiyori, R.; Kaneko, S.; Igawa, K.; Shirakawa, S. *Eur. J. Org. Chem.* **2018**, 2022-2027.

11. (a) Xiao, B.; Sun, J.; Wang, J.; Liu, C.; Cheng, W. *Synth. Commun.* **2013**, *43*, 2985-2997. (b) Werner, T.; Büttner, H. *ChemSusChem* **2014**, *7*, 3268-3271. (c) Wilhelm, M. E.; Anthofer, M. H.; Cokoja, M.; Markovits, I. I. E.; Herrmann, W. A.; Kühn, F. E. *ChemSusChem*, **2014**, *7*, 1357-1360. (d) Büttner, H.; Steinbauer, J.; Werner, T.

ChemSusChem **2015**, *8*, 2655-2669. (e) Alves, M.; Grignard, B.; Gennen, S.; Méreau, R.; Detrembleur, C.; Jerome, C.; Tassaing, T. *Catal. Sci. Technol.* **2015**, *5*, 4636-4643.

12. (a) Han, L.; Choi, H.-J.; Choi, S.-J.; Liu, B.; Park, D.-W. *Green Chem.* **2011**, *13*, 1023-1028. (b) Tharun, J.; Mathai, G.; Kathalikkattil, A. C.; Roshan, R.; Kwak, J.-Y.; Park, D.-W. *Green Chem.* **2013**, *15*, 1673-1677. (c) Dai, W.; Jin, B.; Luo, S.; Luo, X.; Tu, X.; Au, C. -T. *Applied Catalysis A: General* **2014**, *470*, 183-188.

13. (a) Hardman-Baldwin, A. M.; Mattson, A. E. *ChemSusChem* **2014**, *7*, 3275-3278. (b) Velásquez-Hernández, M. J.; Torres-Huerta, A.; Hernández-Balderas, U.; Martínez-Otero, D.; Núñez-Pineda, A.; Jancik, V. *Polyhedron* **2017**, *122*, 161-171.

14. Sopeña, S.; Martin, E.; Escudero-Adán, E. C.; Kleij, A. W. *ACS Catal.* **2017**, *7*, 3532-3539.

15. Gennen, S.; Alves, M.; Méreau, R.; Tassaing, T.; Gilbert, B.; Detrembleur, C.; Jerome, C.; Grignard, B. *ChemSusChem* **2015**, *8*, 1845-1849.

16. Rulev, Y. A.; Gugkaeva, Z. T.; Lokutova, A. V.; Maleev, V. I.; Peregudov, A. S.; Wu, X.; North, M.; Belokon, Y. N. *ChemSusChem* **2017**, *10*, 1152-1159.

17. Fan, Y.; Kass, S. R. *Org. Lett.* **2016**, *18*, 188-191.

18. Alunni, S.; Pero, A.; Reichenbach, G. *J. Chem. Soc. Perkin Trans. 2* **1998**, 1747-1750.

19. Solid carbon dioxide was added to a stainless steel vessel to achieve the higher pressure. This undoubtedly led to some variation in the reaction temperature but only a 16% conversion was observed after 1.5 h and this is virtually the same (18%) as when an atmospheric pressure of CO_2 was used.

20. Fan, Y.; Kass, S. R. *J. Org. Chem.*, submitted for publication.

21. (a) Aoyagi, N.; Furusho, Y.; Endo, T. *Chem. Lett.* **2012**, *41*, 240-241. (b) Liu, X.; Zhang, S.; Song, Q.; Liu, X.; Ma, R.; He, L. *Green Chem.* **2016**, *18*, 2871-2876.

22. Marques-Lopez, E.; Alcaine, A.; Tejero, T.; Herrera, R. P. *Eur. J. Org. Chem.* **2011**, 3700-3705.

23. We also examined the catalytic performance of added organic salts, acids and bases under the same reaction conditions for comparison. More details are provided in the Appendix.

24. (a) Zhao, D.; Liu, X.-H.; Shi, Z.-Z.; Zhu, C.-D.; Zhao, Y.; Wang, P.; Sun, W.-Y. *Dalton Trans.* **2016**, *45*, 14184-14190. (b) Zhou, F.; Xie, S.-L.; Gao, X.-T.; Zhang, R.; Wang, C.-H.; Yin, G.-Q.; Zhou, J. *Green Chem.* **2017**, *19*, 3908-3915.

25. Single point B3LYP/aug-cc-pVDZ/6-311+G(d)//B3LYP/aug-cc-pVDZ/6-311G(d) energies were used but the B3LYP/aug-cc-pVDZ/6-311G(d) optimized values are all within 0.13 kcal mol^{-1} of the given values.

26. A transition structure involved in the conversion of **6** to **4** was located, and the displacement of iodide by the sulfur atom of the deprotonated thiourea was found to have a B3LYP/aug-cc-pVDZ/6-311+G(d) barrier that is 37.5 kcal mol^{-1} (i.e., 9.3 kcal mol^{-1} smaller than for TS_S).

27. Riches, S. L.; Saha, C.; Filgueira, N. F.; Grange, E.; McGarrigle, E. M.; Aggarwal, V. K. *J. Am. Chem. Soc.* ***2010****, 132*, 7626-7630.

28. Edwards, D. R.; Du, J.; Crudden, C. M. *Org. Lett.* **2007**, *9*, 2397-2999.

29. Bonini, B. F.; Maccagnani, G.; Mazzanti, G.; Zani, P. *Tetrahedron Lett.* **1979**, *20*, 3987-3990.

30. Torde, R. G.; Therrien, A. J.; Shortreed, M. R.; Smith, L. M.; Lamos, S. M. *Molecules*, **2013**, *18*, 14977-14988.

31. Bertucci, M. A.; Lee, S. J.; Gagne, M. R. *Chem. Commun.* **2013**, *49*, 2055-2057.

32. Varga, S.; Jakab, G.; Drahos, L.; Holczbauer, T.; Czugler, M.; Soos, T. *Org. Lett.* **2011**, *13*, 5416-5419.

33. Additional signals in the spectra appear to be due to the presence of a tautomer.

34. (a) Rokicki, G.; Kuran, W.; Pogorzelska-Marciniak, B. *Monatsh. Chem.* **1984**, *115*, 205-214. (b) Corsano, S.; Strappaghetti, G.; Ferrini, R.; Sala, R. *Arch. Pharm.* **1988**, *321*, 731-734. (c) Clegg, W.; Harrington, R. W.; North, M.; Pasquale, R. *Chem. Eur. J.* **2010**, *16*, 6828-6843. (d) Wu, L.; Yang, H.; Wang, H.; Lu, J. *RSC Adv* **2015**, *5*, 23189-23192. (e) Kumatabara, Y.; Okada, M.; Shirakawa, S. *ACS Sustainable Chem. Eng.* **2017**, *5*, 7295-7301. (f) Tiffner, M.; Gonglach, S.; Haas, M.; Schöfberger, W.; Waser, M. *Chem. Asian J.* **2017**, *12*, 1048-1051.

35. Iwasaki, T.; Kihara, N.; Endo, T. Reaction of Various Oxiranes and Carbon Dioxide. Synthesis and Aminolysis of Five-Membered Cyclic Carbonates. *Bull. Chem. Soc. Jpn.* **2000**, *73*, 713-719.

36. Buckley, B. R.; Patel, A. P.; Wijayantha, K. G. U. *RSC Adv.* **2014**, *4*, 58581-58590.

37. Kozak, J. A.; Wu, J.; Su, X.; Simeon, F.; Hatton, T. A.; Jamison, T. F. *J. Am. Chem. Soc.* **2013**, *135*, 18497-18501.

38. Kaneko, S.; Shirakawa, S. *ACS Sustainable Chem. Eng.* **2017**, *5*, 2836-2840.

39. Spartan 14v1.2 (2014) Wavefunction, Inc., Irvine.

40. (a) Becke, A. D. Density‐Functional Thermochemistry. III. The Role Of Exact Exchange. *J. Chem. Phys*. **1993**, *98*, 5648-5652. (b) Lee, C.; Yang, W.; Parr, R. G. Development Of The Colle-Salvetti Correlation-Energy Formula Into A Functional Of The Electron Density. *Phys. Rev. B* **1988**, *37*, 785–789.

41. (a) Hay, P. J.; Wadt, W. R. Ab Initio Effective Core Potentials For Molecular Calculations. Potentials For The Transition Metal Atoms Sc To Hg. *J. Chem. Phys.*, **1985**, *82*, 270-283. (b) Wadt, W. R.; Hay, P. J. Ab Initio Effective Core Potentials For Molecular Calculations. Potentials For Main Group Elements Na To Bi. *J. Chem. Phys.*, **1985**, *82*, 284-298. (c) Hay, P. J.; Wadt, W. R. Ab Initio Effective Core Potentials For Molecular Calculations. Potentials For K To Au Including The Outermost Core Orbitals. *J. Chem. Phys.*, **1985**, *82*, 299-310.

42. Frisch, M. J.; Trucks, G. W.; Schlegel, H. B.; Scuseria, G. E.; Robb, M. A., *et al*. Gaussian 09. Gaussian, Inc., Wallingford CT, 2009.

43. Dunning, Jr., T. H. Gaussian Basis Sets For Use In Correlated Molecular Calculations. I. The Atoms Boron Through Neon And Hydrogen. *J. Chem. Phys*. **1989**, *90*, 1007-1023.

44. Glukhovstev, M. N.; Pross, A.; McGrath, M. P.; Radom, L. Extension Of Gaussian‐2 (G2) Theory To Bromine- and Iodine-Containing Molecules: Use Of Effective Core Potentials. *J. Chem. Phys*. **1995**, *103*, 1878-1885.

References for Chapter 5

1. (a) Etter, M. C. *Acc. Chem. Res.*, **1990**, *23*, 120-126. (b) Wittkopp, A.; Schreiner, P. R. *Catalysis of Diels–Alder Reactions in Water and in Hydrogen Bonding Environments*, ed. Z. Rappoport, Wiley-Interscience, Chichester, **2000**. (c) Schreiner, P. R. *Chem. Soc. Rev.* **2003**, *32*, 289-296. (d) Renzi, P.; Bella, M. *Chem. Commun.* **2012**, *48*, 6881-6896.

2. For selected reviews of asymmetric organocatalysis, see: (a) Berkessel, A.; Gröger, H. *Asymmetric Organocatalysis*; Wiley: New York, **2005**. (b) Yamamoto, H. *Tetrahedron* **2007**, *63*, 8377-8412. (c) Allen, A. E.; Macmillan, D. W. C. *Chem. Sci.* **2012**, *3*, 633-658 and references cited therein.

3. For recent reviews of hydrogen bonding catalysis, see: (a) Doyle, A. G.; Jacobsen, E. N. *Chem. Rev.* **2007**, *107*, 5713-5743. (b) *Hydrogen Bonding in Organic Synthesis*; Pihko, P. M., Ed.; Wiley-VCH: Weinheim, Germany, **2009**. (c) Wende, R. C.; Schreiner, P. R. *Green Chem.* **2012**, *14*, 1821-1849. (d) Auvil, T. J.; Schafer, A. G.; Mattson, A. E. *Eur. J. Org. Chem.* **2014**, 2633-2646 and references cited therein.

4. For recent reviews of thiourea organocatalysis, see: (a) Takemoto, Y. *Org. Biomol. Chem.* **2005**, *3*, 4299-4306. (b) Connon, S. J. *Chem. -Eur. J.* **2006**, *12*, 5418-5427. (c) Taylor, M. S.; Jacobsen, E. N. *Angew. Chem., Int. Ed*. **2006**, *45*, 1520-1543. (d) Zhang, Z.; Schreiner, P. R. *Chem. Soc. Rev.* **2009**, *38*, 1187-1198. (e) Serdyuk, O. V.; Heckel, C. M.; Tsogoeva, S. B. *Org. Biomol. Chem.* **2013**, *11*, 7051-7071. (f) Fang, X.; Wang, C.-J. *Chem. Commun.* **2015**, *51*, 1185-1197.

5. (a) Jensen, K. H.; Sigman, M. S. *Angew. Chem. Int. Ed.* **2007**, *46*, 4748-4750. (b) Jensen, K. H.; Sigman, M. S. *J. Org. Chem.* **2010**, *75*, 7194-7201. (c) Li, X.; Deng, H.; Zhang, B.; Li, J.; Zhang, L.; Luo, S.; Cheng, J.-P. *Chem. -Eur. J.* **2010**, *16*, 450-455.

6. Schreiner, P. R.; Wittkopp, A. *Org. Lett.* **2002**, *4*, 217-220.

7. (a) Wittkopp, A.; Schreiner, P. R. *Chem. - Eur. J.* **2003**, *9*, 407-414. (b) Jakab, G.; Tancon, C.; Zhang, Z.; Lippert, K. M.; Schreiner, P. R. *Org. Lett.* **2012**, *14*, 1724-1727. (c) Lippert, K. M.; Hof, K.; Gerbig, D.; Ley, D.; Hausmann, H.; Guenther, S.; Schreiner, P. R. *Eur. J. Org. Chem.* **2012**, 5919-5927.

8. For selected examples of asymmetric thiourea organocatalysts bearing a 3,5-bis(trifluoromethyl)phenyl group, see: (a) Herrera, R. P.; Sgarzani, V.; Bernardi, L.; Ricci, A. *Angew. Chem. Int. Ed.* **2005**, *44*, 6576-6579. (b) Klausen, R. S.; Jacobsen, E. N. *Org. Lett.* **2009**, *11*, 887-890. (c) Zhang, Z.; Lippert, K. M.; Hausmann, H.; Kotke, M.; Schreiner, P. R. *J. Org. Chem.* **2011**, *76*, 9764-9776. (d) Marques-Lopez, E.; Alcaine, A.; Tejero, T.; Herrera, R. P. *Eur. J. Org. Chem.* **2011**, 3700-3705.

9. Fan, Y.; Kass, S. R. *Org. Lett.* **2016**, *18*, 188-191.

10. For other *N*-alkylpyridinium ion containing catalysts, see: (a) Samet, M.; Buhle, J.; Zhou, Y.; Kass, S. R. *J. Am. Chem. Soc.* **2015**, *137*, 4678-4680. (b) Ma, J.; Kass, S. R. *Org. Lett.* **2016**, *18*, 5812-5815.

11. Related hydrogen bond catalysts that introduce an additional N–H bond (i.e., protonated species) have been reported. For example, see: (a) Corey, E. J.; Grogan, M. J. *Org. Lett.* **1999**, *1*, 157-160. (b) Schuster, T.; Kurz, M.; Göbel, M. W. *J. Org. Chem.* **2000**, *65*, 1697-1701. (c) Huang, J.; Corey, E. J. *Org. Lett.* **2004**, *6*, 5027-5029. (d)

Nugent, B. M.; Yoder, R. A.; Johnston, J. N. *J. Am. Chem. Soc.* **2004**, *126*, 3418-3419. (e) Takenaka, N.; Sarangthem, R. S.; Seerla, S. K. *Org. Lett.* **2007**, *9*, 2819-2822. (f) Ganesh, M.; Seidel, D. *J. Am. Chem. Soc.* **2008**, *130*, 16464-16465.

12. (a) Min, C.; Mittal, N.; Sun, D. X.; Seidel, D. *Angew. Chem. Int. Ed.* **2013**, *52*, 14084-14088. (b) Zhao, C.; Seidel, D. *J. Am. Chem. Soc.* **2015**, *137*, 4650-4653. (c) Min,C.; Lin, C.-T.; Seidel, D. *Angew. Chem. Int. Ed.* **2015**, *54*, 6608-6612.

13. (a) Olah, G. A. *Friedel-Crafts and Related Reactions*, Vol. II, part 1, Wiley-Interscience, New York, 1964. (b) Roberts, R. M.; Khalaf, A. A. *Friedel-Crafts Alkylation Chemistry A Century of Discovery*, Marcel Dekker, New York, 1984. (c) Olah, G. A.; Krishnamurty, R. G.; Prakash, K. S. in *Comprehensive Organic Synthesis*, Vol. III (Eds.: Trost, B. M.; Fleming, I.), Pergamon, Oxford, 1st ed., 1991, p. 293. (d) Kleeman, A.; Engel, J.; Kutscher, B.; Reichert, D. *Pharmaceutical Substances*, Thieme, New York, 4th ed., 2001.

14. For recent reviews on organocatalytic Friedel-Crafts alkylation reactions, see: (a) Marqués-López, E.; Diez-Martinez, A.; Merino, P.; Herrera, R. P. *Curr. Org. Chem.* **2009**, *13*, 1585-1609. (b) You, S.-L.; Cai, Q.; Zeng, M. *Chem. Soc. Rev.* **2009**, *38*, 2190-2201. (c) Terrasson, V.; de Figueiredo, R. M.; Campagne, J. M. *Eur. J. Org. Chem.* **2010**, 2635-2655. (d) Zeng, M.; You, S.-L. *Synlett* **2010**, 1289-1301. (e) Bhadury, P. S.; Pang, J. *Curr. Org. Chem.* **2014**, *18*, 2108-2124.

15. Marqués-López, E.; Alcaine, A.; Tejero, Tomás; Herrera, R. P. *Eur. J. Org. Chem.* **2011**, 3700-3705.

16. Use of *N*-methylindole under the same conditions led to a 90% conversion after 3 h, but an *er* of ~50 : 50. Similar results were reported in ref. 8a with **5** as the catalyst.

17. Itoh, J.; Fuchibe, K.; Akiyama, T. *Angew. Chem. Int. Ed.* **2008**, *47*, 4016-4018.

18 This is in accord with previous findings but different than for a disiloxanediol catalyzed process recently reported. For more details, see ref. 9, 10 and Diemoz, K. M.; Hein, J. E.; Wilson, S. O.; Fettinger, J. C.; Franz, A. K. *J. Org. Chem.* **2017**, *82*, 6738-6747.

19. For previous observations of thiourea aggregation, see: (a) Rho, H. S.; Oh, S. H.; Lee, J. W.; Lee, J. Y.; Chin, J.; Song, C. E. *Chem. Commun.* **2008**, 1208-1210. (b) Gimeno, M. C.; Herrera, R. P. *Cryst. Growth Des.* **2016**, *16*, 5091-5099.

20 A related mechanistic pathway was reported. For details, see: Roca-López, D.; Marqués-López E.; Alcaine, A.; Merino, P.; Herrera, R. P. *Org. Biomol. Chem.* **2014**, *12*, 4503-4510.

21, Selectivities often correlate with reactivity. For example, see ref. 5.

22. See the supporting information for experimental details.

23. Sawa, M.; Moriyama, H.; Yamada, T.; Shitashige, M.; Kawase, Y.; Uno, Y. Patent: US2013/317218 A1, **2013**; Location in patent: Paragraph 0068-0070; 0199.

24. Humphreys, P. G.; Bamborough, P.; Chung, C.; Craggs, P. D.; Gordon, L.; Grandi, P.; Hayhow, T. G.; Hussain, J.; Jones, K. L.; Lindon, M.; Michon, A.-M.; Renaux, J. F.; Suckling, C. J.; Tough, D. F.; Prinjha, R. K. *J. Med. Chem.* **2017**, *60*, 695-709.

25. For the preparation of **9a** and **10a**, see ref. 9.

26. Kyasa, S.; Meier, R.; Pardini, R.; Truttmann, T.; Kuwata, K.; Dussault, P. *J. Org. Chem.* **2015**, *80*, 12100-12114.

27. For the preparation of **9h**, see: Luo, R.; Laitinen, T.; Teng, L.; Nevalainen, T.; Lahtela-Kakkonen, M.; Zheng, B.; Wang, H.; Poso, A.; Zhang, X. *Lett. Drug Des. Discovery* **2013**, *10*, 640-650.

Appendices

Appendix for Chapter 2

Table S1. Friedel–Crafts reaction data.

[β-nitrostyrene]$_0$ = 80 mM, [*N*-methylindole]$_0$ = 239 mM		
catalyst, solvent	time (h)	conversion (%)
no catalyst, $CDCl_3$	167.4	3.6
	193.5	4.6
	264.8	9.3
[1] = 8.3 mM, $CDCl_3$	144.3	1.5
	190.3	5.6
	241.5	9.9
[**2**] = 8.3 mM, $CDCl_3$	25.0	47.9
	47.0	68.0
	72.5	76.6
	94.7	87.7
	121.2	92.4
[**3**] = 8.3 mM, $CDCl_3$	0.5	7.0
	0.9	13.3
	1.5	20.8
	2.7	39.5
	3.5	41.2
	18.6	91.5
[**4**] = 8.3 mM, $CDCl_3$	0.2	71.4
	0.3	90.9
	0.4	96.2
[**4**] = 4.2 mM, $CDCl_3$	0.2	39.5
	0.4	60.2
	0.5	65.8
	0.6	73.5
[**4**] = 2.1 mM, $CDCl_3$	0.3	12.8
	0.6	18.8
	1.7	34.4
	2.6	44.6
[**4**] = 0.83 mM, $CDCl_3$	2.25	0.0
	28.9	6.1
	100.0	21.8
	146.0	36.5
	197.0	51.5
[**4**] = 4.2 mM, toluene-d_8	0.1	45.9
	0.2	59.2
	0.4	69.9

[**4**] = 4.2 mM, CD_2Cl_2	0.1	81.3
	0.2	93.5
	0.3	97.0

Table S2. Diels–Alder reaction data.

[cyclopentadiene]$_0$ = 0.50 M, [methyl vinyl ketone]$_0$ = 0.17 M, solvent = $CDCl_3$		
catalyst	time (min)	conversion (%)
no catalyst	10.0	5.4
	20.0	10.3
	30.0	15.3
[2] = 1.7 mM	8.0	12.4
	20.0	19.7
	30.0	25.6
[**3**] = 1.7 mM	10.0	48.0
	20.0	65.9
	25.0	71.1
	30.0	77.1
[**4**] = 1.7 mM	10.0	71.1
	15.0	93.1
	20.0	> 99

Table S3. Aminolysis reaction data.

[styrene oxide]$_0$ = [aniline]$_0$ = 4.9 M			
catalyst	temp (˚C)	time (h)	conversion (%)
no catalyst	60	0.5	0.9
		2.3	5.8
[2] = 49 mM	60	2.0	39.8
		2.7	50.4
		3.3	63.9
[**4**] = 49 mM	60	0.5	93
[**4**] = 4.9 mM	60	0.5	54.1
		1.0	75.8
		2.3	93.5
[**4**] = 4.9 mM	23	2.3	7.9
		24.0	32.0
		48.3	61.3

Appendix for Chapter 3

Table S1. Friedel–Crafts reaction data.

[β-nitrostyrene]$_0$ = 83 mM, [*N*-methylindole]$_0$ = 250 mM, [cat] = 8.3 mM, solvent = $CDCl_3$		
catalyst	Time (h)	Conversion (%)
5	47.5	5.3
	120.0	14.0
	168.0	18.0
	240.0	24.0
	312.0	29.9
6	1.0	25.4
	2.0	41.0
	3.0	50.8
	3.7	58.5
7	1.0	9.7
	3.2	27.2
	5.3	41.2
	23.5	80.6
	29.0	86.2
8	0.2	27.9
	0.3	44.6
	0.4	53.2
	0.5	60.6
	0.7	69.0
	0.8	75.8
9	0.8	28.8
	1.8	55.6
	2.9	73.5
10	0.1	46.1
	0.3	75.2
	0.4	78.7
[β-nitrostyrene]$_0$ = 83 mM, [*N*-methylindole]$_0$ = 250 mM, [cat] = 8.3 mM, solvent = C_6D_6		
catalyst	Time (h)	Conversion (%)
4	0.2	9.3
	2.7	51.8
	3.7	57.1
	4.0	57.5

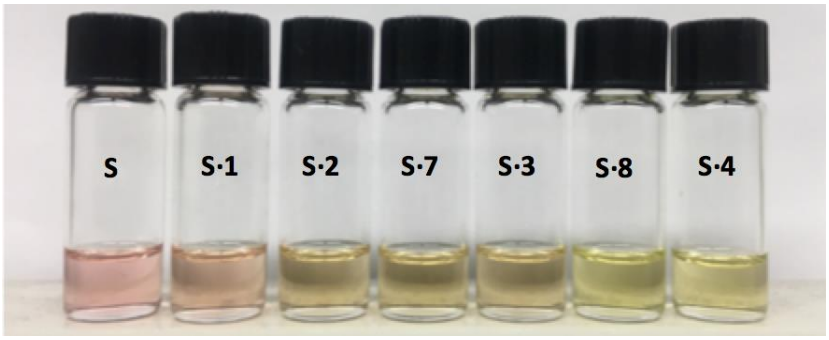

Figure S1. Color changes upon adding the indicated thioureas to dilute solutions of **S** (2.22 x 10^{-5} M) in CH_2Cl_2.

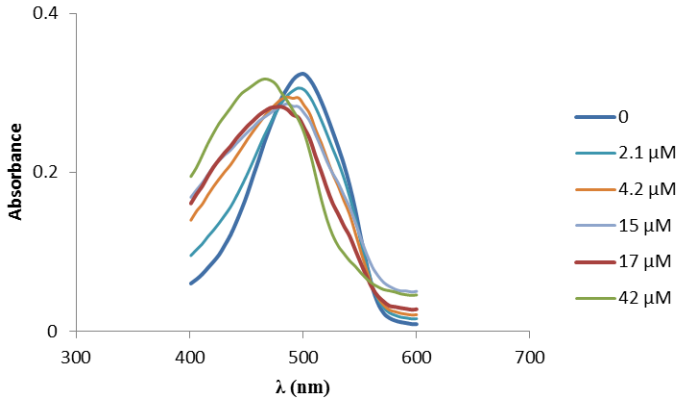

Figure S2. UV-Vis spectra of **S** in CH_2Cl_2 (2.22 x 10^{-5} M) upon addition of thiourea **4**.

General Procedure for UV-Vis Titrations.[1]

Preparation of stock solutions.

In a 5 mL volumetric flask, 5.0 mg (2.22×10^{-2} mmol) of sensor **S**[2] was diluted with anhydrous CH_2Cl_2 to afford a 4.44×10^{-3} M solution (**A**). In another 5 mL volumetric flask, 25 μL of **A** was added and diluted with CH_2Cl_2 to produce a 2.22×10^{-5} M solution (**B**). In 1 mL volumetric flasks, catalyst stock solutions with the desired concentrations ($[catalyst]_0$) were prepared in CH_2Cl_2.

Titration procedure.

For UV titration experiments with each catalyst, 0.50 mL of stock solution **B** was transferred to a 10 mm quartz UV cuvette and the solution level was marked. Aliquots of the catalyst stock solution with the indicated volumes were sequentially added to the cuvette via syringe and the 0.50 mL total volume was maintained to the marked line by evaporation under a flow of argon. A spectrum of the λ_{max} value was recorded after each addition of the catalyst. This was continued until λ_{max} no longer changed. Titration curves of **S** with different catalysts were made by plotting the λ_{max} values versus the corresponding catalyst concentrations.

1 ($[1]_0$ = 0.111 M)

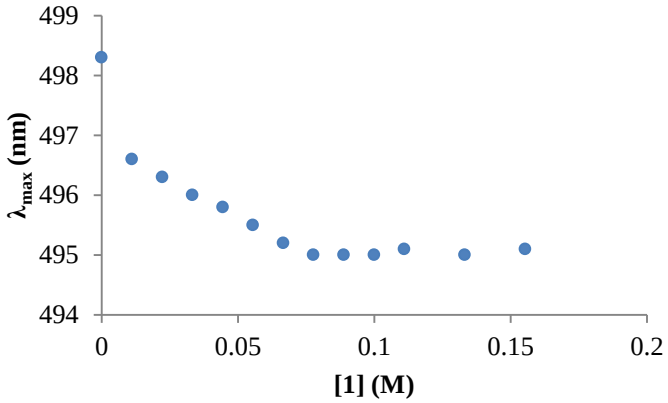

V (µL) **1**	[**1**] (M)	catalyst equivalents	λ_{max} (nm)
0	0	0	498.3
50	0.0111	500	496.6
100	0.0222	1000	496.3
150	0.0333	1500	496.0
200	0.0444	2000	495.8
250	0.0555	2500	495.5
300	0.0666	3000	495.2
350	0.0777	3500	495.0
400	0.0888	4000	495.0
450	0.0999	4500	495.0
500	0.111	5000	495.1
600	0.133	6000	495.0
700	0.155	7000	495.1

2 ($[2]_0$ = 0.00560 M)

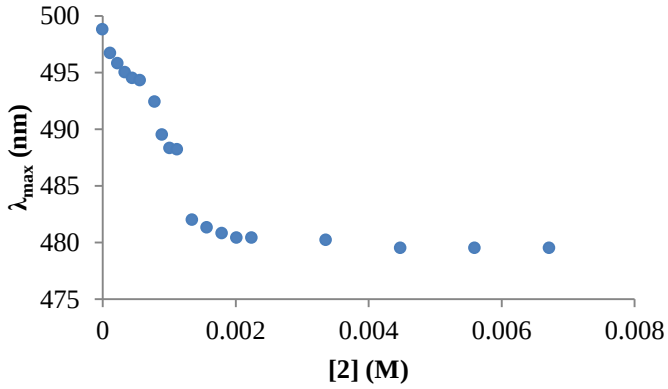

V (µL) **2**	[**2**] (M)	catalyst equivalents	λ_{max} (nm)
0	0	0	498.8
10	0.000112	5	496.7
20	0.000224	10	495.8
30	0.000336	15	495.0
40	0.000448	20	494.5
50	0.000560	25	494.3
70	0.000784	35	492.4
80	0.000895	40	489.5
90	0.00101	45	488.3
100	0.00112	50	488.2
120	0.00134	61	482.0
140	0.00157	71	481.3
160	0.00179	81	480.8
180	0.00202	91	480.4
200	0.00224	101	480.4
300	0.00336	151	480.2
400	0.00448	202	479.5
500	0.00560	252	479.5
600	0.00672	303	479.5

3 ($[3]_0$ = 0.00208 M)

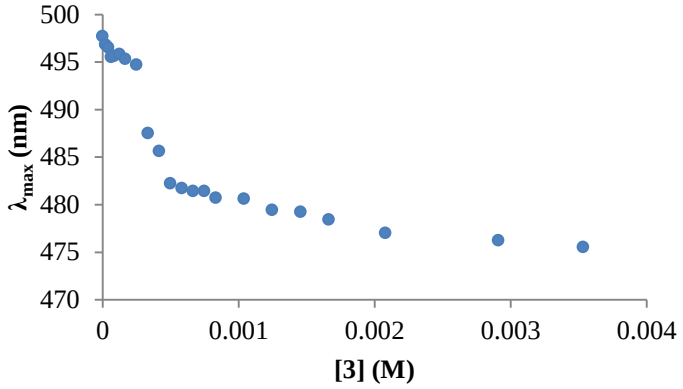

V (µL) **3**	[**3**] (M)	catalyst equivalents	λ_{max} (nm)
0	0	0	497.7
5	0.0000208	0.9	496.8
10	0.0000416	1.9	496.5
15	0.0000623	2.8	495.5
20	0.0000831	3.7	495.6

30	0.000125	5.6	495.8
40	0.000166	7.5	495.3
60	0.000249	11	494.7
80	0.000332	15	487.5
100	0.000416	19	485.6
120	0.000499	23	482.2
140	0.000582	26	481.7
160	0.000665	30	481.4
180	0.000748	34	481.4
200	0.000831	37	480.7
250	0.00104	47	480.6
300	0.00125	56	479.4
350	0.00145	66	479.2
400	0.00166	75	478.4
500	0.00208	94	477.0
700	0.00291	131	476.2
850	0.00353	159	475.5

4 ($[4]_0$ = 0.00106 M)

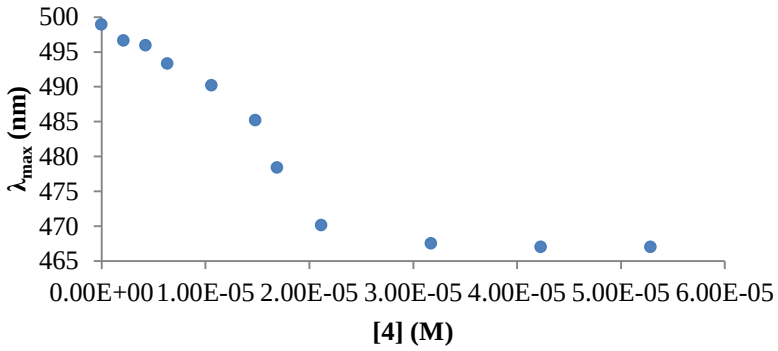

V (µL) **4**	[**4**] (M)	catalyst equivalents	λ_{max} (nm)
0	0	0.0	498.9
1	0.00000211	0.1	496.6
2	0.00000423	0.2	495.9
3	0.00000634	0.3	493.3
5	0.0000106	0.5	490.2
7	0.0000148	0.7	485.2
8	0.0000169	0.8	478.4
10	0.0000211	1.0	470.1
15	0.0000317	1.4	467.5
20	0.0000423	1.9	467.0
25	0.0000529	2.4	467.0

5 ($[5]_0$ = 0.104 M)

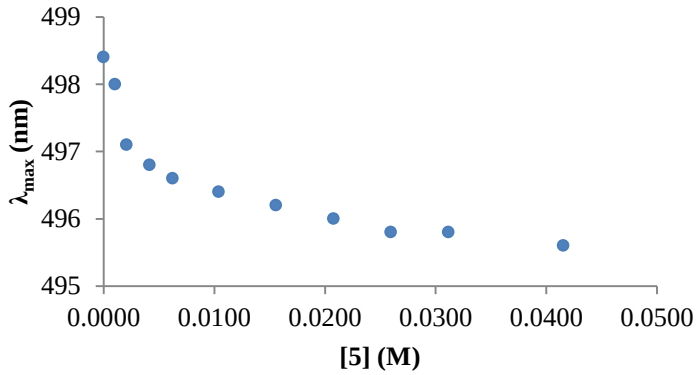

V (µL) **5**	[5] (M)	catalyst equivalents	λ_{max} (nm)
0	0	0	498.4
5	0.00104	47	498.0
10	0.00208	94	497.1
20	0.00415	187	496.8
30	0.00623	281	496.6
50	0.0104	468	496.4
75	0.0156	702	496.2
100	0.0208	936	496.0
125	0.0260	1169	495.8
150	0.0312	1403	495.8
200	0.0415	1871	495.6

6 ($[6]_0$ = 0.00352 M)

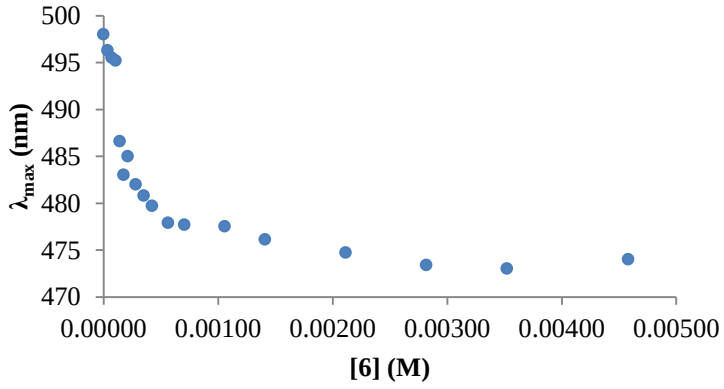

V (µL) **6**	[**6**] (M)	catalyst equivalents	λ_{max} (nm)
0	0	0	498.0
5	0.0000352	1.6	496.3

10	0.0000705	3.2	495.5
15	0.000106	4.8	495.2
20	0.000141	6.3	486.6
25	0.000176	7.9	483.0
30	0.000211	9.5	485.0
40	0.000282	13	482.0
50	0.000352	16	480.8
60	0.000423	19	479.7
80	0.000564	25	477.9
100	0.000705	32	477.7
150	0.00106	48	477.5
200	0.00141	63	476.1
300	0.00211	95	474.7
400	0.00282	127	473.4
500	0.00352	159	473.0
650	0.00458	206	474.0

7 ($[7]_0$ = 0.00358 M)

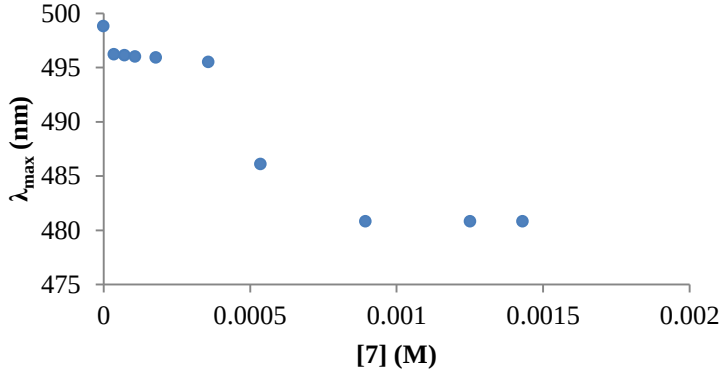

V (µL) **7**	[**7**] (M)	catalyst equivalents	λ_{max} (nm)
0	0	0	498.8
5	0.0000358	1.6	496.2
10	0.0000715	3.2	496.1
15	0.000107	4.8	496.0
25	0.000179	8.1	495.9
50	0.000358	16	495.5
75	0.000536	24	486.1
125	0.000894	40	480.8
175	0.00125	56	480.8
200	0.00143	64	480.8

8 ($[8]_0$ = 0.00321 M)

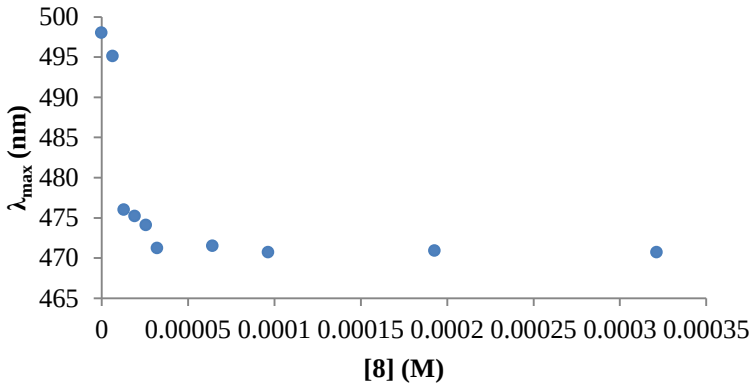

V (µL) **8**	[**8**] (M)	catalyst equivalents	λ_{max} (nm)
0	0	0	498.0
1	0.00000643	0.3	495.1
2	0.0000129	0.6	476.0
3	0.0000193	0.9	475.2
4	0.0000257	1.2	474.1
5	0.0000321	1.4	471.2
10	0.0000643	2.9	471.5
15	0.0000964	4.3	470.7
30	0.000193	8.7	470.9
50	0.000321	14	470.7

9 ($[9]_0$ = 0.00797 M)

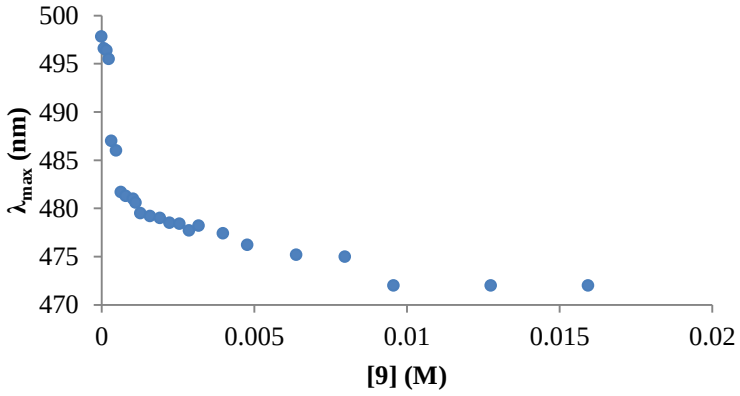

V (µL) **9**	[**9**] (M)	catalyst equivalents	λ_{max} (nm)
0	0	0	497.8
5	0.0000797	3.6	496.6

10	0.000159	7.2	496.4
15	0.000239	11	495.5
20	0.000319	14	487.0
30	0.000478	22	486.0
40	0.000637	29	481.7
50	0.000797	36	481.3
65	0.00104	47	481.0
70	0.00112	50	480.6
80	0.00127	57	479.5
100	0.00159	72	479.2
120	0.00191	86	479.0
140	0.00223	100	478.5
160	0.00255	115	478.4
180	0.00287	129	477.7
200	0.00319	144	478.2
250	0.00398	179	477.4
300	0.00478	215	476.2
400	0.00637	287	475.2
500	0.00797	359	475.0
600	0.00956	431	472.0
800	0.0127	574	472.0
1000	0.0159	718	472.0

10 ($[10]_0$ = 0.00312 M)

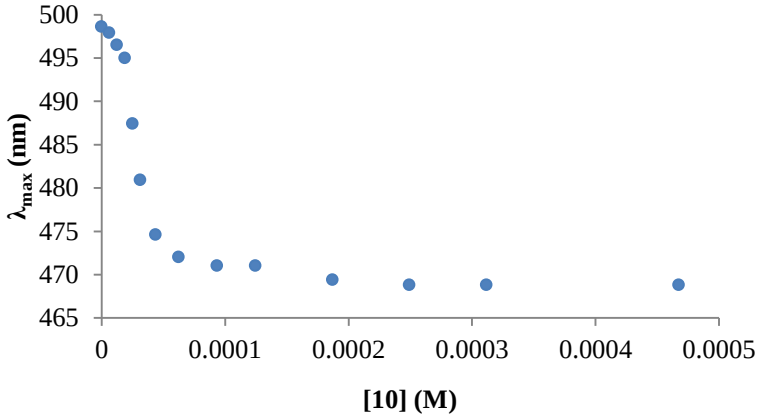

V (µL) **10**	[**10**] (M)	catalyst equivalents	λ_{max} (nm)
0	0	0	498.6
1	0.00000623	0.3	497.9
2	0.0000125	0.6	496.5

3	0.0000187	0.8	495.0
4	0.0000249	1.1	487.4
5	0.0000312	1.4	480.9
7	0.0000436	2.0	474.6
10	0.0000623	2.8	472.0
15	0.0000935	4.2	471.0
20	0.000125	5.6	471.0
30	0.000187	8.4	469.4
40	0.000249	11	468.8
50	0.000312	14	468.8
75	0.000467	21	468.8

Calculation of association equilibrium constants (K)

Based on Kozlowski's report,[1b] the equilibrium binding constant can be calculated as follows:

$$K = \frac{[\mathbf{S}\cdot\text{catalyst}]}{[\mathbf{S}][\text{catalyst}]} = \frac{[\mathbf{S}\cdot\text{catalyst}]_{eq}}{[\mathbf{S}]_{eq}[\text{catalyst}]_{eq}} = \frac{1}{[\text{catalyst}]_{eq}}$$

$$[\text{catalyst}]_{eq} = [\text{catalyst}]_{total} - [\mathbf{S}\cdot\text{catalyst}]_{eq} = [\text{catalyst}]_{total} - 1.11 \times 10^{-5}\,\text{M}$$

where $[\mathbf{S}\cdot\text{catalyst}]_{eq}$, $[\mathbf{S}]_{eq}$ and $[\text{catalyst}]_{eq}$ are their concentrations at the equivalence point (i. e., $[\mathbf{S}\cdot\text{catalyst}]_{eq} = [\mathbf{S}]_{eq} = 1.11 \times 10^{-5}$ M) and $[\text{catalyst}]_{total}$ is the total concentration of bound and unbound catalyst.

Table S2. Equilibrium catalyst concentrations and binding constants.

catalyst	$[\text{catalyst}]_{total}$ (M^{-1})	$[\text{catalyst}]_{eq}$ (M^{-1})	K (M^{-1})
1	0.0500	0.0500	20.0
2	7.41E-04	7.30E-04	1.21E+03
3	2.54E-04	2.43E-04	4.12E+03
4	1.46E-05	3.50E-06	2.08E+05
5	1.04E-03	1.03E-03	9.72E+02
6	1.10E-04	9.89E-05	1.01E+04
7	3.88E-04	3.77E-04	2.65E+03
8	2.67E-05	1.56E-05	6.41E+04

9	2.46E-04	2.35E-04	4.26E+03
10	1.40E-04	1.29E-04	1.02E+05

Computed Cartesian coordinates.

M06-2X/cc-pVDZ

1	6	0	3.563222	-0.337757	2.087645
2	6	0	4.903781	-0.057095	1.999870
3	6	0	4.439186	2.252277	2.229465
4	6	0	3.112171	2.026057	2.299270
5	6	0	1.386372	0.242998	2.181319
6	6	0	1.599905	-1.195075	2.035066
7	1	0	5.632581	-0.843887	1.820396
8	1	0	4.859154	3.254303	2.235217
9	1	0	2.359361	2.807219	2.360224
10	6	0	0.560194	-2.228131	1.994569
11	6	0	-0.793084	-1.899944	1.825125
12	6	0	0.928082	-3.579661	2.128498
13	6	0	-1.760224	-2.904967	1.783110
14	1	0	-1.097347	-0.859862	1.702070
15	6	0	-0.039728	-4.577351	2.091455
16	1	0	1.978944	-3.823644	2.293412
17	6	0	-1.385584	-4.241032	1.918046
18	1	0	-2.806502	-2.637721	1.622003
19	1	0	0.253237	-5.622042	2.213351
20	1	0	-2.146500	-5.023078	1.891537
21	8	0	0.361896	0.971003	2.218771
22	6	0	6.745434	1.530391	1.850161
23	1	0	6.833687	1.878586	0.812432
24	1	0	7.081215	2.296704	2.560224
25	1	0	7.349704	0.626742	1.987121
26	7	0	2.904039	-1.498892	1.966494
27	7	0	5.347770	1.206127	2.115738
28	7	0	2.660193	0.724838	2.265337
29	1	0	-0.451345	1.451278	0.828923
30	1	0	1.127959	0.840049	-0.791374
31	7	0	-1.124299	1.755958	0.089643
32	7	0	0.244348	0.396309	-1.091274
33	6	0	-0.939261	1.158083	-1.117541
34	16	0	-1.870422	1.261953	-2.478348
35	6	0	0.270855	-0.961666	-1.258608
36	6	0	-0.867505	-1.769539	-1.445379
37	6	0	1.509009	-1.599943	-1.124011
38	6	0	-0.717540	-3.148047	-1.473691
39	1	0	-1.861913	-1.324627	-1.479147
40	1	0	2.419770	-1.038694	-0.916868
41	6	0	0.528453	-3.728802	-1.304188
42	1	0	0.698405	-4.801818	-1.270519

43	6	0	-2.252702	2.348487	0.623457
44	6	0	-2.221410	2.651865	1.993666
45	6	0	-3.437087	2.589903	-0.076911
46	6	0	-3.349881	3.169658	2.610409
47	1	0	-1.313820	2.425472	2.557450
48	1	0	-3.551843	2.330799	-1.125128
49	6	0	-4.500329	3.373476	1.871265
50	1	0	-5.433908	3.737688	2.293724
51	7	0	1.602608	-2.936753	-1.133389
52	1	0	-1.591753	-3.788510	-1.577814
53	1	0	-3.352757	3.392675	3.675384
54	6	0	2.926773	-3.509005	-0.851659
55	1	0	3.641810	-3.112497	-1.581749
56	1	0	3.216455	-3.199791	0.163081
57	1	0	2.865854	-4.598858	-0.925960
58	7	0	-4.506402	3.092086	0.558508
59	6	0	-5.780219	3.163162	-0.174043
60	1	0	-5.566805	3.263511	-1.242235
61	1	0	-6.304910	2.219326	0.022101
62	1	0	-6.347571	4.029200	0.183128
63	16	0	4.058870	1.482152	-1.263471
64	8	0	5.371610	1.068580	-0.716298
65	8	0	2.897164	0.948333	-0.465068
66	6	0	3.895710	0.455389	-2.800378
67	9	0	4.713345	0.859857	-3.761773
68	9	0	2.641455	0.491855	-3.254331
69	9	0	4.182298	-0.833841	-2.521813
70	8	0	3.913983	2.872431	-1.706676
71	6	0	-5.039411	-0.596880	-1.371669
72	16	0	-4.504912	-0.625471	0.409838
73	8	0	-4.830993	-1.992082	0.851655
74	8	0	-3.049076	-0.319642	0.297127
75	8	0	-5.311345	0.474844	0.999258
76	9	0	-4.178524	-1.266193	-2.145260
77	9	0	-6.245925	-1.133304	-1.527411
78	9	0	-5.097375	0.670153	-1.830830

B3LYP/cc-pVDZ

1	6	0	-3.580338	-2.627302	1.107615
2	6	0	-4.946905	-2.575407	0.995645
3	6	0	-4.753111	-2.410140	-1.370199
4	6	0	-3.403408	-2.447284	-1.306752
5	6	0	-1.473667	-2.502421	0.289767
6	6	0	-1.527890	-2.574613	1.753594
7	1	0	-5.580172	-2.582323	1.880337
8	1	0	-5.276756	-2.254973	-2.309184
9	1	0	-2.759319	-2.336604	-2.174294
10	6	0	-0.389924	-2.531571	2.675463
11	6	0	0.906293	-2.180291	2.245668
12	6	0	-0.601311	-2.810019	4.043006

13	6	0	1.960365	-2.099952	3.160045
14	1	0	1.089216	-1.958111	1.195704
15	6	0	0.454865	-2.744488	4.948006
16	1	0	-1.606637	-3.075394	4.372438
17	6	0	1.737165	-2.386748	4.510406
18	1	0	2.951859	-1.797171	2.815398
19	1	0	0.278736	-2.970547	6.002942
20	1	0	2.563631	-2.327847	5.222980
21	8	0	-0.525558	-2.411730	-0.539683
22	6	0	-6.962370	-2.155664	-0.338372
23	1	0	-7.062733	-1.072966	-0.511636
24	1	0	-7.406862	-2.715694	-1.174019
25	1	0	-7.476162	-2.438846	0.589405
26	7	0	-2.794987	-2.660418	2.197191
27	7	0	-5.542276	-2.487994	-0.224447
28	7	0	-2.796024	-2.559207	-0.070100
29	1	0	0.240576	-1.093714	-1.145875
30	1	0	-1.116008	0.781962	-0.574621
31	7	0	0.898791	-0.459146	-1.665588
32	7	0	-0.146627	1.119738	-0.406327
33	6	0	0.844978	0.868231	-1.372088
34	16	0	1.724808	2.098292	-2.083194
35	6	0	0.008411	2.019518	0.618449
36	6	0	1.269085	2.367895	1.155928
37	6	0	-1.136551	2.561134	1.221239
38	6	0	1.329646	3.272358	2.210010
39	1	0	2.170262	1.876916	0.785801
40	1	0	-2.134826	2.268176	0.896057
41	6	0	0.167363	3.807502	2.749906
42	1	0	0.153215	4.513155	3.578381
43	6	0	1.852178	-1.151737	-2.394798
44	6	0	1.553702	-2.461272	-2.813203
45	6	0	3.139316	-0.655683	-2.646953
46	6	0	2.509524	-3.196203	-3.510778
47	1	0	0.585403	-2.889048	-2.548892
48	1	0	3.466005	0.308333	-2.274015
49	6	0	3.750227	-2.639746	-3.775164
50	1	0	4.539178	-3.157239	-4.317001
51	7	0	-1.033573	3.424967	2.254274
52	1	0	2.295084	3.547244	2.634999
53	1	0	2.296482	-4.209524	-3.850521
54	6	0	-2.279182	3.921365	2.872013
55	1	0	-3.055950	3.988387	2.101602
56	1	0	-2.599698	3.223397	3.659085
57	1	0	-2.096323	4.911819	3.305557
58	7	0	4.036108	-1.394148	-3.328648
59	6	0	5.391458	-0.826441	-3.499050
60	1	0	5.316900	0.109583	-4.068746
61	1	0	5.786881	-0.643394	-2.488077
62	1	0	6.012802	-1.547184	-4.041983
63	16	0	-4.101543	0.965859	-1.203208
64	8	0	-5.384252	0.588385	-0.541544
65	8	0	-2.876946	0.703336	-0.335082

66	6	0	-4.153703	2.854637	-1.197996
67	9	0	-5.184445	3.327207	-1.902330
68	9	0	-3.017166	3.371337	-1.695655
69	9	0	-4.276542	3.316779	0.079519
70	8	0	-3.928570	0.602563	-2.633315
71	6	0	5.334518	1.457662	0.602615
72	16	0	4.621392	-0.291831	0.618102
73	8	0	4.915420	-0.797229	1.984344
74	8	0	3.166559	-0.036322	0.312363
75	8	0	5.363615	-0.952294	-0.509571
76	9	0	4.624460	2.279044	1.414308
77	9	0	6.610069	1.483356	1.006778
78	9	0	5.278544	1.978318	-0.643477

References:

1. Titration experiments followed a similar general procedure to those by Kozlowski *et al*. For further details, see: (a) Huynh, P. N. H.; Walvoord, R. R.; Kozlowski, M. C. *J. Am. Chem. Soc.* **2012**, *134*, 15621-15623. (b) Walvoord, R. R.; Huynh, P. N. H.; Kozlowski, M. C. *J. Am. Chem. Soc.* **2014**, *136*, 16055-16065.

2. Barlin, G. B.; Brown, D. J.; Kadunc, Z.; Petrič, A; Stanovnic, B; Tišler, M. *Aust. J. Chem.* **1983**, *36*, 1215-1220.

The complete citation to ref. 19 in the manuscript is as follows: Frisch, M. J.; Trucks, G. W.; Schlegel, H. B.; Scuseria, G. E.; Robb, M. A.; Cheeseman, J. R.; Scalmani, G.; Barone, V.; Mennucci, B.; Petersson, G. A.; Nakatsuji, H.; Caricato, M.; Li, X.; Hratchian, H. P.; Izmaylov, A. F.; Bloino, J.; Zheng, G.; Sonnenberg, J. L.; Hada, M.; Ehara, M.; Toyota, K.; Fukuda, R.; Hasegawa, J.; Ishida, M.; Nakajima, T.; Honda, Y.; Kitao, O.; Nakai, H.; Vreven, T.; Montgomery, Jr., J. A.; Peralta, J. E.; Ogliaro, F.; Bearpark, M.; Heyd, J. J.; Brothers, E.; Kudin, K. N.; Staroverov, V. N.; Kobayashi, R.;

Normand, J.; Raghavachari, K.; Rendell, A.; Burant, J. C.; Iyengar, S. S.; Tomasi, J.; Cossi, M.; Rega, N.; Millam, J. M.; Klene, M.; Knox, J. E.; Cross, J. B.; Bakken, V.; Adamo, C.; Jaramillo, J.; Gomperts, R.; Stratmann, R. E.; Yazyev, O.; Austin, A. J.; Cammi, R.; Pomelli, C.; Ochterski, J. W.; Martin, R. L.; Morokuma, K.; Zakrzewski, V. G.; Voth, G. A.; Salvador, P.; Dannenberg, J. J.; Dapprich, S.; Daniels, A. D.; Farkas, O.; Foresman, J. B.; Ortiz, J. V.; Cioslowski, J.; Fox, D. J. *Gaussian 09*, Gaussian, Inc., Wallingford, CT, 2009.

Appendix for Chapter 4

Table S1. Additive screening for the reaction of 2-phenyloxirane with CO_2.

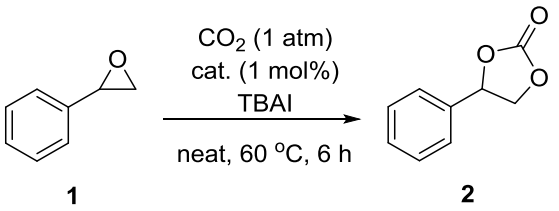

entry	additive	TBAI (mol%)	conversion (%)
1	NH_4OAc	1	37
2	NH_4I	0	-
3	PyOTs	1	18
4	MsOH	2	16
5	TFA	2	19
6	DMAP[a]	0	-
7	-	2	56

[a]DMAP (2 mol%) was used.

Table S2. Racemization of (*R*)-2-phenyloxirane in the presence of **T1** and TBAI at 60 ˚C.

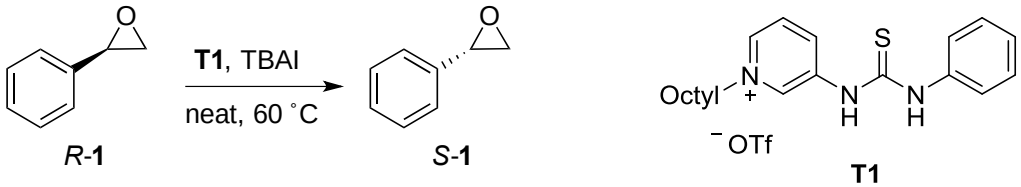

entry	**T1** (mol%)	TBAI (mol%)	t (h)	*R*-**2** : *S*-**2**[a]
1	1	2	1	93 : 7
2	1	2	18	50 : 50

3	1	100	2	90 : 10
4	1	100	6	72 : 28
5	-	100	6	98 : 2
6	1	-	3	-[b]

[a]The enantiomeric ratio was determined by HPLC with a chiral column (RegisPack™, hexanes/ *i*-PrOH = 95 : 5, flow rate = 1.00 mL/min, λ = 220 nm, t_R = 5.9 min, t_S = 6.5 min or a Chiracel OD-H column with hexanes/*i*-PrOH = 85 : 15, flow rate = 1.00 mL/min, and retention times 22.9 and 29.3 min). [b]2-Phenylacetaldehye was formed.

Table S3. Application scope of catalysts **T7** and **T8**.[a]

entry	catalyst	epoxide (and carbonate **3**)	t (h)	T (˚C)	mg (yield %)
1	**T7**	R = Ph, R', R'' = H (**2a**)	4	120	628 (96)
2	**T8**	R = Ph, R', R'' = H (**2a**)	24	60	315 (96)
3	**T7**	R = *p*-ClC_6H_4, R', R'' = H (**2b**)	4	120	758 (95)
4	**T8**	R = *p*-ClC_6H_4, R', R'' = H (**2b**)	24	60	386 (97)
5	**T7**	R = *p*-FC_6H_4, R', R'' = H (**2c**)	4	120	688 (94)
6	**T8**	R = *p*-FC_6H_4, R', R'' = H (**2c**)	24	60	345 (95)
7	**T7**	R = $PhOCH_2$, R', R'' = H (**2f**)	4	120	760 (98)
8	**T8**	R = $PhOCH_2$, R', R'' = H (**2f**)	24	60	376 (97)
9	**T8**	R = $ClCH_2$, R', R'' = H (**2g**)	24	60	263 (96)
10	**T8**	R = CH_2=$CHCH_2CH_2$, R', R'' = H (**2h**)	24	60	271 (95)
11	**T8**	R = CH_2=CH, R', R'' = H (**2i**)	24	60	206 (90)

[a]Reactions were carried out as described for catalyst **T5** but using 1 mol% of **T7** or **T8** and no added TBAI.

Table S4. Kinetic isotope data for the reactions illustrated in eq. 4 in the manuscript.[a]

time (h)	product (%)[a]			kinetic isotope effect	
	3a-d_0	**3a-d_1**	**3a-d_2**	k_H/k_{D1}[b]	k_H/k_{D2}[c]
2	19	18	12	1.06	1.58
3	28	26	18	1.08	1.56
4	41	38	25	1.08	1.64
5	46	46	29	1.00	1.59

6	57	56	37	1.02	1.54
8	72	76	49	0.95	1.47
average				**1.03**	**1.56**

[a]Separate reactions were run for **2a**-d_0, **2a**-d_1 and **2a**-d_2 and the corresponding yields of aliquots determined by ^{1}H NMR at various times are provided. [b]Obtained from the **3a-d$_0$**/**3a-d$_1$** product ratio. [c]Obtained from the **3a-d$_0$**/**3a-d$_2$** product ratio.

HPLC profiles:

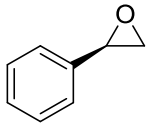

Racemic

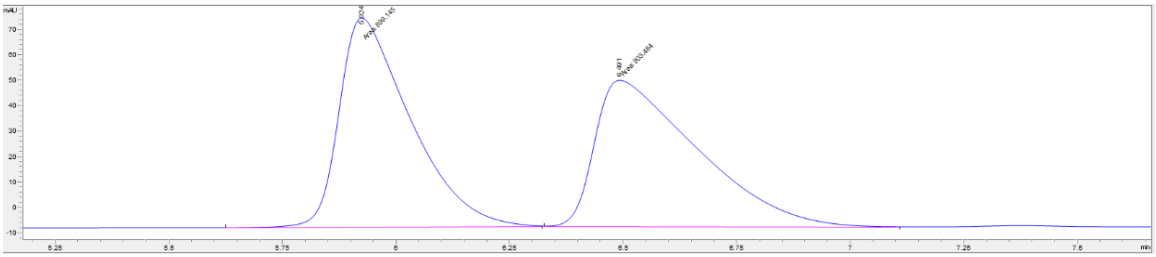

#	Time	Area	Height	Width	Area%	Symmetry
1	5.924	899.1	82.6	0.1814	49.880	0.465
2	6.491	903.5	57.7	0.2611	50.120	0.319

(*R*)-**2** : (*S*)-**2** = 72 : 28

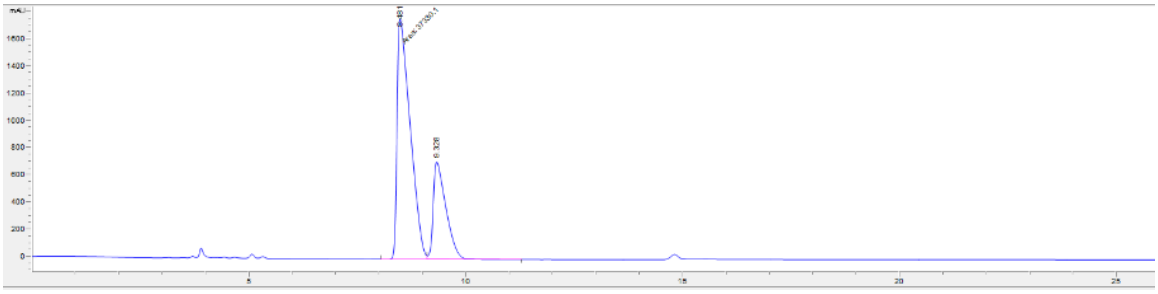

#	Time	Area	Height	Width	Area%	Symmetry
1	8.481	37330.1	1771.9	0.3511	71.887	0.315
2	9.328	14598.4	717.6	0.3013	28.113	0.368

Enantiopure (*R*)-**2**

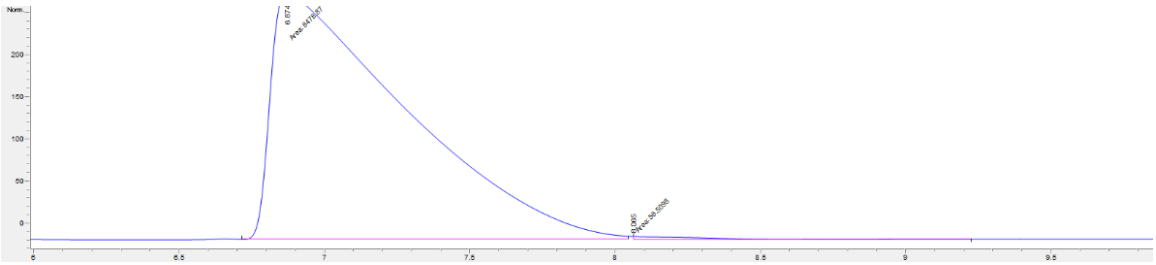

#	Time	Area	Height	Width	Area%	Symmetry
1	6.874	8478.9	262.4	0.5385	99.338	0.149
2	8.065	56.5	3.5	0.213	0.662	0

Appendix for Chapter 5

Table S1. Chemical shifts of indoles and the alkylation products used for reaction conversion calculations (in $CDCl_3$).

Indoles	R = H	5-OMe	6-OMe	5-Cl	6-Cl			
δ (ppm)	6.58	6.49	6.50	6.51	6.55			
Products	Ar = Ph R = H	Ph 5-OMe	Ph 6-OMe	Ph 5-Cl	Ph 6-Cl	4-MeC_6H_4 H	2-ClC_6H_4 H	3-BrC_6H_4 H
δ (ppm)	5.20	5.14	5.15	5.14	5.16	5.16	5.75	5.17

Table S2. Friedel–Crafts reaction kinetic data (T = –35 ˚C).

$[\beta$-nitrostyrene$]_0$ = 83 mM, $[$indole$]_0$ = 250 mM, solvent = $CDCl_3$		
[**4a**] (mM)	time (h)	conversion (%)
0.83 mM	71	23
	95	33
	117	39
4.2 mM	51	42
	96	67
	123	76
8.3 mM	24	44
	48	76
	71	86
	95	93
17 mM	1.5	8.8
	4	15
	28	88

Table S3. Evaluation of **4b** under various conditions.

entry	solvent	[βNS] (mM)	[indole] (mM)	temp.(˚C)	t (h)	Conv. (%)[b]	*er*[c]
1	CD_2Cl_2	83	250	-35	98	33	92 : 8
2	$C_6D_5CD_3$	83	250	-35	98	36	88 : 12
3	$CDCl_3$	83	250	-35	48	41	93 : 7
4	$CDCl_3$	166	250	-35	47	56	90 : 10
5	$CDCl_3$	200	300	-35	49	57	92 : 8
6	$CDCl_3$	250	125	-35	92	85	88 : 12
7	$CDCl_3$	250	250	-35	94	75	88 : 12
8	$CDCl_3$	250	375	-35	48	60	95 : 5
9	$CDCl_3$	250	500	-35	94	99	89 : 11
10	$CDCl_3$	250	750	-35	71	99	92 : 8
11	$CDCl_3$	300	450	-35	48	66	91 : 9
12	$CDCl_3$	400	600	-35	48	71	89 : 11
13	$CDCl_3$	500	750	-35	48	83	90 : 10
14	$CDCl_3$	250	375	-30	48	84	91 : 9
15	$CDCl_3$	250	375	-45	90	70	92 : 8

[a]Standard conditions of 10 mol% catalyst were used. [b]Conversions were determined by ^{1}H NMR analysis of crude reaction mixtures. [c]Enantiomeric ratios were determined by chiral HPLC.

Table S4. Evaluation of **4c** under various conditions.[a]

entry	solvent	[βNS] (mM)	[indole] (mM)	t (h)	Conv. (%)[b]	*er*[c]
1	CD_2Cl_2	83	250	96	33	89 : 11
2	$C_6D_5CD_3$	83	250	96	27	83 : 17
3	$CDCl_3$	29	83	144	12	92 : 8
4	$CDCl_3$	83	250	49	48	93 : 7
5	$CDCl_3$	166	250	47	45	92 : 8
6	$CDCl_3$	250	250	46	49	91 : 9
7	$CDCl_3$	250	375	48/70	58/87	92 : 8
8	$CDCl_3$	250	500	47	80	91 : 9
9	$CDCl_3$	250	750	46	88	91 : 9
10	$CDCl_3$	500	750	47	82	90 : 10

[a]Standard conditions of 10 mol% catalyst under -35 ℃ were used. [a]Conversions were determined by ^{1}H NMR analysis of crude reaction mixtures. [b]Enantiomeric ratios were determined by chiral HPLC.

Table S5. Evaluation of **4e** under various conditions.[a]

entry	cat. loading (mol%)	[βNS] (mM)	[indole] (mM)	temp.(˚C)	t (h)	Conv. (%)[b]	*er*[c]
1	10	83	125	-35	71	63	93 : 7
2	10	83	250	-35	72	78	91 : 9
3	10	100	150	-35	71	64	93 : 7
4	10	166	166	-35	71	65	93 : 7
5	10	166	250	-35	73	84	94 : 6
6	10	166	333	-35	70	95	93 : 7
7	10	166	500	-35	69	99	94 : 6
8	10	200	300	-35	70	88	93 : 7
9	10	250	375	-35	70	96	92 : 8
10	10	250	750	-25	45	77	90 : 10
11	5	166	250	-35	74	47	91 : 9
12	5	166	500	-35	74	61	90 : 10
13[d]	10	166	250	-35	70	94	93 : 7
14[e]	10	166	250	-35	70	96	92 : 8
15[f]	10	166	250	-35	88	15	79 : 21
16[g]	10	166	250	-35	88	8	77 : 23

[a]Standard conditions of $CDCl_3$ as solvent were used. [b]Conversions were determined by ^{1}H NMR analysis of crude reaction mixtures. [c]Enantiomeric ratios were determined by chiral HPLC. [d]5-Methoxyindole was used as substrate. [e]6-Methoxyindole was used as substrate. [f]5-Chloroindole was used as substrate. [g]6-Chloroindole was used as substrate.

Table S6. Evaluation of **4f** under various conditions.[a]

entry	[βNS] (mM)	[indole] (mM)	t (h)	Conv. (%)[b]	*er*[c]
1	29	83	48	13	83 : 17
2	83	125	47	40	91 : 9
3	83	250	46	70	93 : 7
4	166	250	47	73	92 : 8
5	166	500	48	78	92 : 8
6	250	375	47	81	92 : 8
7	250	750	47	91	92 : 8

[a]Standard conditions of 10 mol% catalyst in $CDCl_3$ under -35 ℃ were used.[b]Conversions were determined by ^{1}H NMR analysis of crude reaction mixtures. [c]Enantiomeric ratios were determined by chiral HPLC.

HPLC profiles:

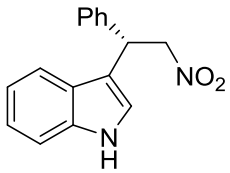

Regiscell column, hexanes : *i*-PrOH = 75 : 25, flow rate 1.00 mL/min, λ = 250 nm

Racemic

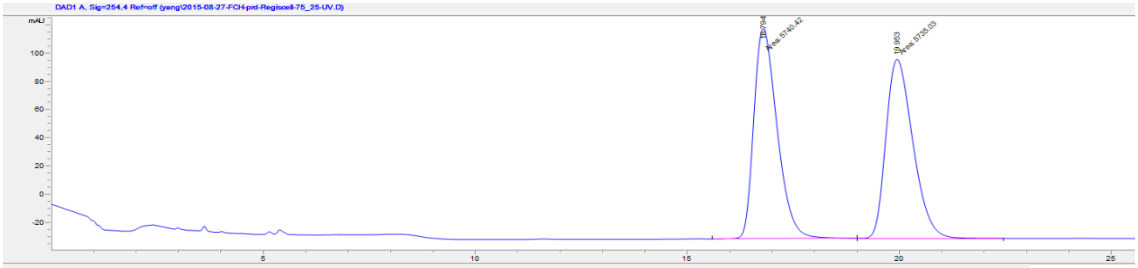

#	Time	Area	Height	Width	Area%	Symmetry
1	16.794	5740.4	149.7	0.6391	50.023	0.655
2	19.953	5735	127.9	0.7476	49.977	0.677

Enantiomerically enriched

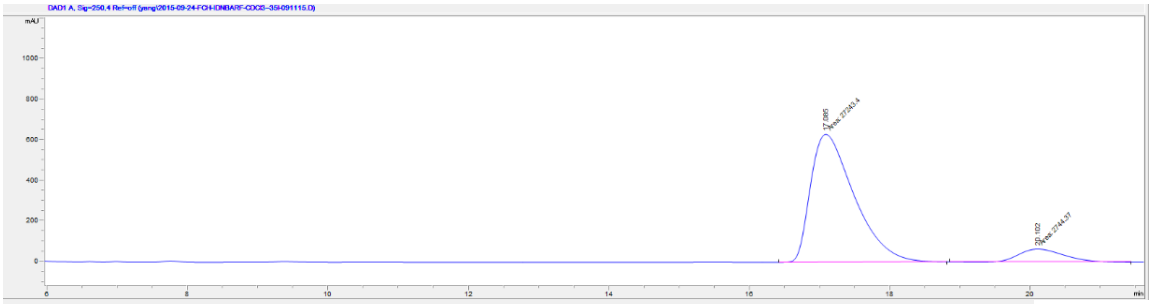

#	Time	Area	Height	Width	Area%	Symmetry
1	17.085	27243.4	630.6	0.7201	90.848	0.522
2	20.102	2744.4	63	0.7261	9.152	0.731

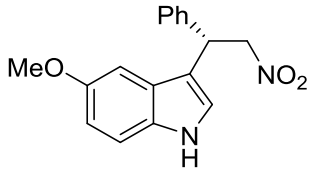

Regiscell column, hexanes : *i*-PrOH = 75 : 25, flow rate 1.00 mL/min, λ = 250 nm

Racemic

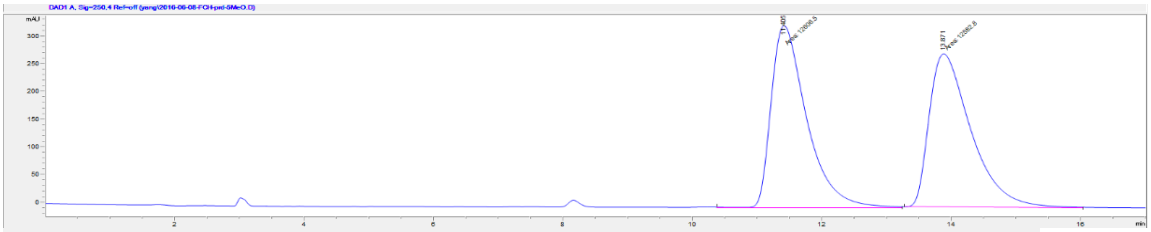

#	Time	Area	Height	Width	Area%	Symmetry
1	11.405	12606.5	329.9	0.6369	50.047	0.551
2	13.871	12582.8	277.9	0.7547	49.953	0.509

Enantiomerically enriched

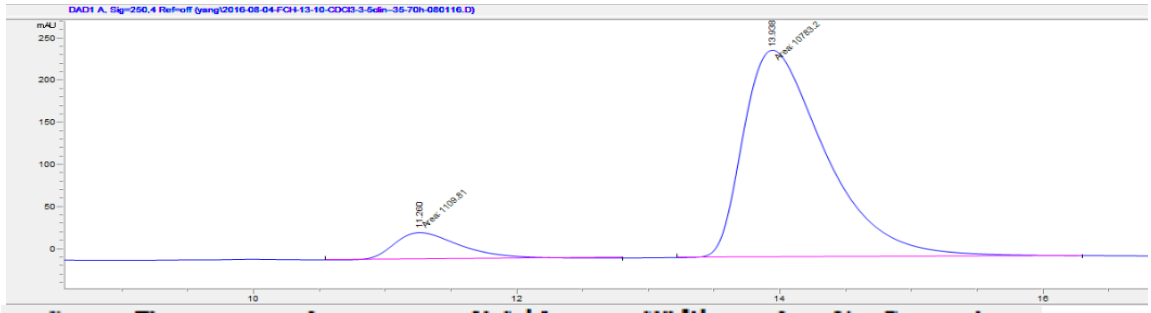

#	Time	Area	Height	Width	Area%	Symmetry
1	11.26	1109.8	31.7	0.5839	9.332	0.605
2	13.938	10783.2	246.8	0.7282	90.668	0.525

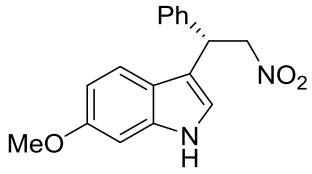

Regiscell column, hexanes : *i*-PrOH = 75 : 25, flow rate 1.00 mL/min, λ = 250 nm

Racemic

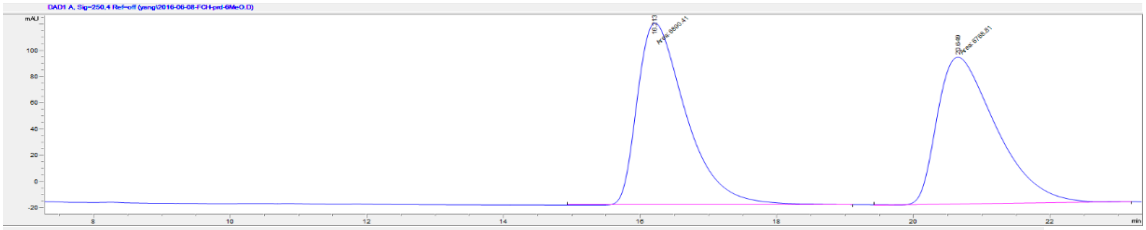

#	Time	Area	Height	Width	Area%	Symmetry
1	16.213	6890.4	138.6	0.8287	50.445	0.544
2	20.649	6768.8	112.2	1.0059	49.555	0.525

Enantiomerically enriched

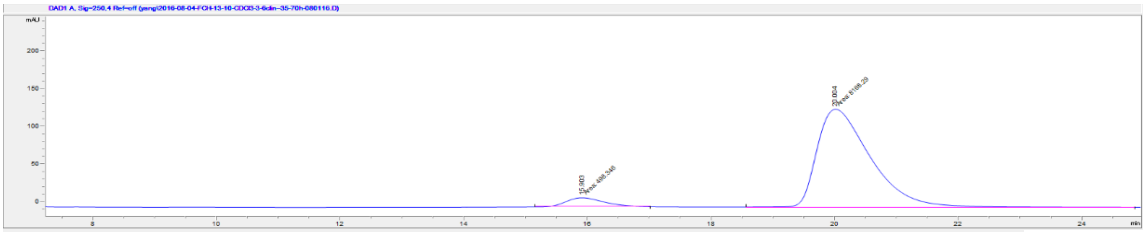

#	Time	Area	Height	Width	Area%	Symmetry
1	15.903	498.3	11.8	0.7066	5.750	0.686
2	20.004	8168.3	131	1.0391	94.250	0.505

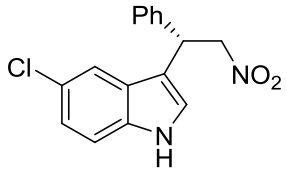

Regiscell column, hexanes : *i*-PrOH = 75 : 25, flow rate 1.00 mL/min, λ = 250 nm

Racemic

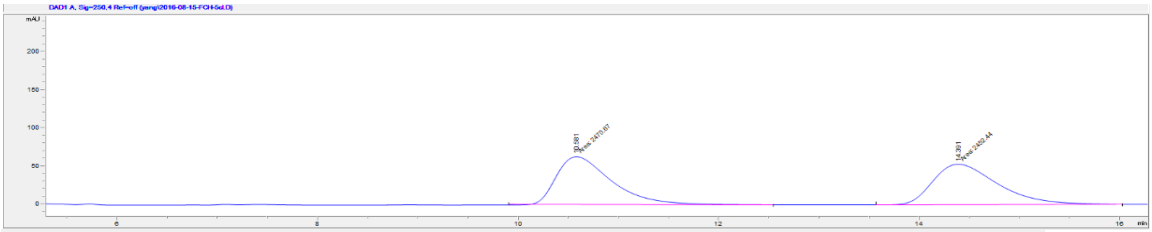

#	Time	Area	Height	Width	Area%	Symmetry
1	10.581	2470.7	63.3	0.6506	50.185	0.539
2	14.391	2452.4	53.6	0.7627	49.815	0.612

Enantiomerically enriched

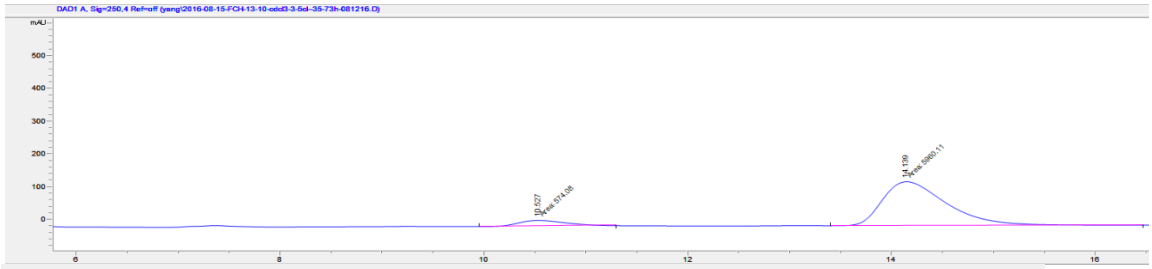

#	Time	Area	Height	Width	Area%	Symmetry
1	10.527	574.1	17.6	0.5421	8.786	0.748
2	14.139	5960.1	134.6	0.7381	91.214	0.582

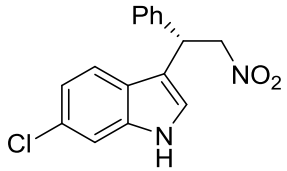

Regiscell column, hexanes : *i*-PrOH = 85 : 15, flow rate 1.00 mL/min, λ = 250 nm

Racemic

#	Time	Area	Height	Width	Area%	Symmetry
1	18.383	5258.6	90.7	0.9668	50.020	0.567
2	21.831	5254.3	82.2	1.0648	49.980	0.584

Enantiomerically enriched

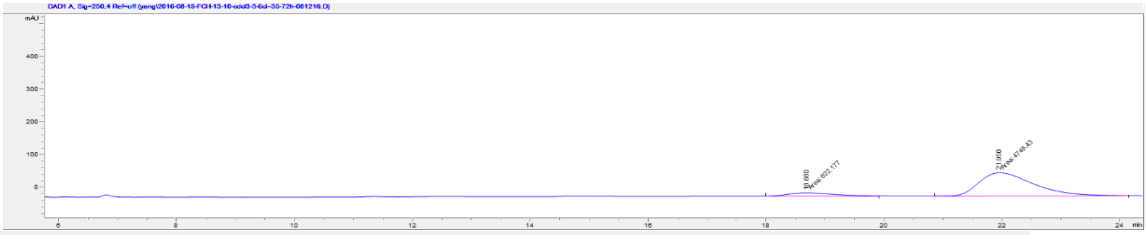

#	Time	Area	Height	Width	Area%	Symmetry
1	18.68	622.2	10.6	0.9819	11.589	0.627
2	21.95	4746.4	72	1.0985	88.411	0.618

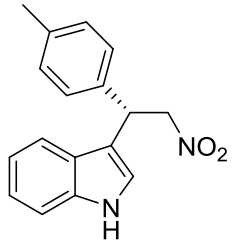

Regiscell column, hexanes : *i*-PrOH = 80 : 20, flow rate 1.00 mL/min, λ = 250 nm

Racemic

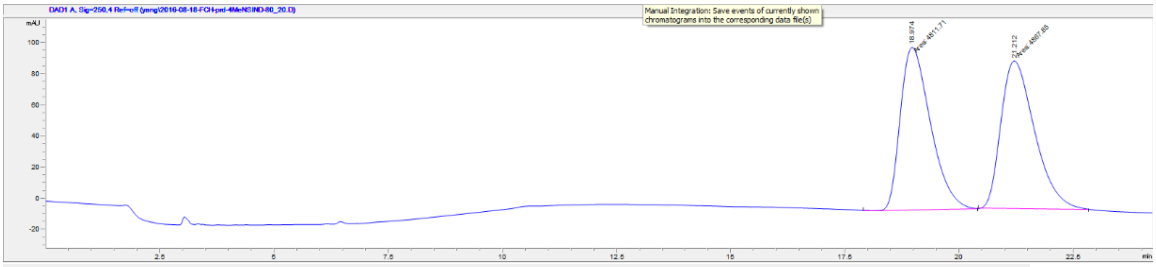

#	Time	Area	Height	Width	Area%	Symmetry
1	18.974	4811.7	104.4	0.7684	49.710	0.632
2	21.212	4867.8	94.7	0.8564	50.290	0.639

Enantiomerically enriched

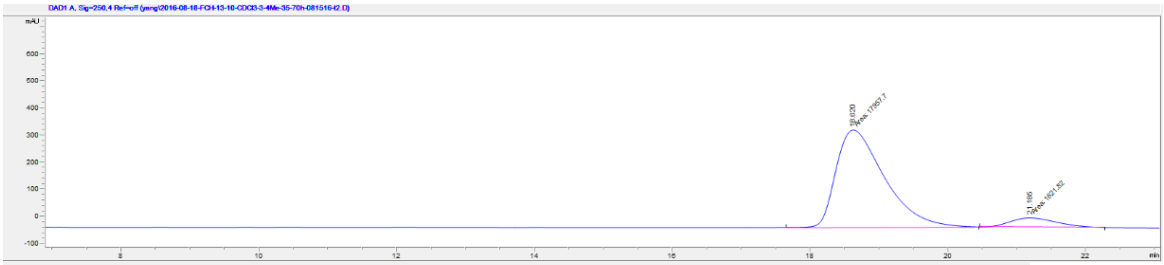

#	Time	Area	Height	Width	Area%	Symmetry
1	18.974	4811.7	104.4	0.7684	49.710	0.632
2	21.212	4867.8	94.7	0.8564	50.290	0.639

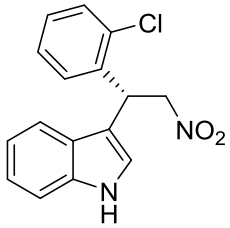

Regiscell column, hexanes : *i*-PrOH = 75 : 25, flow rate 1.00 mL/min, λ = 250 nm

Racemic

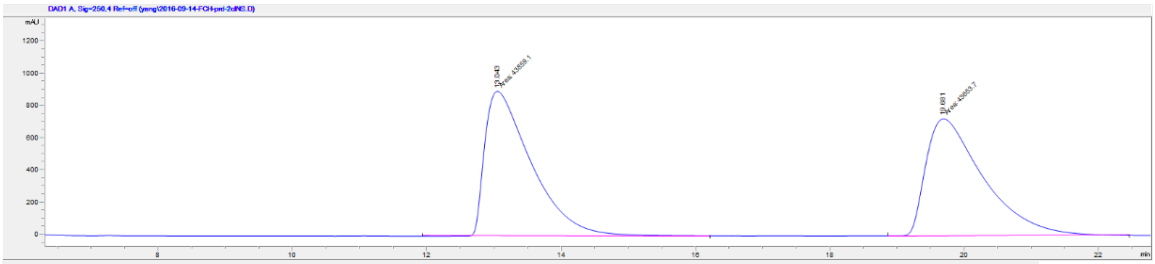

#	Time	Area	Height	Width	Area%	Symmetry
1	13.043	43859.1	900.3	0.8119	50.117	0.356
2	19.681	43653.7	730.3	0.9963	49.883	0.431

Enantiomerically enriched

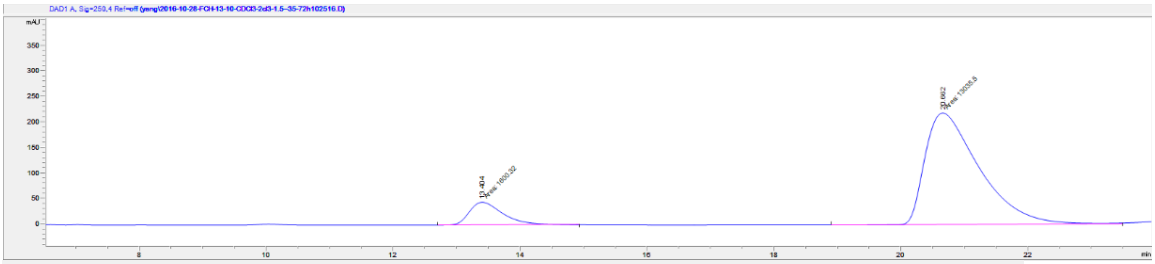

#	Time	Area	Height	Width	Area%	Symmetry
1	13.404	1600.3	44.3	0.6019	10.934	0.623
2	20.662	13035.5	218.8	0.9928	89.066	0.472

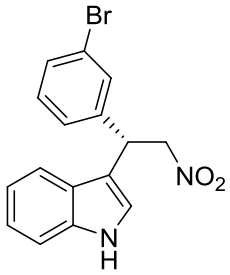

Regiscell column, hexanes : *i*-PrOH = 80 : 20, flow rate 1.00 mL/min, λ = 250 nm

Racemic

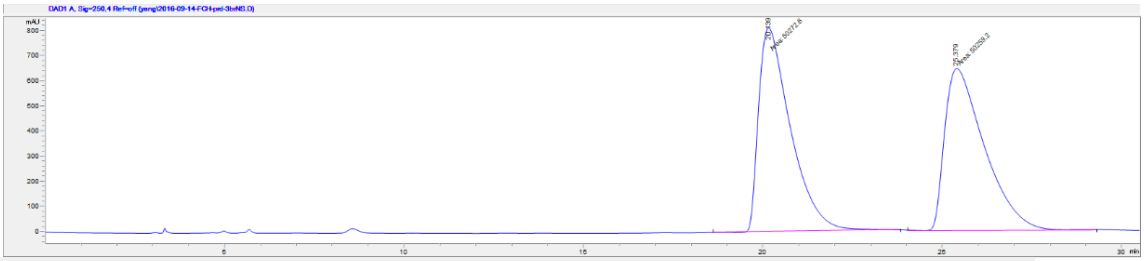

#	Time	Area	Height	Width	Area%	Symmetry
1	13.404	1600.3	44.3	0.6019	10.934	0.623
2	20.662	13035.5	218.8	0.9928	89.066	0.472

Enantiomerically enriched

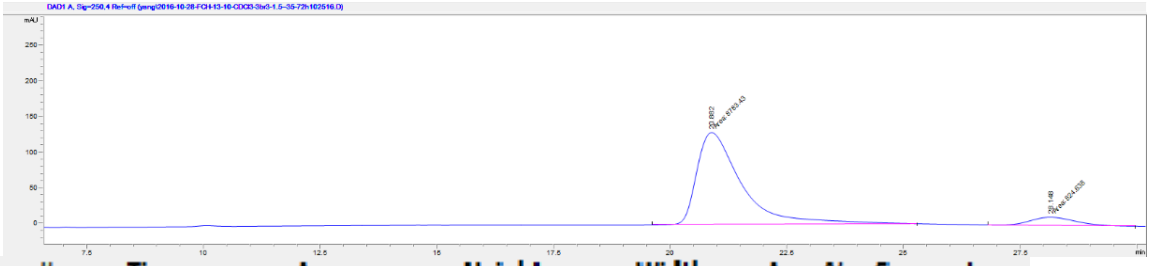

#	Time	Area	Height	Width	Area%	Symmetry
1	20.882	8783.4	129.9	1.1265	91.417	0.468
2	28.148	824.6	11.9	1.1563	8.583	0.845